THE UNIVERSITY OF CHICAGO

DYSFUNCTIONAL CD8^{+} T CELLS AND THE IMMUNE SUPPRESSIVE TUMOR MICROENVIRONMENT

A DISSERTATION SUBMITTED TO
THE FACULTY OF THE DIVISION OF THE BIOLOGICAL SCIENCES
AND THE PRITZKER SCHOOL OF MEDICINE
IN CANDIDACY FOR THE DEGREE OF
DOCTOR OF PHILOSOPHY

COMMITTEE ON IMMUNOLOGY

BY
JASON BRUCE WILLIAMS

CHICAGO, ILLINOIS
JUNE 2018

One, remember to look up at the stars and not down at your feet.

Two, never give up work. Work gives you meaning and purpose and life is empty without it.

Three, if you are lucky enough to find love, remember it is there and don't throw it away.

- Stephen Hawking - 1942-2018

TABLE OF CONTENTS

LIST OF FIGURES

LIST OF TABLES

ACKNOWLEDGMENTS

The scientific discoveries and advancement of knowledge presented in this thesis, as well as the progress I have made as a scientist, is a product of a truly collaborative effort made by many individuals, to whom I give my deepest gratitude.

First, to my thesis advisor, Tom Gajewski; your unabashed enthusiasm for science, the art of discovery and your projects that continue to push the boundary of tumor immunology, make you a unparalleled mentor. Your advocacy for scientific excellence, precision, and your dedication to us, is truly inspirational, and has made every lab member a better scientist and individual. You have taught me that science is not just an accumulation of data and figures, but is a story, that is eager to be shared. For this, and much more, I thank you.

To the Gajewski Lab members: you are all fantastic scientists and individuals, without whom, I would not be where I am today. First, thank you to the "old" Gajewski Lab members. Thank you to Stefani and Leticia for showing me the ropes when I first joined the lab. Your friendliness and collaboration always made me feel welcome and eager to do science. A shining example of your geniality was when Stefani brought me coffee early in the morning after I pulled an all-night experiment, and Leticia for a wonderful coffee mug (which I use everyday) for simply continuing an experiment in her absence. To Seng-Ryoung Woo, thank you for sharing your expertise and techniques, your good spirits and laboratory whistling; I will always remember.

A sincere thank you to those on the "island of misfits" in the Gajewski Lab: Ayelet, Brendan, and Kyle; who joined the lab pre-primed with expertise. To Ayelet Sivan, your ability to think critically about every aspect of an experiment was truly enlightening. I am honored to have worked with you, your jokes and jovial personality always made the lab a warm place to work. I thank you for all you have taught me. To Brendan, because our projects intertwined you were an invaluable source for insights, ideas, inspiration, and...data. I could not have had a better neighboring desk and bench space partner. You are a gifted scientist and I am excited for the discoveries you will unveil in the future. To Kyle, your

eagerness to help anyone in lab was a blessing, thank you. In addition, your enthusiasm for sports kept us tied to reality. To Blake, your depth of knowledge of the field is inspiring, you had an answer to every question I asked you...followed by in-depth apt conversations. A special thank you to Shuyin Li, your key discovery of the importance of the IFN-γ pathway in rendering tumor cells resistance to T cell killing, drove a significant proportion of the data presented in this thesis. You collaborated with me without hesitation and we have worked side-by-side to uncover significant insights, likely to make a meaningful impact in the field. Your earthy humor and deep knowledge of intricate laboratory techniques make you a pleasure to work with and an invaluable asset to the lab. In addition, you always took my beloved cat Neutrino into your home with open arms. A thank you to Vyara, Jessica, and Randy; you were always full of encouragement and your excitement about science was superbly contagious.

To the new members of the Gajewski Lab: Alex, Andrea, Emily, Jon, Jeff, and Manja; you have continued to make this lab feel like a family. Alex, I thank you for all the conversations about science and life in general. Emily, thank you for your eagerness to collaborate, I'm excited to see your achievements to come. Andrea, thank you for taking the helm on future projects. Your determination and love for science will serve you well as you continue your career in the Gajewski Lab.

I couldn't have done this without my thesis committee: Marisa Alegre, Pete Savage, and Justin Kline. You have provided insightful comments throughout my thesis work and provided encouragement, especially when I most needed it.

Graduate school would not have been as enjoyable without the friends and colleagues I made along the way: Alex Bobe, Natha Torres, Kevin Lei, Sanja Milkin, Michelle Miller, Junior Emmanuel, Katie Igartua and Ken Barr.

To my amazing family, you have loved and supported me though this path I have taken. I started my scientific career as a teenager genotyping mice in my father's lab. I was blessed to have had the opportunity to work a few years with both my mother and father after

college, where I feel in love with science. I owe everything to you. To my sister Brooke, her husband Joseph, and my adorable niece and nephew, Birch and Bruce, I could not have done this without your love and support. Our family discussions of science and all things life, have rooted a firm desire to continue my path. Thank you.

To my incredible wife Yesika, you fill every day with happiness. You are my anchor, from helping me during the late nights in lab to listening to me recite my presentations endlessly, I would not be who am I today without you. I love you.

ABSTRACT

Although the presence of tumor-infiltrating lymphocytes (TILs) indicates the generation of an endogenous antitumor immune response, immune regulatory pathways often subvert the effector phase of the immune response and enable tumor escape. Negative regulatory pathways include extrinsic suppressive mechanisms, but also a T cell-intrinsic dysfunctional state. A more detailed study has been hampered by a lack of cell surface markers defining dysfunctional TILs, and it is clear that PD-1 alone is not sufficient. Our laboratory previously identified the transcription factor Egr2 as a critical component in controlling the anergic state *in vitro*. Identified Egr2 target genes were used as a means to focus on cell surface markers that might characterize the dysfunctional state, and those with robust staining by flow cytometric analysis were applied towards study of $CD8^+$ T cells in the tumor microenvironment. We found that the Egr2-driven cell surface proteins, LAG-3 and 4-1BB, identify dysfunctional tumor antigen-specific $CD8^+$ TILs. Co-expression of 4-1BB and LAG-3 was seen on a majority of $CD8^+$ T cells within the tumor microenvironment but not in secondary lymphoid organs. Functional analysis revealed defective production of IL-2 and TNF-α, while Treg-recruiting chemokines and IFN-γ remained highly expressed. Transcriptional and flow cytometric characterization identified co-expression of multiple additional co-stimulatory and co-inhibitory receptors by this subset of TIL. Administration of anti-LAG-3 plus anti-4-1BB mAbs was therapeutic against tumors *in vivo*, which correlated with reversal of TIL dysfunction and restoration of an effector phenotype. The striking feature of heightened and prolonged production of IFN-γ by T cells within the tumor led us to investigate the role IFN-γ played during the setting of chronic T cell activation within the tumor site. While IFN-γ has been reported to be necessary for tumor elimination, IFN-γ also mediates a form of adaptive resistance by upregulating PD-L1 and indoleamine-2,3-dioxygenase (IDO) in the tumor microenvironment. On the other hand, loss of IFN-γ sensing by tumor cells has been proposed to lead to secondary resistance to checkpoint blockade therapy. Therefore, to determine whether the effects of IFN-γ on tumor cells are pro-immune or im-

mune regulatory we rendered tumor cells insensitive to IFN-γ by selectively mutating the IFNγR2 or Jak1 genes in tumor cells. When implanted into mice, IFN-γ-insensitive tumors were better controlled *in vivo*. This phenotype was true across several tumor models and was not due to off-target effects from CRISPR/Cas9 mutagenesis. Spontaneous control of mutant tumors was dependent on $CD8^+$ T cells and was associated with a marked increase in the frequency of tumor antigen-specific $CD8^+$ T cells. The mechanism of improved tumor control was mapped to defective PD-L1 upregulation in response to IFN-γ produced by $CD8^+$ TILs, which phenocopied PD-L1 blockade. Retroviral-mediated re-expression of PD-L1 on IFN-γ-insensitive tumor cells was sufficient to restore progressive tumor growth. These results indicate that in settings in which the major source of PD-L1 is on tumor cells within the tumor microenvironment, then the dominant effect of IFN-γ on cancer cells can be immunoregulatory.

Part I

Introduction

Chapter 1

An Overview: Cancer Immunity

The immune system plays a critical role in protecting the host from cancer [1]. The innate sensing of tumor cell-derived factors can lead to an adaptive T cell response through the presentation of tumor-associated antigens (TAAs) generated from genetic mutations and epigenetic changes that occur during carcinogenesis [2]. Spontaneously primed $CD8^+$ T cells can home to tumor sites and accumulate there, even if tumors are not completely eliminated [3, 4]. These tumor-infiltrating lymphocytes (TIL) have the ability to recognize tumor cells and are thought to be critical in controlling tumor growth in cancer patients, based on the correlation of TILs with improved prognosis in multiple types of cancer [5, 6, 7, 8]. However, without additional manipulation, this endogenous antitumor response is usually not sufficient to promote complete rejection of an established tumor [9, 10, 11]. Data accumulated over the past decade have indicated that tumors can co-opt mechanisms of immune suppression normally used to maintain immune homeostasis and prevent auto-immunity to subvert the effector phase of the antitumor T cell response. Such mechanisms include expression of ligands for inhibitory receptors expressed by activated T cells [12], recruitment of suppressive cell populations including $CD4^+Foxp3^+$ regulatory T (Treg) cells [13] and suppressive myeloid cell populations [14], and metabolic dysregulation by immunosuppressive enzyme activity such as indoleamine-2,3-dioxygenase (IDO) and the ectonucleotidases CD39 and CD73 [15, 16, 17]. Independent of these extrinsic modes of suppression, T cells themselves can enter a state of intrinsic dysfunction [18, 19, 20, 21]. Much of the body of work presented in this thesis is centered on the dysfunctional state of TILs and its role in contributing to immune regulation within the tumor microenvironment. Efforts over the past 10 years have led to novel immunotherapies centered on blockade of negative regulatory processes within the tumor microenvironment. However, this area of research is still in its infancy, and a comprehensive understanding of the dysfunctional state of $CD8^+$ TILs has the potential to open up new therapeutic opportunities.

1.1 The innate and adaptive immune system

The immune system can be divided into two main components: the innate arm and the adaptive arm. The innate immune system responds rapidly at the first encounter of an infectious agent through a set of evolutionary conserved germline-encoded pattern recognition receptors (PRRs). In the context of infection, the array of PRRs expressed by an antigen-presenting cell (APC) can recognize conserved features of pathogens known as pathogen-associated molecular patterns (PAMPs), or molecules released from stressed or dying cells known as damage-associated molecular patterns (DAMPs). The adaptive immune system takes longer to respond and utilizes different mechanisms to control pathogens. The exquisite specificity, sensitivity, and memory of the adaptive immune system provides the host with sterilizing immunity. The adaptive immune system is composed of two main cell types, T and B lymphocytes. The T cell expresses a T cell receptor (TCR) responsible for recognizing peptides derived from foreign antigens presented on major histocompatibility complex (MHC) molecules. During T cell development, the T cell receptor is generated through random combinatorial rearrangements of germline encoded DNA, providing the T cell compartment with a vast diversity of TCRs. It is thought that T cells have the potential to recognize virtually any pathogen because of the vast number of unique TCRs that can be generated. It is estimated that random gene rearrangement during T cell development can generate 10^{15}-10^{20} distinct TCRs [22, 23], however only 10^7 and 10^6 TCR clonotypes exist at one time in an individual human or mouse body respectively [24, 25]. The collective TCR repertoire provides the T cell compartment with the ability to respond to almost any exogenous antigen. During an immune response, T cells recognizing a cognate antigen undergo significant proliferation, which skews the TCR repertoire towards those abundant clonotypes. The critical component of the TCR dictating antigen recognition is the complementarity-determining region 3 (CDR3), which is the most variable region of the TCR. By measuring the skewness of the TCR repertoire during an immune response, the enriched clones represent subsets of cells that are antigen-specific. This analysis can be accomplished in several

ways. Deep sequencing of the CDR3 region of the TCR alpha or beta chain can provide population statistics used to determine responding clonotypes. A second method, termed spectratyping, determines the distribution of CDR3 nucleotide lengths. The spectratype of a naïve T cell repertoire conforms to a Gaussian distribution, but during an immune response the TCR spectratype is skewed due to overrepresentation of different CDR3 lengths, which reflects oligoclonal T cell expansion.

APCs communicate with T cells and induce their activation through the processing and presentation of antigens that are loaded as peptides onto MHCI and MHCII molecules. $CD8^+$ and $CD4^+$ T cells are restricted to MHCI:peptide and MHCII:peptide interactions, respectively. Antigens can be derived from many different sources. APCs routinely degrade self-proteins and present self-peptides on the cell surface, primarily in the context of MHC molecules. Extracellular antigens, such those derived from bacteria, are endocytosed and degraded in endocytic vesicles, which become merged with MHCII-containing endosomal vesicles where peptides are loaded and transported to the cell surface. Intracellular antigens are frequently derived from self-proteins, viruses, or intracellular bacteria that eventually are transported to the endoplasmic reticulum (ER), where they are loaded onto MHCI and transported to the cell surface. Surface-presented class I MHC:peptide or class II MHC:peptide complexes are then available for potential recognition by specific T cells bearing the corresponding TCR.

The random generation of TCRs and the extraordinary diverse nature of the TCR repertoire inevitably leads to T cells capable of recognizing self-antigens. Therefore, during T cell development, T cells with high affinity TCRs towards self-antigens undergo clonal deletion. While central tolerance is very efficient, auto-reactive T cells do escape the thymus. These auto-reactive T cells are suppressed by layers of peripheral tolerance mechanisms [26]. One dominant peripheral tolerance mechanism is mediated through Treg cells, which suppress auto-reactive T cells at steady-state, and also dampen the magnitude of the immune response during infection to minimize host injury. The importance of Treg cells is exemplified

by humans and mice that lack Foxp3, the forkhead box transcription factor required for Treg development and function. In the absence of Foxp3, fatal systemic autoimmunity develops in both mouse and human [27]. A second layer of peripheral tolerance is imposed upon autoreactive T cells that interact with APCs in the absence of pro-inflammatory signals. These interactions can induce T cell deletion or a hypofunctional state that has been termed T cell anergy [28].

For many years it was unclear whether tolerance mechanisms and a paucity of defined tumor antigens prevented T cells from recognizing tumors. However, a T cell infiltrate in the tumor microenvironment of patients has been shown to have significant prognostic benefit in multiple cancer types and associates with clinical responses to immunotherapy [7].

1.2 Tumor antigens

At the core of the endogenous antitumor immune response are T cells that have the ability to recognize tumor-specific antigens. Tumor antigens can fall under three main classifications: tumor-specific (TSA), tumor-associated (TAA) and cancer-testis (CTA) antigens. TSAs, also referred to as neoantigens, are completely absent from normal cells, are recognized as foreign by the host immune system, and are derived from non-synonymous driver or passenger mutations and viral genes. TAAs are comprised of proteins expressed at disproportionally greater levels in tumor cells compared to normal cells, and can be derived from gene amplification events and post-translational modifications [29]. CTAs are expressed by various tumor types and cells of reproductive tissues such as testes and fetal ovaries but have limited expression on normal host cells. Expression of CTAs and TAAs occur among cancer bearing individuals, providing the opportunity to treat many cancer patients by targeting T cell activation, by vaccination for example.

T cell responses to human tumor antigens have been well documented over the past 20 years [29]. However, as tumors are derived from normal tissues, how these antigens arise and how the innate immune system initiates an effector rather than an tolerogenic adaptive

immune response had remained unclear. Recent data have indicated that many tumor-specific antigens are derived from mutational processes that also drive oncogenesis. Defects in DNA repair machinery, exposure to mutagens (e.g. UV light and tobacco smoking), and abnormalities of enzymes that modify DNA can lead to somatic mutations, chromosomal translocations and alterations in gene expression as part of the process of carcinogenesis [2]. These processes lead to diverse mutational landscapes, with some commonly mutated oncogenes or tumor-suppressor genes that are characteristics of certain cancer types but also with a spectrum of unique mutations specific to an individual tumor [30].

CTAs and TAAs have been the targets of several types of immunotherapies including cancer-vaccines and adoptive cell transfer (ACT) therapy [31]. Cancer vaccines incorporating TAAs have shown only modest benefit, likely due to tolerance mechanisms against self-antigens [32] or induction of T cells with low affinity TCRs. ACT therapy uses TILs expanded *ex vivo* or TCR gene-modified T cells. ACT therapy can lead to strong clinical responses; however, some patients experience life-threatening autoimmune toxicities due to low or unknown expression of these antigens in other tissues [33, 34]. TSAs are a more attractive target because they are not likely to be regulated by homeostatic central and peripheral tolerance mechanisms. Since antigen expression is restricted to tumor cells, therapies that target TSAs are less likely to induce autoimmune toxicities. Further, several studies have found that TSAs appear to be dominant antigens driving the endogenous antitumor T cell response in many patients [35, 36, 37, 38]. In addition, the therapeutic responses in patients receiving ACT or immune-checkpoint blockade therapy, was dominated by neoantigen-specific T cells [39, 40, 41]. It will be important in future studies to determine the neoantigen-specific T cell repertoire as a prospective measure of effective checkpoint blockade therapy.

1.3 Innate recognition of tumor derived material

In order for a productive T cell response to be induced against tumor antigens, it is thought that APCs need to be recruited to the tumor site and become activated. The process by

which APCs are initially recruited to the tumor site is not fully understood and likely depends on the chemokine repertoire produced by tumor cells or the surrounding tumor stroma. Tumor cells produce chemokines that can promote their growth, survival, and metastasis [42]. Genomic aberrations such as oncogenic pathways can impact the array of chemokines expressed. For instance, in a melanoma model, B-Raf pathway activation led to production of the chemokine CCL4, which contributed to the recruitment of Batf3-lineage DCs, known to be essential for priming antitumor $CD8^+$ T cell responses. However, if active β-catenin signaling was also present, CCL4 transcription was silenced, which impaired the recruitment of Batf3-lineage DCs, and subsequent spontaneous T cell priming [43]. It is likely that other chemokines produced by tumor cells contribute to the recruitment of additional cell types within the tumor microenvironment.

Beyond recruitment, the mechanisms of DC activation in the tumor context are beginning to be understood. A clue in identifying potential innate immune pathways that might be necessary for productive adaptive immunity was the observation that tumors containing a T cell infiltrate exhibited a type I IFN gene signature [3, 44]. Studies in mice revealed an essential role for type I IFN signaling on host DCs for spontaneous priming of $CD8^+$ T cells against tumor antigens. Specifically, type I IFN signaling had to occur in Batf3-lineage DCs [4, 45]. This DC subset is specialized to acquire exogenous antigen and cross-present peptides on MHCI to $CD8^+$ T cells [46]. The functional role for type I IFNs prompted investigation of the DAMP that could induce type I IFN production in a sterile tumor environment. Early studies identified several DAMPs that could be released by stressed or dying tumor cells and lead to productive T cell priming. For example, high-mobility group protein B1 (HMGB1) and ATP, recognized by TLR4 and the inflammasome respectively, were both reported to induce DC maturation and subsequent activation of antitumor T cells [47, 48]. However, not all studies supported a mandatory role for TLR4 or extracellular ATP [49]. Subsequent work has provided evidence that tumor-derived DNA is a potential initiator of the endogenous antitumor immune response. DCs recruited to the tumor microenvironment have shown

to engulf tumor-derived DNA, resulting in STING-dependent production of type I IFNs. STING is a cytosolic adaptor molecule that is activated by cyclic dinucleotides generated by cGAMP synthase. The mechanism by which tumor-derived DNA gains access to the cytosol of DCs to activate the STING pathway has yet to be elucidated. Regardless, a critical role for STING in sensing tumors was found in preclinical models, immunogenic tumors rejected in normal mice, grow progressively in STING$^{-/-}$ mice, and spontaneous priming of CD8$^+$ T cells against tumor antigens is nearly ablated.

1.4 The priming and effector phase of CD8$^+$ T cell activation

The priming of naïve CD8$^+$ T cells involves a complex series of spatial, biochemical, transcriptional, proliferative, and differentiation events that engender clonal populations of activated T cells with effector programs. Naïve CD8$^+$ T cells enter and leave the blood stream to traffic through peripheral lymphoid organs (e.g. lymph nodes (LNs)), where they survey thousands of APCs in search of cognate peptide:MHCI complexes [50]. Naïve CD8$^+$ T cells can exit the lymph node via a sphingosine-1-phosphate (S1P) gradient and reenter lymph nodes using CCR7 through a CCL21 chemokine gradient [51]. Activated DCs carrying tumor-derived antigens exit the tumor, traffic to the tumor-draining draining lymph node (TdLN), and communicate contextual information to CD8$^+$ T cells via the interaction of co-stimulatory receptors and ligands and through the production of cytokines, including IL-12 and type I IFNs. During the first few days of priming, CD8$^+$ T cells remain in the TdLN to interact with DCs and undergo initial activation events. This is accomplished by upregulating CD69 which binds the S1P receptor (S1PR) in trans, inducing its internalization. After interaction with a DC expressing cognate antigen, CD8$^+$ T cells undergo programming to rapidly proliferate, expand, and differentiate [52]. A critical factor influencing the magnitude of an antitumor T cell response is the precursor frequency of CD8$^+$ T cells in the naïve repertoire capable of recognizing tumor-derived antigens [53]. After CD8$^+$ T cell activation and proliferative expansion, CD8$^+$ T cells differentiate into cytotoxic T

lymphocytes (CTLs) expressing effector molecules that endow CTLs with the capacity to effectively target and lyse tumor cells. After the priming phase, $CD8^+$ T cells exit the LN by down regulating CD69, whereby they reenter the circulation and have the potential to traffic to the tumor site. However, effector cell trafficking into the tumor microenvironment requires proper homing signals expressed within tumor sites. A strong correlation between the presence of $CD8^+$ T cells and expression of CXCL9 and CXCL10 has been observed across a range of tumor types [3, 54, 55]. Consistent with these data, a recent mechanistic study found that CXCR3 was indispensable for $CD8^+$ T cell recruitment to the tumor [56]. This finding is in line with the importance of CXCR3 in T cell homing to sites of tissue inflammation [57]. While the source of these chemokines in the initial recruitment of $CD8^+$ T cells has been attributed to tumor cells in some settings [3, 58], in a murine model of oncogene-induced melanoma, Batf3-lineage dendritic cells were identified to be the major source of CXCL9 and CXCL10 within the tumor microenvironment, and those DCs were required to recruit activated $CD8^+$ T cells to the tumor site in a CXCR3-dependent manner [59].

At the tumor site, CTLs traverse and identify tumor cells through specific interactions, thereby enabling the release of their cytotoxic functions. Generally, this requires the formation of an immunological synapse with peptide:MHC-TCR interactions at its core, although noncognate interactions have also been implicated [60]. Two main modes of cytotoxicity have been defined by which CTLs can lyse target cells: the granule exocytosis pathway and the expression of death receptor ligands. In either mode, an interaction between the CTL and tumor cells must occur. The granule exocytosis pathway is executed by the release of specialized cytoplasmic granules containing a pore forming protein, perforin (Prf1), along with granzymes, which are a family of serine proteases. Once inside the target cell, granzymes cleave critical proteins controlling cell survival and induce caspase-mediated apoptosis. For the second mode of cytoxocity, CTLs can express ligands that when bound to their receptor on tumors cells can induce intrinsic cell death pathways. Two well-characterized death

receptor ligands are Fas ligand (FasL/CD95) and TNF-related apoptosis inducing ligand (TRAIL). Binding of FasL or TRAIL to their receptors, Fas and TRAIL-R1/2 respectively, induces receptor oligomerization and caspase-8 mediated cell death. Recent evidence suggests that either the granule exocytosis or the death ligand pathway alone can be sufficient to control tumor growth in different models and contexts. These pathways may also act synergistically with each other [61]. CTLs also produce cytokines and chemokines within the tumor microenvironment that can further modulate immune responses, both positively and negatively.

1.5 Immunosuppressive mechanisms within the tumor microenvironment

It is clear that multiple cancer types can be infiltrated by $CD8^+$ T cells [62], and in most scenarios, a proportion of these T cells are specific for tumor antigens. However, despite influx of $CD8^+$ T cells into the tumor microenvironment, most tumors grow progressively, indicating a failure of the immune response to ultimately eliminate malignant cells. Based on a broad set of correlative data, as well as preclinical mechanistic studies, this immune escape can be largely attributed to immune suppressive pathways that become recruited or upregulated within the tumor microenvironment [63, 64]. Several local tissue perturbations during carcinogenesis lead to a microenvironment that is suboptimal for supporting T cell function. These factors include hypoxia, acidosis, and nutrient deprivation [65]. Glycolytic pathways, for example, have been shown to be critical for the acquisition and maintenance of effector T cell function, and competition with tumor cells for glucose likely limits availability for T cells [66, 67]. However, another array of negative regulatory mechanisms are not directly tumor-driven but rather are part of an immune system-intrinsic negative feedback process that dampens T cell function during settings of chronic inflammation. These mechanisms include upregulated expression of PD-L1, which engages the inhibitory receptor PD-1 ex-

pressed by activated T cells; indoleamine-2,3-dioxygenase (IDO), a tryptophan-catabolizing enzyme reported to lead to inhibition of T cell function; and recruitment of $Foxp3^+$ regulatory T (Treg) cells, which suppress the activation of conventional T cells [64, 68]. These pathways converge, often in concert, to blunt the effector function of $CD8^+$ TILs.

The T cell dysfunction that nearly universally is present in tumors is reminiscent of that first described in chronic viral infection and is referred to as T cell "exhaustion". These parallels derive in part from the upregulation of PD-1 on antigen-specific T cells, which is observed in both contexts. However, preliminary data from our laboratory had indicated that $CD8^+$ TILs may in fact retain some functional properties, which are necessary to activate several negative regulatory properties in tumors. For example, IFN-γ produced by $CD8^+$ T cells induces the upregulation of PD-L1 and IDO within the tumor microenvironment. In addition, chemokines produced by $CD8^+$ TIL, such as CCL22, contribute to the recruitment of Treg cells [63]. These and other related data have prompted a deeper investigation into the functional and molecular characteristics of dysfunctional $CD8^+$ T cells within the tumor microenvironment, and that overarching idea has provided the impetus for my dissertation project.

Treg cells are key modulators of immune responses. They possess potent immune suppressive capacity and are required to prevent systemic autoimmunity. Given the prevalence of Treg cells in many cancer types, it is thought that Treg cells represent a major barrier to productive antitumor immune responses. For some human tumors, the presence of intratumoral Treg cells is an indicator of poor prognosis [69], consistent with the notion that Treg cells promote tumor growth. However, the negative prognostic association of Treg cells has not been uncovered in cancer, likely because the presence of Treg cells also indicates that a spontaneous antitumor T cell response has been raised, which has positive prognostic value. Therefore, the ratio of $CD8^+$ T cells to Treg cells within the tumor microenvironment may be a more appropriate biomarker. Studies in mice have shown that depletion of Treg cells, through a variety of targeted approaches, can lead to tumor regression and augment

the effector function of $CD8^+$ TILs [70, 71, 72, 73, 74]. However, clinical trials using an anti-human CD25 antibody or a IL-2-diptheria-toxin fusion protein to deplete Treg cells, have shown little benefit [75, 76, 77]. On the contrary, because Treg cells express high levels of CTLA-4 it has been proposed that one mechanism of action by anti-CTLA-4 antibody therapy in humans is through the depletion of Treg cells [78]. Other strategies to target Treg cells have focused on inhibiting their suppressive functions. For example, one potential target is Neuropilin-1 (Nrp1), which is highly expressed on intratumoral Treg cells. Nrp1 is thought to maintain Treg function in the tumor through interactions with its ligand Sema4a [79] and blocking Nrp1 with mAbs delayed tumor growth [80]. Conditional deletion of Nrp1 in Treg cells destabilizes their suppressive function at the tumor site while retaining tissue homeostasis elsewhere [81]. Effectively depleting Treg cells or inhibiting their function remains an enticing avenue for future therapies.

1.6 $CD8^+$ T cell dysfunction in the tumor microenvironment

During initial antigen encounter, $CD8^+$ T cells recognizing their cognate antigen undergo proliferation and differentiation into effector CTLs. After clearance of antigen, and subsidence of inflammation, a contraction phase ensues where a majority of the responding $CD8^+$ T cells undergo cell death and are removed from the circulating $CD8^+$ T cell population. A smaller population (5-10%) of $CD8^+$ T cells differentiate into self-renewing memory cells with functional capacities to respond rapidly to secondary antigen challenge [82]. These memory cells are divided into subsets defined by their migrational patterns to survey lymphoid and non-lymphoid tissues and their capacity to rapidly respond and regain effector function in response to secondary pathogen encounter. However, if antigen is not cleared, as in the context of chronic viral infections or a growing tumor, immunological memory formation breaks down and responding T cells can enter into a state of dysfunction. Much of the work done dissecting this state has been performed in chronic viral models, namely LCMV clone 13, and this state has been termed T cell "exhaustion". Virus-induced exhaus-

tion is characterized by a gradual and sequential loss of effector functions: first the capacity to produce IL-2 is lost, followed by TNF-α and then IFN-γ; and finally, cytotoxicity and proliferative capacity are lost at late stages of "exhaustion" [83, 84]. Due to key features that parallel chronic infection and cancer, i.e. the persistence of antigen and inflammation, it has long been proposed that dysfunctional $CD8^+$ TILs resemble virally-exhausted $CD8^+$ T cells [85, 86]. However, the metabolic provisions and demands on the immune response, the anatomical localization of the process, and the cellular components involved in these two chronic diseases are disparate. Therefore, whether $CD8^+$ TILs are truly analogous to viral-induced exhausted $CD8^+$ T cells remains unclear. Indirect evidence suggests that the functional state of $CD8^+$ TILs may differ compared to viral-induced exhausted $CD8^+$ T cells. For instance, the therapeutic efficacy of adoptive cell transfer therapy by inoculation of *ex vivo* expanded tumor antigen-specific $CD8^+$ TILs [87, 39, 88, 89], suggests that not all $CD8^+$ TILs are not terminally exhausted. When analyzed directly *ex vivo*, $CD8^+$ TILs have been reported to produce IFN-γ [90, 91]. In addition, tumor antigen-specific $CD8^+$ TILs also retain expression of perforin and granzyme B [92], suggesting that $CD8^+$ TILs contain effector molecules to lyse cancer cells, but fail to do so due to suppressive mechanisms in the tumor microenvironment. Importantly, $CD8^+$ T cell dysfunction in the tumor microenvironment is believed to be reversible. In pre-clinical cancer models, administration of mAbs blocking activity of CTLA-4, PD-1, TIM-3 and LAG-3 were shown to improve $CD8^+$ T cell function [10]. Accordingly, the success of current immunotherapies targeting PD-1 and CTLA-4 is thought to be, at least in part, due to restored function of tumor antigen-specific $CD8^+$ TILs.

In vitro models have revealed that T cells can transition into a state of dysfunction through chronic TCR stimulation without adequate co-stimulation. This dysfunctional state has been termed clonal anergy, and is thought to represent *in vivo* settings in which high levels of antigen might be encountered in the absence of innate immune activation or inflammation. The induction phase of anergy appears to be driven by excessive calcium signaling and NFAT

transcriptional activity. Under those conditions, factors become induced that inhibit the activation of the Ras pathway through TCR/CD28 ligation; one of those defined factors is the lipid phosphatase diacylglycerol kinase (DGK) [93]. *In vivo*, anergy has been observed after transfer of TCR transgenic cells into a naïve host expressing cognate self-antigen [94]. Anergic T cells can persist for weeks but fail to proliferate and produce reduced levels of cytokines in response to subsequent stimulation. Inducing anergy in self-reactive T cells is a peripheral tolerance mechanism responsible for sequestering potentially harmful T cells that escape central tolerance. More recently, a subpopulation of self-reactive polyclonal anergic $CD4^+$ T cells was shown to differentiate into peripherally induced Treg (iTreg) cells [95], providing an additional layer of peripheral tolerance. In the context of cancer, it is thought that T cell anergy may occur because tumor cells and intratumoral DCs often express low levels of co-stimulatory molecules [96]. Additionally, introduction of the CD28 co-stimulatory ligands CD80 or CD86 into tumor cells can lead to spontaneous tumor regression in preclinical models, supporting the idea that improved co-stimulation can enable T cell-mediated tumor rejection [97, 98, 99].

A phenotypic parallel encompassing anergized, virally exhausted, and dysfunctional $CD8^+$ TILs is the expression of cell surface receptors that regulate T cell functions. These receptors can be classified as co-stimulatory or co-inhibitory and act as a rheostat controlling fine tuning T cell activation. In response to specific antigen encounter, the expression of co-inhibitory molecules serves to modulate the intensity of an immune response after antigen clearance, presumably to prevent unintended tissue damage [100]. However, in chronic-viral models, exhausted $CD8^+$ T cells upregulate and maintain expression of an array of co-inhibitory receptors, including PD-1, CTLA-4, and LAG-3 [101]. In the tumor microenvironment, a similar pattern of co-inhibitory receptor expression has been observed on $CD8^+$ TILs from mouse [21, 102, 20] and human [90] tumors. Engagement of these receptors has been shown to blunt proliferation and cytokine production by T cells, and blocking interactions between these receptors and their corresponding ligands can restore T cell function.

1.7 Immunotherapies based on restoring T cell function within the tumor microenvironment

The expression of co-inhibitory receptors on $CD8^+$ TILs has led to the development of monoclonal antibodies to block the interaction of these receptors with their corresponding ligands in hopes of restoring T cell effector function. These co-inhibitory receptors are broadly referred to as checkpoints of immune activation and function, and the administration of antibodies to neutralize their activity has been termed "checkpoint blockade therapy". One of the most well studied checkpoint blockade therapies is anti-PD-1/anti-PD-L1 antibody therapy. PD-1 is expressed on $CD8^+$ T cells after activation and remains expressed on a subset of $CD8^+$ TILs in the tumor microenvironment. PD-1 interacts with its ligand PD-L1, which is expressed on tumor cells and non-malignant cells in the tumor environment. Interruption of PD-1/PD-L1 interaction has shown significant clinical efficacy in a wide variety of cancers [103]. While the mode of action of anti-PD-1/PD-L1 therapy is still under investigation, it has been shown that responding patients exhibited a change in $CD8^+$ T cell locality from the invasive tumor margin to inside the tumor [104]. Also observed was an expansion of $CD8^+$ TILs, which are believed to be specific for tumor associated antigens [105]. In fact, recent reports suggest that neoantigen specific $CD8^+$ T cells may play an essential role in tumor rejection after immune checkpoint blockade therapy [106, 107, 108, 41, 38].

Despite the ability of the immune system to recognize cancer cells, not all patients respond to checkpoint blockade therapy. Anti-PD-1/PD-L1 therapy exhibits an almost bimodal response; some patients experience complete eradication of tumors, but a majority derive little or no clinical benefit. A few theories have been proposed to explain this dichotomy. Two major subsets of tumor microenvironments can be defined by the presence or absence of a transcriptional profile indicative of an endogenous antitumor response. The T cell-inflamed tumor subset contained T cell markers (e.g. CD8A and GZMK) and chemokines known to recruit T cells to the tumor (e.g. CXCL9 and CXCL10), whereas the non-T cell-inflamed lacked

these markers. The biology of the T cell-inflamed subset suggests that spontaneous T cell priming and trafficking into the tumor had occurred. By segregating tumors according to the T cell-inflamed or non-inflamed phenotype, we find that the majority of patients responding to checkpoint blockade therapy contain a T cell-inflamed tumor phenotype [109], suggesting that in these patients, the immune system has been restrained, but primed for reinvigoration. However, even in the T cell-inflamed subset, fewer than half of the patients respond to checkpoint blockade therapy, suggesting that additional negative regulatory mechanisms must be overcome to achieve effective clinical responses. The non-T cell-inflamed subtype of tumor is remarkably devoid of immune cell signatures; even the negative regulatory pathways normally seen in the T cell-inflamed tumor [3, 63]. The mechanisms behind the evolution of these tumors is currently under intense investigation [110], and a few recent observations have helped understand this phenotype. By studying and comparing gene expression patterns between the T cell-inflamed and non-T cell-inflamed tumors, our lab recently discovered an immune evasion mechanism driven by oncogenic activation of the Wnt/β-catenin pathway. The mechanism was ascertained to be a loss of chemokines critical for the recruitment of the Batf3-DC lineage to the tumor site, and thus a failure to activate the innate immune system. Also proposed to explain the non-T cell-inflamed phenotype is a lack of tumor-associated antigens to be recognized by T cells. While this may be true in rare instances, a comparison of the mutational load between the T cell-inflamed versus non-T cell-inflamed did not reveal any correlation, suggesting that other mechanisms are contributing to the exclusion of intratumoral T cells [111].

To convert non-T cell-inflamed tumors into tumors with a T cell-inflamed phenotype, researchers and physicians are interrogating a plethora of immunomodulatory targets and combinatorial strategies. A prime example is the synergistic effect of combinatorial anti-PD-1/PD-L1 and anti-CTLA-4 checkpoint blockade therapy [112]. This has led to the development of other inhibitors of additional negative regulatory molecules. For example, LAG-3, much like PD-1, is upregulated after activation and is known to diminish T cell function

[113]. In pre-clinical models, blocking LAG-3 synergizes with anti-PD-L1 therapy inducing potent tumor control [114]. Clinical trials targeting LAG-3 are ongoing, but have shown modest efficacy to date [115, 116]. Therapies targeting other inhibitory receptors including TIGIT and TIM-3 are in the early stages of development, but have shown robust efficacy in murine cancer models [100]. The molecular mechanisms underlying the function of these co-inhibitory receptors is largely unknown and under active investigation. In addition to interfering with co-inhibitory receptor pathways, co-stimulatory receptors, also expressed on T cells after activation and in the tumor, are promising candidates for immunotherapy. These include the TNFR superfamily members 4-1BB, OX-40, and GITR [12]. Agonistic antibodies against several co-stimulatory receptors have shown therapeutic efficacy in mouse models. These include antibodies against 4-1BB [117], GITR [118], and OX-40 [119]. However, the deep mechanism of action of these approaches has not been completely elucidated. It is also unknown whether endogenous co-stimulation in the tumor microenvironment is sufficient for the functional activity of anti-PD-1/PD-L1 checkpoint blockade therapy. Recent studies revealed that PD-1 can blunt T cell function by dampening CD28 signaling [120] and the efficacy of anti-PD-L1 therapy depends on CD28 signaling [121]. This has led to an emerging idea that $CD8^+$ T cells in the tumor microenvironment are primed to receive co-stimulatory signals but fail to do so due to the absence of ligand in the tumor milieu or due to active suppression of co-stimulatory signaling through the cross-talk of co-inhibitory receptors. Therefore, it will be important to determine if agonist antibodies against co-stimulatory molecules can augment the efficacy of checkpoint blockade therapies and increase the number of patients that are able to benefit from immunotherapy.

A core problem in the development of therapies targeting tumor antigen-specific $CD8^+$ T cells to reinvigorate their effector function, has been a lack of positive cell surface markers to identify these cells. Identifying the cell surface phenome may provide new additional targets for immunotherapy as well as provide a means to study tumor antigen-specific $CD8^+$ TILs with minimal manipulation. Also important to understand is the function of $CD8^+$

TILs during tumor progression. Even when $CD8^+$ TILs fail to control tumor growth, it is thought that they are not inert; therefore, it is important to determine whether dysfunctional $CD8^+$ TILs actively modulate the tumor microenvironment in a pro- or antitumor manner. In addition, examining the functional and phenotypic changes that occur in $CD8^+$ TILs after effective immunotherapy will lead to a better understanding of $CD8^+$ T cell biology in the tumor microenvironment and may give rise to new ways to reinvigorate these cells. Therefore, as a bridge to study dysfunctional $CD8^+$ TILs, our lab turned to a model of *in vitro* T cell anergy to first characterize the genetic profile of anergic T cells. In these studies, we uncovered a role for the transcription factor Egr2 in regulating anergized $CD4^+$ T cell clones [122]. The Egr2-driven transcriptional profile included expression of the co-inhibitory molecule LAG-3, and co-stimulatory molecule 4-1BB, both previously found to be expressed on $CD8^+$ TILs. As I will demonstrate in the results section, these markers provided a useful strategy to study dysfunctional $CD8^+$ TILs in great detail and investigate the function of these cells in shaping the antitumor response before and after effective immunotherapy.

Part II

Materials and Methods

Mice and tumor inoculation

Female C57BL/6 mice ranging from 6 to 8 weeks were purchased from Taconic Farms. CD45.1 and $Rag2^{-/-}$ mice on the C57BL/6 background were obtained from Taconic Farms and bred at the University of Chicago. $2C/Rag2^{-/-}$ and $P14/Rag2^{-/-}$ mice have been previously described [123]. B16.SIY.dsRed [61], C1498.SIY.GFP [124], and MC57.SIY [125] tumor cells were engineered to express either dsRed or GFP in frame with the H2-K^b-restricted model antigen SIYRYYGL and have all been previously described [125]. For experiments, mice were 6 to 9 weeks of age and received $2x10^6$ tumor cells subcutaneously on either the left flank or both the left and right flank. All mice were maintained according to the National Institute of Health Animal Care guidelines and studied under IACUC-approved protocols. To generate the targeting construct for the Egr2EGFP knock-in reporter mice (generated by Dr. Jonathon Powell, Johns Hopkin University), a 12.6kb mouse genomic DNA fragment including the Egr2 gene was excised with SacII and cloned into a pEasy-Flox vector adjacent to the thymidine kinase (TK) selection marker. A cassette containing IRES2-eGFP and a LoxP-flanked neomycin selection marker was inserted into an Nhel site between the translation stop codon (TGA) and the polyadenylation signal of the egr2 gene. ES cell clones from 129 mice were electroporated and selected for Neomycin resistance. ES cell clones were verified for homologous insertion in the endogenous locus by PCR and southern blot with 5' and 3' probes. Mice were backcrossed to C57BL/6 for over 8 generations.

TIL isolation

Tumors were harvested from mice at the indicated time points. Tumors were dissociated through a 50 μm filter and washed with PBS. TILs were further enriched by layering Ficoll-Hypaque beneath the cell suspension followed by centrifugation without breaks for 30 min at 400 x g. The buffy-layer was isolated and washed twice with PBS before staining. For isolating specific cell populations by FACS, tumors were pooled when indicated and the

cell layer was re-purified by Ficoll-Hypaque centrifugation twice. For day 28 tumors, after Ficoll-Hypaque separation T cells were further purified by negative bead selection according to manufacturer's instructions (MagniSort, eBiosciences). Cells were then washed with PBS, stained at 4°C for 15 minutes before resuspending in complete DMEM (cDMEM: 10% FBS, 100U/mL Penicillin-Streptomycin, 1% MEM Non-Essential Amino Acids, 50 μM β-ME, 0.01M MOPS), and were sorted into either RLT lysis buffer (QIAGEN) or cDMEM depending on the experimental assay. Cells sorted into RLT buffer were put directly on dry ice as soon as the sort was finished.

Flow cytometry and antibodies

Cell suspensions were washed twice in PBS before staining an FACS buffer (10% FBS, 2mM EDTA, 0.001% NaN3). Cells were stained for 30 min on ice and fixed in 1% PFA. Antibodies against the following molecules were used: CD3 (17A2, AX700), 2B4 (2B4, FITC), CD127 (A7R34, PE), OX-40 (OX-86, PE), 4-1BB (17B5, Biotin, APC), CD160 (7H1, PE-Cy7), LAG-3 (C9B7W, PerCPeFluor710), PD-1 (RMP1-30, PE-Cy7), NRP1 (3E12, BV421), GITR (DTA-1, FITC), ICOS (7E.17G9, BV421), KLRG-1 (2F1, eF450, BV605), TIGIT (1G9, APC), TIM-3 (RMT3-23, PE), CD4 (RM4-5, BV605), CD45.1 (A20, FITC), CD45.2 (104, PE), CD8α (53-6.7, BV711). Fixable Viability Dye 506 (eBioscience) was used for live/dead discrimination. Staining of SIY-specific T cells was performed utilizing the SIYRYYGL-Pentamer (PE) (Proimmune); a SIINFEKL-pentamer (PE) was used as a non-specific control. All flow cytometric analysis was conducted on an LSRFortessa (BD) and analyzed using FlowJo software (Tree Star).

Quantitative real-time PCR

Total RNA was extracted from sorted cell populations using the RNEasy Micro Kit (QIAGEN) following the manufacturer's protocol. cDNA was synthesized using the High Ca-

pacity cDNA Reverse Transcription kit (Applied Biosystems) according to manufacturer's instructions. Transcript levels were determined using primer-probe sets (Table 3.2) developed through the online ProbeFinder Software and the Universal Probe Library (Roche) with the exception of IL-2 (Mm00434256_m1) and 18S (Hs99999901_s1). To minimize batch effect, when possible, all samples probed for a gene were run on the same 96-well qRT-PCR plate. All primer-probe sets either contained a primer spanning an exon-exon boundary or primers spanning an intron. Expression levels of transcripts were normalized to 18S expression.

In vivo proliferation assay

in vivo proliferation was measured by a BrdU pulse 24 hours prior to flow cytometric analysis. Each mouse received 0.8 mg BrdU injected i.p. on day 12 after tumor inoculation. TILs were isolated and surface stain was performed as described above. Following surface staining, cells were fixed and permeabilized using the Foxp3 staining kit (BD), according to manufacturer's protocol, and incubated with 100 µl PBS/DNase solution (300 µg/ml) for 30 minutes at 37°C. Cells were washed and incubated for 30 minutes at room temperature with anti-BrdU (FITC, Bu20a) and then washed with and resuspended in PBS.

In vitro stimulation assays

Tissue culture-treated 96-well round bottom plates were coated with anti-CD3ε (1 µg/ml; 2C11) in DPBS overnight at 4°C or for 2 hours at 37°C. Cells were sorted into cold cDMEM media and put on ice as soon as the sort was finished. Cells were then pelleted, resuspended in 50 µl cDMEM and incubated with soluble anti-CD28 (2 µg/ml; PV-1) for 10-12 hours for a final volume of 100 µl. After stimulation supernatants were removed for ELISA or bead-based immunoassay (LegendPlex), and cells were washed once with DPBS and resuspended in 25 µl of RNAlater Stabilization Solution (QIAGEN) or 300 µl of RLT buffer. Cells were stored at -80°C until RNA isolation was performed.

Protein quantification

Measurement of protein concentration was determined either by a standard ELISA or bead-based immunoassay (LEGENDplex, BioLegend). ELISAs were performed according to manufacturer's protocol (Ready-SET-Go ELISA; eBioscience) on supernatants from *in vitro* stimulations. Absorbance values were obtained at 450 nm using an Emax microplate reader (Molecular Devices) and IL-2 concentration was determined by standard curve. Protein concentration values were normalized to the number of sorted cells plated. LEGENDplex assays were performed according to manufacturer's protocols. IL-2 concentration was confirmed by both methods in separate experiments with no significant difference in IL-2 concentration between the two methods.

Spectratype analysis and sequencing

Mice were injected with 2x10^6 B16.SIY.dsRed tumor cells subcutaneously. 14 days later, tumors were harvested and specific $CD8^+$ TIL subpopulations were sorted into RLT buffer (QIAGEN) and immediately frozen. cDNA was synthesized from sorted cell populations and CDR3 regions were amplified by PCR with 21 different Vβ-5' primers paired with a FAM-Cβ1.1 primer (Table 3.1). Three VβPCR reactions did not reach significant amplification for analysis and were removed from the analysis. For sequencing, Cβ-VβPCR products were purified using the QIAquick PCR purification kit (QIAGEN) and sequenced at the University of Chicago Genomics Core Facility. Cβ-VβPCR products were analyzed by capillary electrophoresis at the University of Chicago Genomics core and CDR3 peaks were aligned using the Liz500 ladder. Spectratype graphs were displayed using the GeneiousR9 software [126]. To generate the frequency profile for each Vβ spectratype, the area under each peak was measured using peak studio (http://fodorlab.uncc.edu/software/peakstudio). The Hamming Distance [127] was calculated between each Vβ spectratype from each $CD8^+$ spleen and TIL population within a given mouse. To determine significance between the HD from

each comparison the HDs for each Vβ from 3 mice were averaged and a One-Way ANOVA with Dunn's correction for multiple comparisons was performed.

TCR transgenic T cell transfer experiments

Cell suspensions were generated from spleens and lymph nodes from congenic 2C/Rag2$^{-/-}$/CD45.1/2 and/or P14/Rag2$^{-/-}$/CD45.2 mice and T cells were purified by CD8^{+} negative selection (Miltenyi Biotechnologies) over magnetic columns according to the manufacturer's protocol. TCR Transgenic (Tg) T cells were washed with PBS, resuspended at a concentration of 10x10^{6}/ml and 1x10^{6} TCR Tg cells were adoptively transferred into CD45.1 tumor bearing mice by tail vein transfer in a volume of 0.1 mL. After indicated times, 2C T cells and corresponding host CD8^{+} T cells were sorted and stimulated as described above.

In vitro cytotoxicity assay

Per individual experiment, 10 C57BL/6 mice were injected s.c. with 2 x 10^{6} B16.SIY cells on both left and right flanks. On day 14, all 20 tumors were pooled and dissociated using the Tumor Dissociation Kit (Miltenyi Biotec) following the manufacturer's protocol. Tumor cell suspensions were washed 3-5 times with PBS and TILs were enriched for by Ficoll-Hypaque gradient centrifugation. TILs were stained, sorted and put directly on ice. TILs were titrated and added directly to a 96-well plate containing 50,000 P815 mastocytoma cells and 1 μg/mL anti-CD3ε. For a positive control, OT-I cells were isolated from OT-I/Rag2$^{-/-}$ mice and stimulated with plate-bound anti-CD3ε (0.25 μg/mL), anti-CD28 (2 μg/mL) and 100 U/mL IL-2 for 2-3 days. For a negative control, P815 cells were cultured alone or cultured with naïve CD8^{+} T cells isolated from lymph nodes. After 12 hours of incubation, cells were stained for Thy1, CD45, CD8α, Fixable Viability Dye 450 (eBioscience) and/or propidium Iodide.

Gene expression analysis

Total RNA for the $CD8^+$ TIL subpopulations was isolated following the manufacturer's protocol (RNEasy Micro Kit: QIAGEN) from sorted cells pooled from 10 mice. Samples were analyzed by the University of Chicago Genomics Facility using Illumina MouseRef8 microarray chips. Two experimental replicates were performed, and the results were log2 transformed and averaged. Probe sets that revealed a 1.5-fold difference abs(log2(ratio)$>$ 1.5)) relative to $CD8^+$4-1BB$^-$LAG-3$^-$PD-1$^-$ cells were identified and used for subsequent analysis. The microarray data are available in the Gene Expression Omnibus database (http://www.ncbi.nlm.nih.gov/gds) under accession number GSE79919. For cross-study comparisons, log2-fold change values were extracted using the GEO2R online software from the hypofunctional $CD8^+$ TIL data set, GSE79858 ((GSM2107353, GSM2107353 and GSM2107355) versus (GSM2107350, GSM2107351, GSM210732)) and the $CD8^+$ T cell exhausted data set, GSE41870 ((GSM1026819, GSM1026820, GSM1026821) versus (GSM1026786, GSM1026787, GSM1026788, GSM1026789)). Upregulated genes showing a 2-fold difference were used for analysis. Multiple genes names with from the GEO2R extracted data were identified and matched to gene names from the Illumina data set. The rank-rank hypergeometric overlap (RRHO) analysis [128] was conducted through the online software (http://systems.crump.ucla.edu/rankrank/index.php) and the associated Bioconductor package "RRHO" [129].

Gene ontology enrichment analysis

In a pair-wise fashion, shared upregulated genes (Supplementary Table 3) were used as the input for the ClueGO software with the Cytoscape application [130]. Both the Biological Process and Immune System Process Gene Ontology Annotations were used for analysis. Only pathways with a Bonferroni step down correction p-value > 0.01 were considered when generating pathway nodes. Non-redundant pathways with the greatest number of genes

found within each node were used.

Antibody and FTY720 treatments

Mice were treated i.p. with 100 μg/mouse of anti-4-1BB (Bio-X-Cell; LOB12.3) antibody and/or 100 μg/mouse anti-LAG-3 (Bio-X-Cell; C9B7W). For tumor outgrowth experiments, mice were treated on day 7, 10, 13 and 16 after tumor inoculation. For ex vivo functional experiments mice were treated on day 7, 10 and 13 and cells were sorted on day 14. For experiments blocking lymph node egress, 25 μg of FTY720 was given by gavage one day prior to first antibody treatment (day 6) and continued every day until endpoint on day 14.

Single cell cloning

Single cell sorting was performed using a FACS Aria II cell Sorter (BD Biosciences). Cells were sorted into single wells of a 96 well plate containing complete DMEM media. Visible colonies from single cells occurred after approximately 2 week. In a temporal sequential order, when single cell clones obtained confluence they were transferred to a 24 well plate and maintained until all single cell clones were acquired or until 18 clones from each single cell sort was obtained. Once achieved, all cell clones were trypsonized and re-seeded in the 24 well plate at approximately 100,000 to normalize cell numbers. After 1-2 days of expansion and cell clones were trypsonized and an aliquot of each clone was tested for disruption of the targeted gene through failure to upregulate H-2K^{b} and/or PD-L1 in response to IFN-γ. Responsiveness to IFN-γ was performed by plating cell clones in a 96 well plate and stimulating with murine IFN-γ (5 ng/mL) for 16-20 hours. Cell clones that exhibited disruption of the target gene were then sequentially expanded in a 100x15 cm^2 petri dish followed by an expansion in a 225cm^2 flask. Stocks of the cell lines were subsequently frozen and stored at -150°C

Lentiviral transduction and transfection

Individual single-guide RNA (sgRNA) expression vectors were constructed as follows. Forward and reverse 26-nt oligonucleotides (Table 5.1) were mixed at 10 mM each in 10 mM Tris-HCl (pH8.0) and 5 mM $MgCl_2$ in a total volume of 100 µl. The mixture was incubated at 95°C for 5 min and cooled to room temperature. The duplex oligonucleotides were then cloned into the BbsI site of pKLV-U6sgRNA(BbsI)-PGKpuro2ABFP (Addgene, #50946). sgRNA sequences targeting IFNγR2 and Jak1 were described previously [131]. To generate the sgRNA sequences for PD-L1 and H-2K^b, the online ATUM guide-RNA design tool was used (www.atum.bio/eCommerce/cas9/input).

The vector pLV-U6g-EPCG expressing Cas9 (Sigma) was used for stable transduction of Cas9. For transient transfection of Cas9, a vector containing Cas9 with a blasticidin resistance gene (Bsr) (a generous gift from Haouchu Huang, University of Chicago) or a Cas9-GFP vector (Sigma) was used.

Vector transfection was performed using Lipofectamine 3000 reagent (Thermo Fisher Scientific) according to the manufacturers protocol. For stable expression of sgRNAs or Cas9-GFP, HEK293T cells were cultured in complete DMEM without antibiotics at 50-70% confluence in a 6 well plate. HEK293T cells were then transfected with lipofectamine particles containing the target vector and a psPAX2 packaging vector (Addgene, #12260). Supernatant was collected and added to tumor cells at 48 and 56 hours after transfection. The day before viral supernatant collection, tumor cells were plated in a 24 well plate at 10,000 tumor cells per well. Cells were transduced with lentiviral supernatant from HEK293T cell culture with a 1:1000 dilution of polybrene (Sigma). At confluence, cells were transferred to a 100x15 cm^2 petri dish and expand for three days. After expansion cells were sorted based on GFP (Cas9) or BFP (sgRNA) expression.

Generation of mutant tumor cell lines

To establish a founder B16.SIY.dsRed tumor cell line, B16.SIY tumor cells were single cell sorted and the intensity of dsRed was measured for each B16.SIY founder line. Two B16.SIY.dsRed founder lines with similar dsRed expression to the polyclonal B16.SIY.dsRed population were engrafted into C57BL/6 mice and measured for tumor growth and responsiveness to anti-PD-L1/anti-CTLA-4 (BioXCell) checkpoint blockade therapy. To generate loss-of-function mutations in the IFNγR2 and Jak1 genes, the #9 B16.SIY.dsRed founder line was transduced with lentiviral supernatant from HEK293T cells with the corresponding sgRNA vectors. Cells were allowed to recover for 3 days and then transfected with the Cas9-Bsr vector. Cells were selected for resistance to blasticidin for 2 days and then single cell sorted based on BFP expression.

To generate IFNγR2 H-2K^{b} double-mutant cells, #9 B16.SIY cell line was first transfected with both Cas9-GFP (Sigma) and pKLV-U6-sgRNA(H-2K^{b})-PGKpuro2ABFP vectors. Cells were single cell sorted for BFP and GFP expression. Single cell clones were then tested for inability to upregulate H-2K^{b} in response to IFN-γ stimulation. One clone was chosen, expanded and transfected with Cas9-GFP and pKLV-U6-sgRNA(IFNγR2)-PGKpuro2ABFP vectors. Cells were single cell sorted and tested for the inability to upregulate PD-L1 in response to IFN-γ stimulation. The #9 B16.SIY IFNγR2 H-2K^{b} double mutant cell line was then transduced with the empty vector pKLV-U6-PGKpuro2ABFP to normalize BFP expression and allow for identification of the tumor cells when performing flow cytometry.

MC38 and B16F10 cells were transduced to stably express Cas9-GFP (Sigma: pLV-U6g-EPCG) and sorted 2-3 times for GFP expression. To generate loss-of-function mutations in the IFNγR2 and Jak1 genes, cells were transiently transfected with the corresponding pKLV-U6-sgRNA-PGKpuro2ABFP vectors and single cell sorted based on GFP and BFP expression and tested for disruption of the targeted gene by IFN-γ stimulation.

All cell lines were routinely tested for mycoplasma contamination using the HEKBlue

(InvivoGen) reporter cell line, following the manufacturer's protocol.

Part III

The EGR2 targets LAG-3 and 4-1BB describe and regulate dysfunctional antigen-specific CD8$^+$ T cells in the tumor microenvironment

Chapter 2

Introduction

Although the presence of tumor-infiltrating lymphocytes (TILs) indicates the generation of an endogenous antitumor immune response by the host, immune regulatory pathways can subvert the effector phase and enable tumor escape. Negative regulatory pathways include extrinsic suppression mechanisms but also a T cell-intrinsic dysfunctional state. Much of the literature on $CD8^+$ T cell dysfunction is derived from studies using chronic viral models. This type of dysfunction has been termed exhaustion, and is characterized by a gradual loss of cytokine production, proliferative capacity, and cytotoxicity. Concordant with a loss of function is an increase in expression of co-inhibitory receptors. One such receptor is PD-1 [132], which is upregulated during T cell activation and binds to two ligands, PD-L1 and PD-L2 [133]. Blockade of PD-1/PD-L1 interaction with an anti-PD-L1 antibody can restore the function of a subset of exhausted $CD8^+$ T cells [134]. PD-1 is also expressed on $CD8^+$ TILs, and anti-PD-1/anti-PD-L1 blockade therapy, has produced durable clinical responses in a variety of malignancies [103], likely through the release of inhibitory effects mediated by PD-1 on tumor antigen-specific $CD8^+$ T cells. Despite the unparalleled success of PD-1 blockade therapy, only a subset of patients are cured or experience long-lasting stable disease. This has led to intense investigation to understand the biological state of $CD8^+$ TILs in the context of failed tumor control, with one aim being to identify additional targetable receptors expressed on tumor antigen-specific $CD8^+$ TILs.

Two methods are generally used to identify and characterize tumor antigen-specific $CD8^+$ T cells: staining and sorting bulk tumor suspensions with peptide-MHC multimers, or *in vitro* expansion of T cells from sorted $CD8^+$ TIL subpopulations. Both methods induce T cell stimulation, which could alter downstream functional analyses. Nonetheless, these approaches have revealed important insights into the phenotypic characteristics of tumor antigen-specific $CD8^+$ TILs. Studies using peptide-MHC multimer staining found high expression of PD-1 on MART-1- [86, 135] or NY-ESO-1-specific [136] $CD8^+$ T cells isolated

from human tumors. In addition to PD-1, work from Speiser and colleagues [90, 137] demonstrated that tumor antigen-specific $CD8^+$ T cells isolated from tumor infiltrated lymphnodes, can co-express multiple co-inhibitory receptors, including TIM-3, LAG-3, 2B4, and BTLA. *In vitro* expansion of sorted $CD8^+$ TIL subpopulations expressing PD-1, LAG-3, or TIM-3 revealed that any of these markers could identify the majority of tumor-reactive $CD8^+$ T cells [138]. Furthermore, inclusion of 4-1BB expression enriched for tumor-reactive $CD8^+$ T cells [138, 139]. These studies promoted the idea that antibody-mediated interference of multiple co-inhibitory receptors may act synergistically to alleviate suppression of tumor antigen-specific $CD8^+$ TILs. Interference of PD-1 in combination with LAG-3 [140] or TIM-3 [136] was able to improve NY-ESO-1-specific $CD8^+$ TIL function *in vitro* and induce robust tumor control in preclinical models [141, 114]. In addition, an attractive approach is to agonize co-stimulatory receptors expressed on tumor antigen-specific $CD8^+$ TILs, such as 4-1BB, while simultaneously blocking co-inhibitory receptors, which may provide augmented T cell stimulation needed to overcome the suppressive effects of co-inhibitory receptors [117]. These studies highlight the general idea that multiple targetable receptors are expressed on tumor antigen-specific $CD8^+$ TILs, however, a comprehensive analysis of the cell surface receptors characterizing dysfunctional tumor antigen-specific TILs has been lacking, which may reveal new therapeutic targets.

Based on chronic viral models and the fact that tumors progress despite a $CD8^+$ T cell infiltrate, it is predicted that $CD8^+$ TILs are in a dysfunctional state similar to T cell exhaustion. However, studies interrogating $CD8^+$ TIL function in cancer patients have revealed conflicting results, mainly surrounding the ability of $CD8^+$ TILs to produce IFN-γ. The capacity to produce IFN-γ is an important readout in models of T cell exhaustion, as the inability to do so is a characteristic terminally differentiated T cells that are not likely to be rescued by PD-1 blockade therapy [84]. By cell sorting Melan-A-specific $CD8^+$ TILs followed by *ex vivo* stimulation, one study found that IFN-γ production was lost [90], yet, in another study, IFN-γ production was maintained [142]. It was proposed that only a subset of

tumor antigen-specific $CD8^+$ TILs enter into an exhausted-like state, which may be identified by expression of PD-1. Melan-A-specific PD-1^+ $CD8^+$ TILs were shown to lack IFN-γ production [86], however, in another study NY-ESO-1-specific PD-1^+ $CD8^+$ TILs retained IFN-γ, and instead the TIM-3^+PD-1^+ fraction was found to produce less IFN-γ [136], albeit IFN-γ production was not completely lost in this population. These studies are convoluted by the use of peptide-MHC multimers, which can alter T cell function. In a different approach, co-expression of PD-1 and CTLA-4 was used to identity antigen-specific $CD8^+$ TILs, and PD-1^+CTLA-4^+ $CD8^+$ TILs were found to retain IFN-γ production [143]. These differing results may be a reflection of the variable nature of the tumor microenvironment. It is possible that each individual tumor exerts different pressures and stresses on $CD8^+$ TILs resulting in different functional characteristics. Alternatively, it may be that the methods used to identify and extract tumor antigen-specific $CD8^+$ TILs alter T cell function, thereby confounding results. Therefore, to aid in the development of new therapeutic approaches, new strategies are needed to identify tumor antigen-specific $CD8^+$ TILs with minimal manipulation in order to accurately measure their function.

Recently, our laboratory identified the transcription factor Egr2 as a critical regulator of the anergic state in $CD4^+$ T cell clones [122, 144]. Egr2 is also involved in negative regulation of T cell activation in several *in vivo* model systems [145]. Egr2 contributes to upregulation of DGK-α and -ζ which act to blunt TCR-mediated Ras pathway activation [93]. By comparing gene expression profiling of anergized cells along with Egr2 ChIP-Seq analysis, we identified multiple additional Egr2-driven gene targets, including Tnfrsf9 (4-1BB) and Lag3, which encode cell surface proteins. We reasoned that flow cytometric analysis for expression of these and other Egr2 targets may identify the subset of T cells with a dysfunctional state in the tumor microenvironment.

In this study, based on the hypothesis that coexpression of 4-1BB and LAG-3 might define dysfunctional T cells in tumors, we investigated the functional characteristics of $CD8^+$ TILs expressing 4-1BB and LAG-3 using mouse tumor models. We found that the co-

expression of 4-1BB and LAG-3 effectively identified tumor antigen-specific, dysfunctional $CD8^+$ TILs enriched in the expression of Egr2 target genes. Functionally, 4-$1BB^+$LAG-3^+ $CD8^+$ TILs failed to secrete IL-2 after *in vitro* stimulation, yet still produced IFN-γ and Treg cell-recruiting chemokines and lysed target cells *ex vivo*, arguing they are not completely functionally inert. Combinatorial treatment of tumor-bearing mice with anti-LAG-3/anti-4-1BB antibodies restored the function of these T cells, and promoted *in situ* accumulation of KLRG-1^{hi} effector cells. Additional gene expression profiling provided a complete phenotyping of this T cell subset, which revealed expression of a broad array of both inhibitory and co-stimulatory receptors. These approaches have enabled the characterization of the population of tumor antigen-specific $CD8^+$ T cells that arise specifically within the tumor microenvironment having altered functional properties, and have highlighted new targets for novel immunotherapeutic approaches to restore desired functionality and promote tumor regression.

Sections of this chapter were published in the Journal of Experimental Medicine [19] and have been reproduced with permission from the copyright holder.

Chapter 3

Results

3.1 4-1BB and LAG-3 identify a major population of CD8$^+$ TILs

To determine whether 4-1BB and LAG-3 could accurately identify tumor antigen-specific dysfunctional CD8$^+$ TILs, we examined the expression pattern of LAG-3 and 4-1BB using the well-characterized B16.SIY model of melanoma. On day 7 following tumor inoculation, the 4-1BB$^+$ LAG-3$^+$ population comprised 15.8% of all CD8$^+$ TILs. The frequency of this population significantly increased to 44% by day 21. The frequency of 4-1BB$^-$ LAG-3$^+$ (4$^-$ L$^+$) population also increased 1.9-fold from day 7 to day 14 to comprise 25% of the CD8$^+$ TIL compartment. In contrast, the frequency of the 4-1BB$^-$ LAG-3$^-$ (4$^-$L$^-$) population decreased by 2.7-fold by day 21. Since there was no significant increase in the proportion or number of 4-1BB$^+$LAG-3$^-$ CD8$^+$ TILs within the time frame of the experiment (Figure 3.1A and B) this population was not studied further. Similar patterns were seen when analyzing absolute numbers of cell subsets (Figure 3.1C and D). Acquisition of these phenotypes was specific for the tumor microenvironment, as they were not observed in the spleen or tumor-draining lymph node (TdLN) (Figure 3.1A). These data suggest that the tumor microenvironment preferentially supports the induced co-expression of 4-1BB and LAG-3.

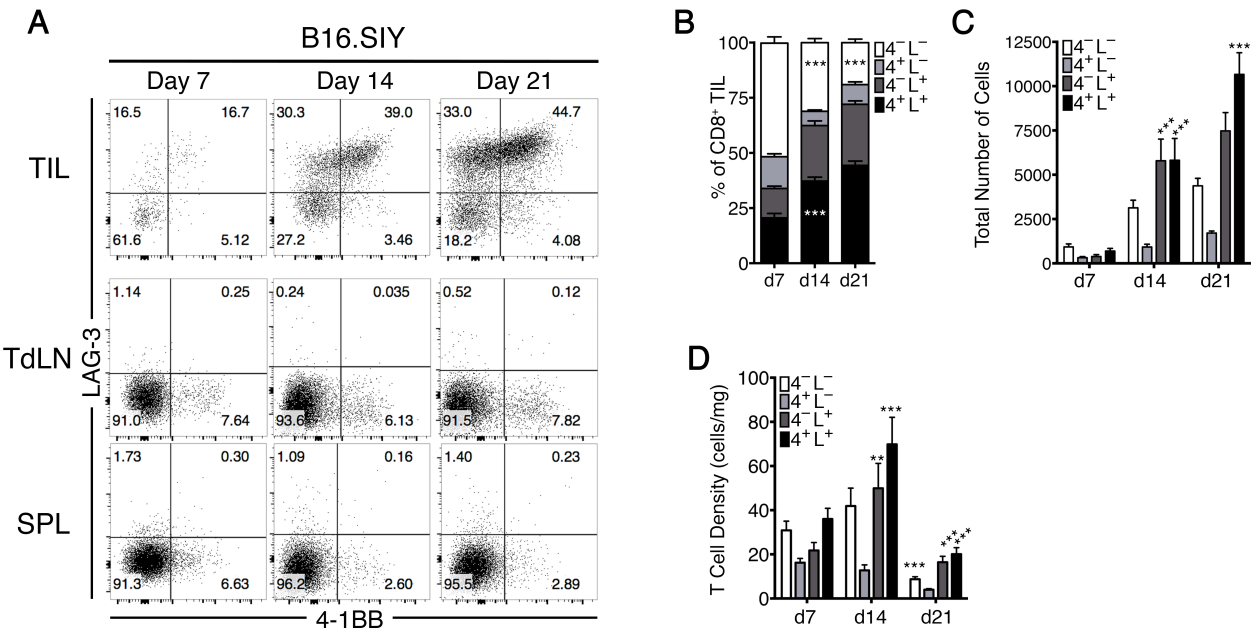

Figure 3.1: Co-expression of 4-1BB and LAG-3 identifies a significant fraction of the CD8$^+$ TIL compartment
(A) Representative analysis of 4-1BB and LAG-3 expression on CD8$^+$ T cells from B16.SIY tumors and the spleen and TdLN from tumor bearing mice on day 7, 14 and 21 after s.c. tumor inoculation. (B-D) Longitudinal summary of the composition, n=5; four to five independent experiments per time point, (C) absolute cell number, n=5; seven to nine independent experiments per time point, and (D) cellular density of the CD8$^+$ 4-1BB/LAG-3 TIL subpopulations, n=5; two to five independent experiments per time point. Absolute cell numbers were determined by acquiring the complete tumor sample by flow cytometery. *P$<$0.05, **P$<$0.01, ***P$<$0.001 A two-way ANOVA with Bonferroni post-hoc test was used for (B, C, D).

The selective increase in cell numbers and proportional shift towards the 4-1BB$^-$ LAG-3$^+$ and 4-1BB$^+$ LAG-3$^+$ populations during tumor progression suggested that expansion of these populations was occurring within the tumor microenvironment. To investigate this possibility, CD8$^+$ TILs were stained for Ki67 at day 14 after tumor inoculation and analyzed by flow cytometry. In fact, 81% of 4-1BB$^-$ LAG-3$^+$ cells and 85% of 4-1BB$^+$ LAG-3$^+$ cells were Ki67$^+$ compared to only 32% of the 4-1BB$^-$ LAG-3$^-$ TILs (Figure 3.2A). To further investigate this process, mice were pulsed with BrdU on day 12, and 24 hours later the CD8$^+$ TIL subpopulations were analyzed for BrdU incorporation. Indeed, the 4-1BB$^-$ LAG-3$^+$ and 4-1BB$^+$ LAG-3$^+$ populations incorporated more BrdU compared to the 4-1BB$^-$

LAG-3$^-$ population (Figure 3.2B). These data suggest that once CD8$^+$ T cells arrive at the tumor site, a fraction of TILs expands within the tumor, and that these expanding TILs can be identified by increased expression of 4-1BB and LAG-3.

To determine if upregulation of LAG-3 and 4-1BB was simply a product of the B16.SIY tumor model or if it is a more general feature of CD8$^+$ T cells within tumors, we analyzed T cells from four additional progressively growing tumor models, C1498.SIY, MC38.SIY, EL4.SIY and B16F10 parental. TILs were analyzed for expression of 4-1BB and LAG-3 at day 14. We found that the pattern of expression was similar to that seen in CD8$^+$ TILs isolated from B16.SIY tumors (Figure 3.2C and E). The results from the B16F10 parental tumor confirm that presence of SIY is not required to see co-expression of 4-1BB and LAG-3. In order to determine whether the 4-1BB$^+$ LAG-3$^+$ TIL subset was generated only in progressing tumors or also in tumors that were rejected, we analyzed T cell phenotypes in the 1969.SIY and MC57.SIY fibrosarcoma tumor models, which are more immunogenic and undergo spontaneous rejection. Interestingly, distinctly fewer 4-1BB$^+$ LAG-3$^+$ cells were found among the CD8$^+$ TIL compartment in the 1969.SIY and MC57.SIY tumors (Figure 3.2D and E). Over time, co-expression of 4-1BB and LAG-3 was maintained in B16.SIY tumors but not MC57.SIY tumors (Figure 3.2F). These data suggest that the acquisition of the 4-1BB$^+$ LAG-3$^+$ TIL phenotype preferentially occurs within the tumor microenvironment and only upon conditions of tumor progression rather than regression.

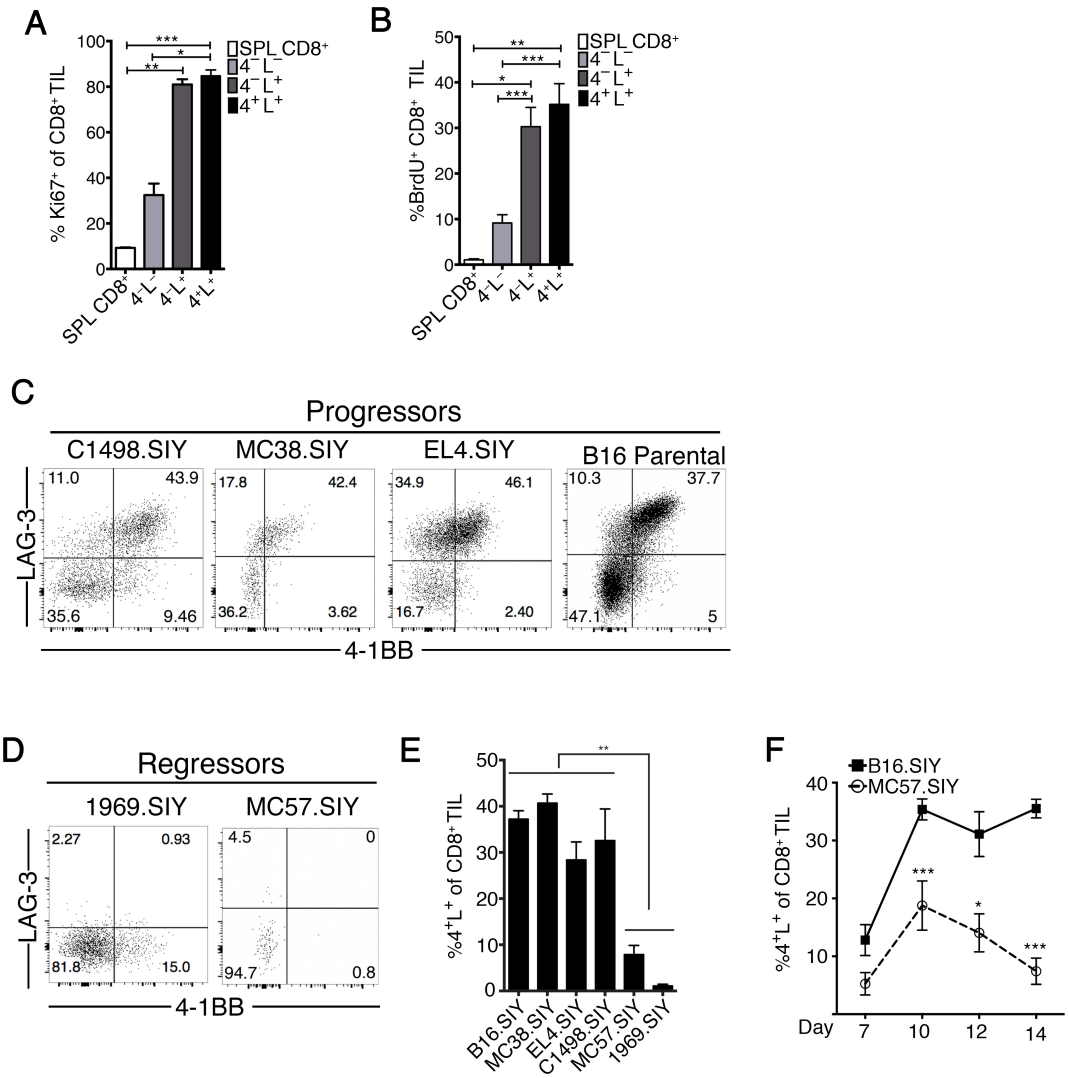

Figure 3.2: Co-expression of 4-1BB and LAG-3 identifies a significant fraction of the CD8$^+$ TIL compartment found in progressing but not regressing tumors (A) Day 14 summary of the proportion of the CD8$^+$ 4-1BB/LAG-3 TIL subpopulations that are Ki67$^+$. n=3-5; two independent experiments. (B) Summary of BrdU uptake on day 13 in the CD8$^+$ 4-1BB/LAG-3 TIL subpopulations after a 24 hour BrdU pulse. n=5; three independent experiments. (C-E) Representative flow plots (C and D) and summary (E) of the 4-1BB/LAG-3 populations in other tumor models. Mice were inoculated with 2x10^6 C1498.SIY, MC38.SIY, EL4.SIY, B16 Parental, MC57.SIY or 1969.SIY subcutaneously and analyzed for 4-1BB and LAG-3 expression on day 14 after tumor inoculation. n=3-5; two to 5 independent experiments for each time point. (F) Mice were inoculated on both flanks with 2x10^6 MC57.SIY or B16.SIY, at indicated time points tumors from each mouse were pooled and analyzed for co-expression of 4-1BB and LAG-3 in the CD8$^+$ TIL compartment. n=3-5; two independent experiments for each time point. All error bars indicate mean SEM. *:P < 0.05, **:P0.01, ***:P < 0.001. A two-way ANOVA with Bonferroni post-hoc test was used for (F) and Kruskal-Wallis (non-parametric) test was used for (A, B, E) analysis at one time-point.

3.2 $CD8^+4\text{-}1BB^+LAG\text{-}3^+$ TILs express Egr2 and multiple Egr2 targets

Based on previous studies describing Egr2 as a critical regulator of T cell activation *in vitro* and *in vivo* [145, 146, 147] accompanied by our previous finding that Egr2 regulates the expression of 4-1BB and LAG-3 in an *in vitro* model of anergy [144], we investigated whether Egr2 expression itself was also characteristic of T cells within the $CD8^+$ TIL compartment. To this end we utilized an Egr2-IRES-GFP (Egr2GFP) knock-in reporter mouse. Approximately 14% of all $CD8^+$ TILs were GFP^+ on both day 7 and day 14 (Figure 3.3A). To confirm that Egr2 is faithfully reported we sorted $CD8^+$ TILs expressing high and low levels of EGFP and subsequently screened for Egr2 and several Egr2 targets by qRT-PCR. The Egr2-GFP^{hi} population expressed greater levels of Egr2 and many Egr2-target genes previously defined using *in vitro* anergy models. These include *Tnfrsf9, Lag3, Ngn, Sema7a, Crtam, Ccl1 and Nrn1* (Figure 3.3B). Expression of 4-1BB and LAG-3 in the Egr2-GFP^{hi} $CD8^+$ TILs was confirmed by flow cytometry. The majority of Egr2-GFP^{hi} cells expressed LAG-3 and/or 4-1BB. The $Egr2GFP^{lo}$ cells also showed expression of 4-1BB and LAG-3 on a subpopulation at day 14 (Figure 3.3C). This result suggests either that $CD8^+$ TILs expressing Egr2 encompass only a subset of the TILs expressing LAG-3 and/or 4-1BB, or that Egr2 is transiently expressed and is subsequently downregulated after the induction of LAG-3 and 4-1BB.

Using previously identified Egr2 target genes [144], we examined the Egr2-driven transcriptional program in sorted $4\text{-}1BB^-LAG\text{-}3^-$ and $4\text{-}1BB^+LAG\text{-}3^+$ cells by qRT-PCR. Of the 43 Egr2 target genes examined, 10 showed detectably increased expression in $4\text{-}1BB^+LAG\text{-}3^+$ population, while expression of a similar subset of genes was increased in the $4\text{-}1BB^-LAG\text{-}3^+$ population (Figure 3.3D). Collectively, these data show that Egr2 is expressed in a subpopulation of $CD8^+$ TILs expressing LAG-3 and/or 4-1BB, and that a subset of known Egr2 targets was detected in these larger T cell populations as a whole.

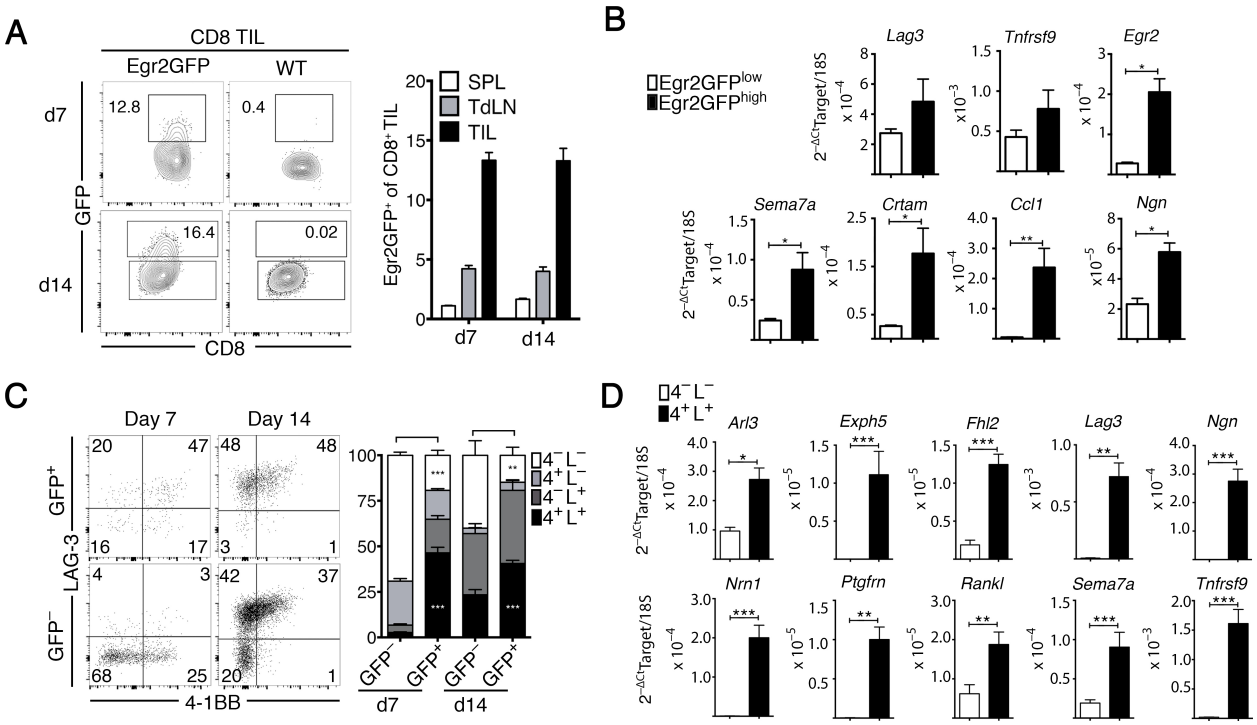

Figure 3.3: Egr2 and a component of the Egr2-transcriptional network are enriched in 4-1BB$^+$LAG-3$^+$ CD8$^+$ TILs

(A) Representative flow plot and summary of Egr2EGFP expression. Egr2EGFP mice were inoculated with 2x10^6 B16.SIY tumors s.c. CD8$^+$ T cells from the tumor, TdLN and spleen were analyzed for Egr2EGFP expression on day 7 and day 14. n=4-5; two-independent experiments. (B) Expression of Egr2 target genes [144]. CD8$^+$ TILs from day 14 tumor bearing mice were sorted based on high or low expression of Egr2EGFP and analyzed directly for expression of Egr2 targets by qRT-PCR. Two tumors on opposite flanks pooled per mouse. n=3; two independent experiments. (C) Representative flow plots and summary of the 4-1BB/LAG-3 subpopulations in CD8$^+$ Egr2GFP^{hi} and Egr2GFP^{lo} TILs on day 7 and 14. n=4-5. Two-independent experiments per time point. (D) Expression of Egr2 targets in the 4-1BB$^+$LAG-3$^+$ and 4-1BB$^-$LAG-3$^-$ subpopulations. The subpopulations were sorted and analyzed directly for the expression of targets by qRT-PCR. Two tumors on opposite flanks pooled per mouse. n=4; two-independent experiments. *:P < 0.05, **:P$<$0.01, ***:P$<$0.001. A two-way ANOVA with Bonferroni post-hoc test was used for longitudinal studies (A and C) and a Mann-Whitney test was used to compute significance in (B, D).

3.3 Egr2 contributes to initial expression of LAG-3 and 4-1BB after T cell entry into the tumor microenvironment

We next examined whether Egr2 was required for expression of LAG-3 and 4-1BB among $CD8^+$ TILs *in vivo*. To this end we utilized $Egr2^{flox/flox}$ X pLCK-CreERT2 x ROSA-YFP mice, in which after oral tamoxifen administration a fraction of the $CD8^+$ T cells delete Egr2 and express YFP (Figure 3.4A). This allowed us to compare both Egr2-sufficient (YFP^-) and Egr2-deficient (YFP^+) $CD8^+$ within the same tumor. To determine that Egr2 was in fact deleted from the YFP^+ fraction, we sorted both YFP^+ and YFP^- $CD8^+$ TILs and measured Egr2 transcripts directly ex vivo and upon restimulation. As expected, the YFP^+ $CD8^+$ TILs expressed substantially less Egr2 transcripts compared to the YFP^- counterparts (Figure 3.4A). To determine if Egr2 is required for 4-1BB and LAG-3 expression we analyzed $CD8^+$ TILs at day 7 and 14 after tumor inoculation and compared the YFP^+ and YFP^- populations to mice not treated with tamoxifen. Indeed, at day 7, the YFP^+ fraction expressed less 4-1BB and LAG-3 compared to the YFP^- population and the WT $CD8^+$ TILs. However, expression of 4-1BB and LAG-3 was not significantly different at day 14 (Figure 3.4B). This suggests that other transcriptional regulators may compensate and contribute to the expression of LAG-3 and 4-1BB.

Egr3 has been shown to have overlapping function with Egr2 [147] and HIF1α can contribute to 4-1BB expression [148]. To investigate whether these transcription factors may compensate for 4-1BB and/or LAG-3 expression we sorted $Egr2GFP^{hi}$ and $Egr2GFP^{lo}$ $CD8^+$ TILs expressing 4-1BB and LAG-3 on day 7 and analyzed expression of Egr3 and HIF1α by qRT-PCR. Egr3 and HIF1α were indeed expressed in both the $Egr2GFP^{hi}$ and $Egr2GFP^{lo}$ populations. We confirmed differential expression of Egr2 and CCL1 between the $Egr2GFP^{hi}$ and $Egr2GFP^{lo}$ populations to assure sort purity (Figure 3.4C). Together, these data indicate that Egr2 contributes to upregulation of 4-1BB and LAG-3 expression at early time points, but that other transcriptional regulators may compensate and drive expression of

LAG-3 and 4-1BB as the T cell-tumor interaction progresses.

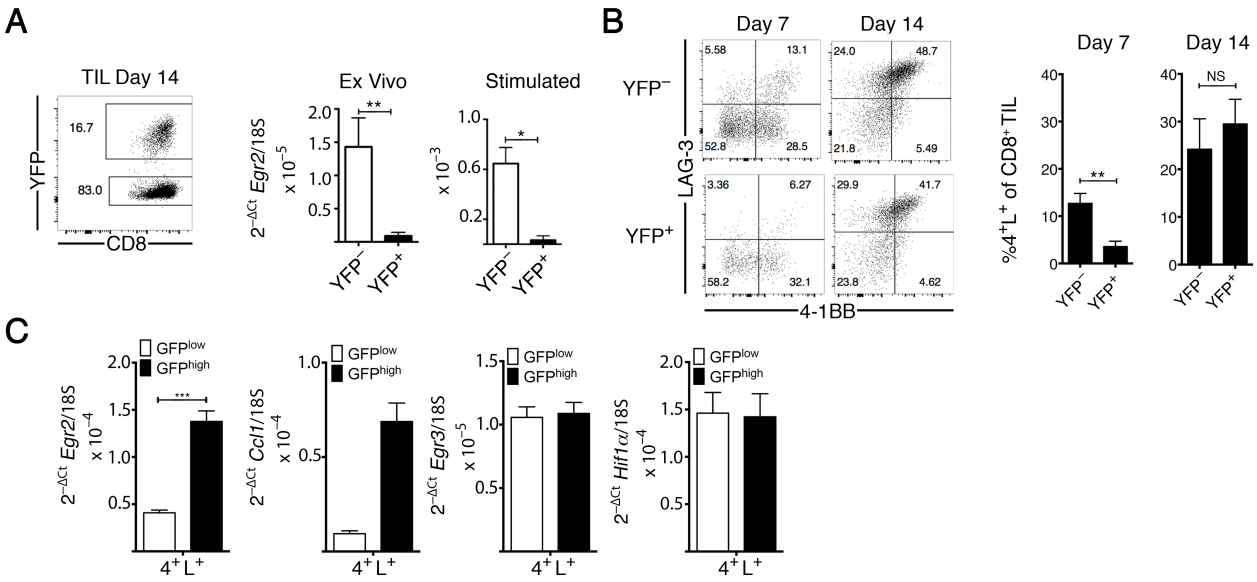

Figure 3.4: Egr2 regulates early expression of 4-1BB and LAG-3 in CD8$^+$ TIL
(A) Egr2$^{flox/flox}$ x pLCKCreERT2 x YFP-Rosa26 mice given 5 doses of tamoxifen by gavage and inoculated 3 days later with 2x10^6 B16.SIY cells. YFP$^+$ or YFP$^-$ CD8$^+$ TILs were sorted and analyzed for Egr2 transcript directly and after *in vitro* stimulation. Two tumors on opposite flanks pooled per mouse. n=3; two independent experiments. (B) Representative flow plots and summary of 4-1BB/LAG-3 co-expression in YFP$^+$ or YFP$^-$ CD8$^+$ TILs on day 7 and 14. n=3; two independent experiments. (C) Expression of Egr3 and Hif1α in Egr2GFP^{hi} and Egr2GFP^{lo} from day 7 CD8$^+$ TILs isolated from Egr2GFP mice. n=5; two-independent experiments. Error bars indicate mean SEM. *:P $<$ 0.05, **:P$<$0.01, ***:P$<$0.001. A Mann-Whitney test was used to compute significance in (A,B,C)

3.4 CD8$^+$4-1BB$^+$LAG-3$^+$ TILs are oligoclonal

Not all T cells in the tumor microenvironment are specific for tumor-associated antigens, as memory T cells specific for irrelevant antigens are often found among TILs, and non-specific T cell trafficking has been documented *in vivo* [149]. We hypothesized that the 4-1BB$^+$LAG-3$^+$ CD8$^+$ TILs are tumor antigen-specific because LAG-3, 4-1BB and Egr2 are upregulated after TCR stimulation and our initial characterization suggested that this population expands within the tumor microenvironment *in situ*. To test this hypothesis, three complementary techniques were employed. First, we isolated the CD8$^+$ TILs based on LAG-3 and 4-1BB expression by cell sorting and performed TCRβ spectratype analysis. Compared to the 4-1BB$^-$LAG-3$^-$ TILs and CD8$^+$ splenocytes, the 4-1BB$^+$LAG-3$^+$ TILs had a non-Gaussian distribution and shared one or two dominant peaks (Figure 3.5A). Analysis of several Vβs displaying one dominant peak revealed that Vβ7 contained a single CDR3β sequence shared between the 4-1BB$^-$LAG-3$^+$ and 4-1BB$^+$LAG-3$^+$ populations, indicating a clonal relationship (Figure 3.5A). To measure the oligoclonality of the CDR3β repertoires, the Hamming Distance (HD) was calculated for each Vβ between the CD8$^+$ TIL subpopulations and the splenic CD8$^+$ population within three separate mice (Figure 3.6). By transforming each spectratype into area under the curve frequency profiles, the HD computes the changes in frequency and reports a value of comparison between 0 and 1, with 0 indicating a completely identical frequency profile and 1 signifying a completely discordant profile. As a control, we calculated the HD of the splenic CD8$^+$ populations between different mice (Figure 3.5B, black bar). Since the splenic CD8$^+$ spectratypes are largely Gaussian this value represents the HD between two similar distributions. Analysis of the HD between the CD8$^+$ TIL subpopulations revealed that the 4-1BB$^+$LAG-3$^+$ and 4-1BB$^-$LAG-3$^+$ but not the 4-1BB$^-$LAG-3$^-$ CDR3β distributions are significantly different (less Gaussian) compared to the splenic CD8$^+$ population (Figure 3.5B). These data indicate that the 4-1BB$^+$LAG-3$^+$ and 4-1BB$^-$LAG-3$^+$ populations are oligoclonal expanded subsets of TILs, suggesting likely antigen specificity in these subpopulations.

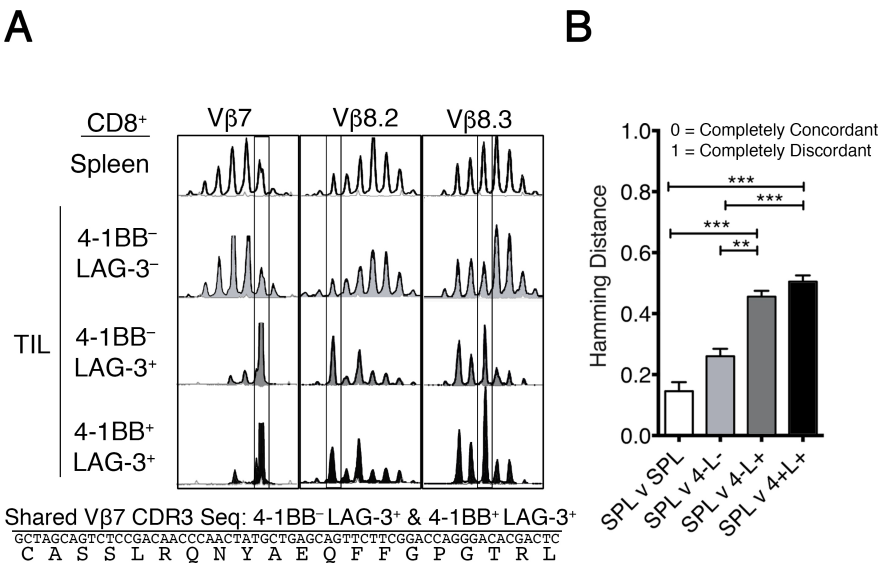

Figure 3.5: CD8$^+$4-1BB$^+$LAG-3$^+$ TILs have a skewed CDR3β repertoire
Co-expression of 4-1BB and LAG-3 identifies tumor antigen-specific TILs in progressing tumors. (A) Representative CDR3β distributions from the different 4-1BB/LAG-3 subpopulations and CD8$^+$ T cells isolated from the spleen. Boxed regions represent dominant peaks in the 4-1BB$^+$LAG-3$^+$ CD8$^+$ TIL subpopulation. (B) As a measure of skewness, the Hamming Distance (HD) for each Vβ spectratype was calculated between each TIL subpopulation and CD8$^+$ T cell spleen population within the same mouse. As a control the HDs from CD8$^+$ splenocyte populations between mice (grey bar) were calculated. *:P $<$ 0.05, **:P$<$0.01, ***:P$<$0.001 A Kruskal-Wallis (non-parameteric) test was used for (B) spectratype analysis.

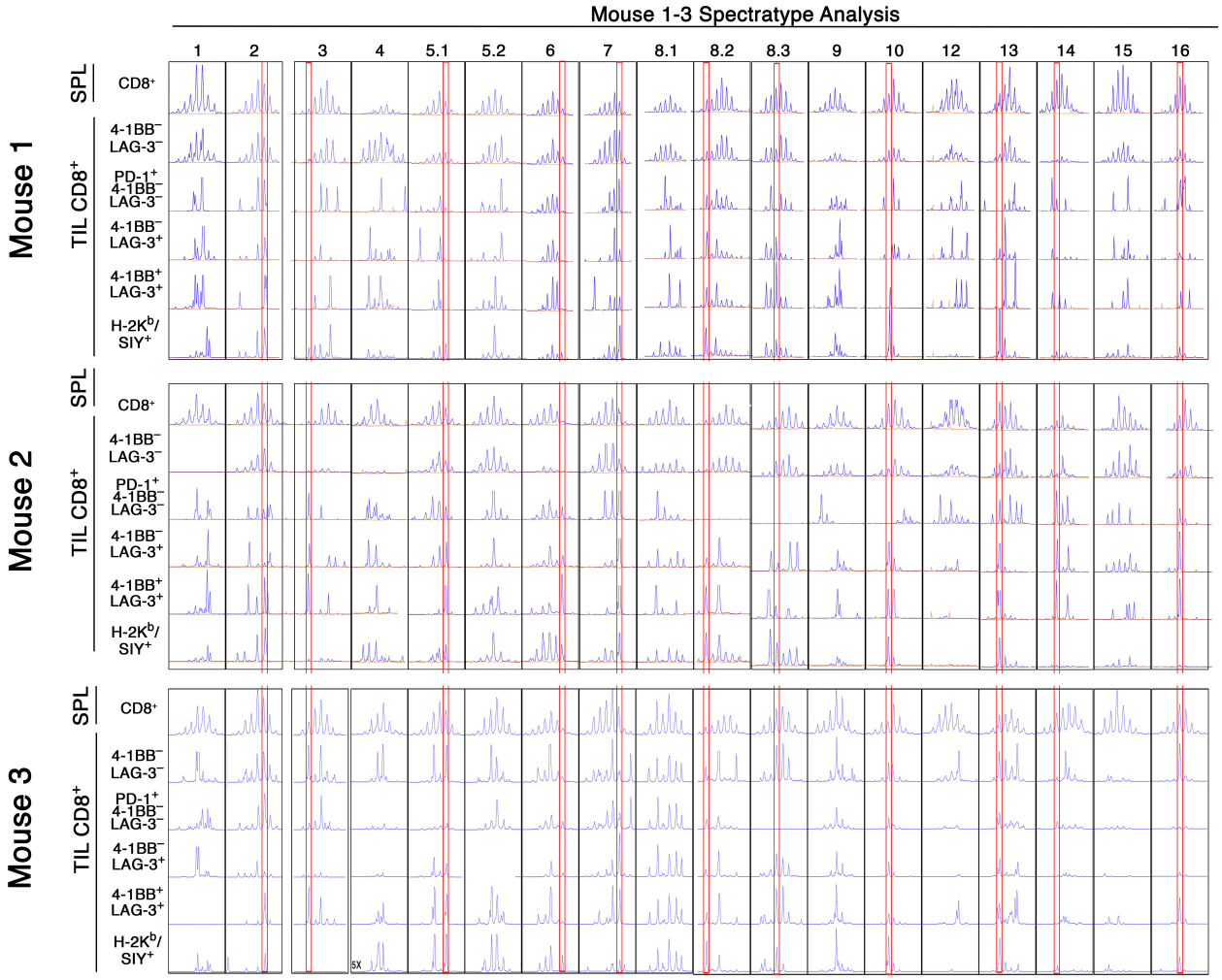

Figure 3.6: Spectratype Analysis of different CD8$^+$ TIL populations
CDR3β distributions in three mice of the different 4-1BB/LAG-3 subpopulations from the tumor and spleen and the H-2K^b/SIY$^+$ CD8$^+$ TILs. Boxed regions represent dominant peaks

3.5 H-2K^b/SIY-specific CD8$^+$ TILs are enriched for 4-1BB and LAG-3 expression in progressing tumors

As a second approach, we utilized the B16.SIY melanoma and MC38.SIY adenocarcinoma models and monitored CD8$^+$ T cells specific for the H-2K^b-restricted SIY epitope (SIYRYYGL). SIYRYYGL/K^b pentamer$^+$ (H-2K^b/SIY) cells were found in expanded numbers within B16.SIY and MC38.SIY tumors at day 14 after tumor inoculation (Figure 3.7A). Nearly 47% of the H-2K^b/SIY$^+$ cells expressed both 4-1BB and LAG-3, in contrast to 32% of the H-2K^b/SIY$^-$ population (Figure 3.7A and C). This enrichment of antigen-specific CD8$^+$ TILs in the 4-1BB$^+$LAG-3$^+$ populations suggests that these markers identify tumor antigen-specific TILs. The H-2K^b/SIY$^-$ cells also contained significant numbers of 4-1BB$^+$LAG-3$^+$ cells, which is consistent with the notion that tumor antigens other than SIY are also recognized by subsets of CD8$^+$ TILs *in vivo* (Figure 3.7C). H-2K^b/SIY$^+$ cells in the spleen (not shown) or TdLN did not co-express 4-1BB and LAG-3, indicating that this phenotype is acquired within the tumor microenvironment.

We also analyzed these features in the context of tumor antigen-specific CD8$^+$ TILs in two spontaneously rejected tumor models. To this end we evaluated H-2K^b/SIY-specific CD8$^+$ TILs cells from MC57.SIY and 1969.SIY tumors. At day 14 after tumor inoculation, approximately 5% of the H-2K^b/SIY-specific CD8$^+$ TILs were found in the 4-1BB$^+$LAG-3$^+$ fraction. As with the B16.SIY tumors, no H-2K^b/SIY-specific CD8$^+$ T cells co-expressed 4-1BB and LAG-3 in the TdLN or spleen (not shown) (Figure 3.7B). Unlike the B16.SIY and MC38.SIY tumors, no significant enrichment of 4-1BB$^+$LAG-3$^+$ H-2K^b/SIY-specific CD8$^+$ TILs was observed in these regressor tumors (Figure 3.7B and C). These data suggest that tumor antigen specificity per se does not determine dysfunctionality, and that this is a feature unique to the microenvironment of progressing tumors.

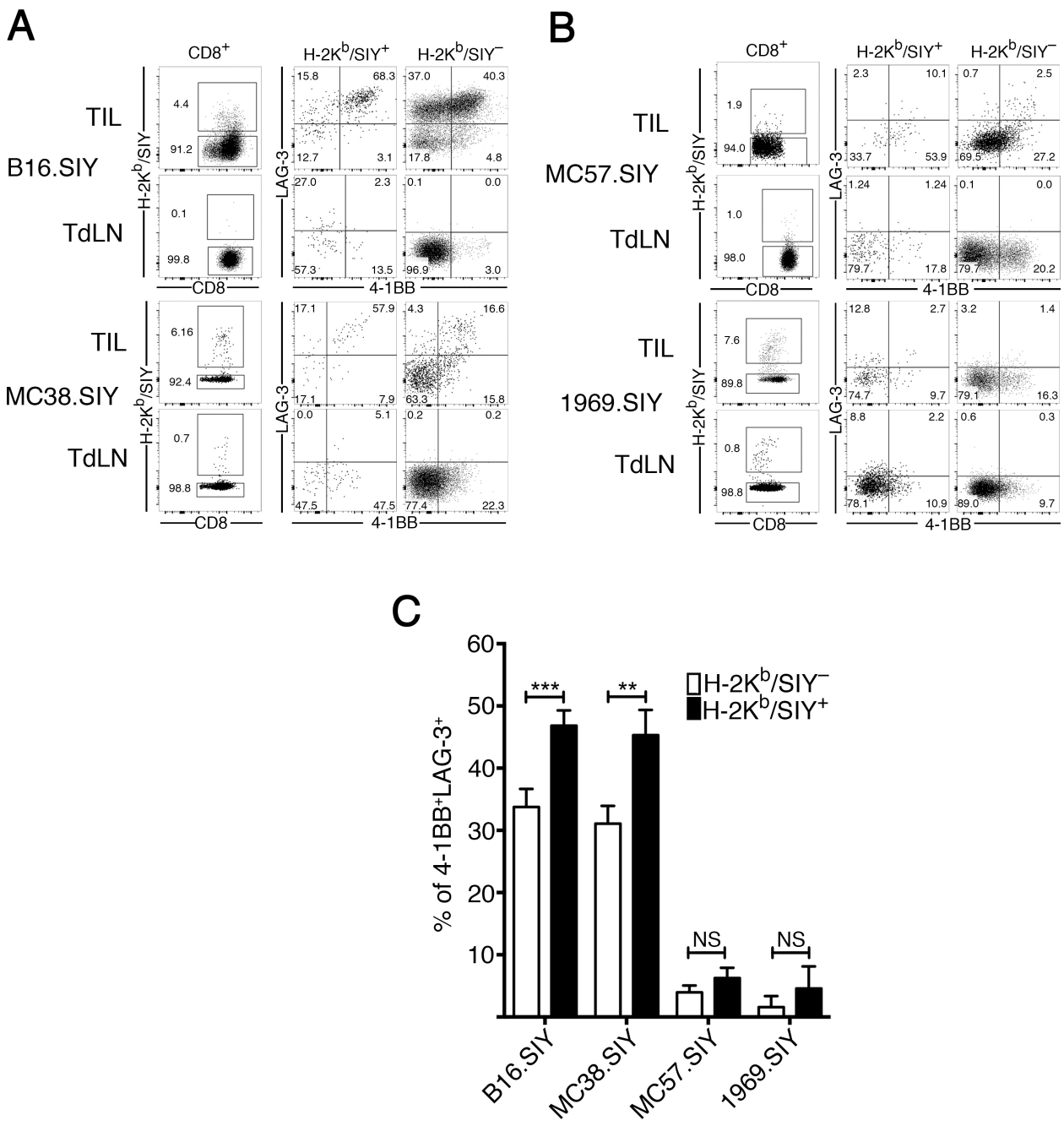

Figure 3.7: H-2K^b/SIY-specific CD8$^+$ TILs in progressing but not regressing tumors express 4-1BB and LAG-3

(A and B) Representative flow analysis of the 4-1BB/LAG-3 subpopulation in H-2K^b/SIY$^+$ and H-2K^b/SIY$^-$ CD8$^+$ TILs on day 14 after B16.SIY and MC38.SIY or (B) MC57.SIY and 1969.SIY tumor inoculation. n=3-4; three to five independent experiments. (C) Summary of the composition of H-2K^b/SIY$^+$ and H-2K^b/SIY$^-$ CD8$^+$ TILs co-expressing 4-1BB and LAG-3 comparing B16.SIY, MC38.SIY, MC57.SIY and 1969.SIY tumors on day 14 after tumor inoculation. n=5; three to four independent experiments. *:P $<$ 0.05, **:P$<$0.01, ***:P$<$0.001. A Kruskal-Wallis (non-parameteric) test was used for (C) H-2K^b/SIY analysis.

3.6 Tumor-specific 2C T cells express 4-1BB and LAG-3 after entry into the TME

As a third measure to determine if tumor antigen-specific $CD8^+$ T cells acquire the 4-$1BB^+LAG\text{-}3^+$ phenotype, we transferred congenically marked 2C and P14 transgenic (Tg) T cells, isolated from $2C/Rag2^{-/-}$ and $P14/Rag2^{-/-}$ mice, into tumor-bearing hosts. The 2C TCR is specific for the SIY model antigen expressed by B16.SIY tumor cells, while P14 is an irrelevant TCR specific for the LCMV-derived gp33-41 epitope; both TCRs are H-$2K^b$-restricted. 2C and P14 Tg $CD8^+$ T cells were transferred via tail vein 7 days after tumor inoculation. Seven days after transfer, tumors and TdLNs were extracted and the phenotypic profile of the transferred populations was analyzed. This system allowed for the analysis of two T cell populations with defined antigen specificities within the same tumor microenvironment, as well as the polyclonal host $CD8^+$ T cells. The 2C T cells were more efficiently recruited and expanded within the tumor microenvironment compared to the P14 T cells and encompassed a large fraction of the total $CD8^+$ TIL population (Figure 3.8A). Of the 2C T cells, nearly all expressed LAG-3 and or 4-1BB while this was true for only a small percentage of the P14 cells (Figure 3.8B and C). Consistent with the SIY/H-$2K^b$-pentamer analysis, the co-expression of LAG-3 and 4-1BB on 2C T cells was not observed in the TdLN. Together, these results firmly demonstrate that the 4-$1BB^+LAG\text{-}3^+$ phenotype is a property of tumor antigen-specific TILs under conditions of tumor progression.

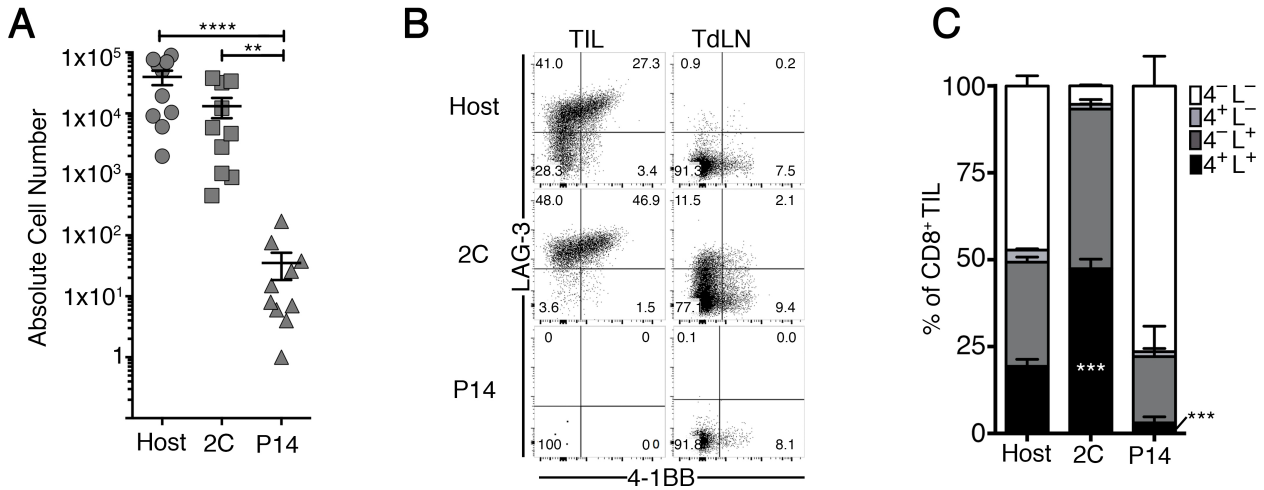

Figure 3.8: Adoptively transferred tumor-specific 2C but not irrelevant P14 TCR Tg T cells co-express 4-1BB and LAG-3 in the tumor

(A-C) On day 7 after tumor inoculation 1x10^6 P14/CD45.2 and 2C/CD45.1/2 Tg T cells were adoptively transferred, via tail vein, into CD45.1 congenic tumor bearing hosts and analyzed for the (A) total number of recovered cells in the tumor, (B and C) profile of 4-1BB and LAG-3 expression in 2C, P14 and host $CD8^+$ TILs. n=5; two-independent experiments. All error bars indicate mean SEM. *:P $<$ 0.05, **:P$<$0.01, ***:P$<$0.001. A Mann-Whitney test was used to compute significance in (A) and a two-way ANOVA with Bonferroni post-hoc test was used for (C).

3.7 $CD8^+$ TILs expressing LAG-3 and 4-1BB exhibit defective IL-2 production

Based on the characteristics of the *in vitro* T cell anergy model that led to the identification of Egr2 as an important regulator, we hypothesized that the tumor antigen-specific 4-1BB^+LAG-3^+ $CD8^+$ TIL population might be dysfunctional in their capacity to produce IL-2. To this end we sorted each subpopulation and stimulated with anti-CD3 and anti-CD28 mAb and analyzed IL-2 production by qRT-PCR and ELISA. Since nearly all $CD8^+$ TILs displayed an activated phenotype we used $CD8^+CD44^+$ splenocytes as a positive control. Indeed, the 4-1BB^+LAG-3^+ cells showed a 100-fold reduction in *Il2* mRNA and as much as a 40-fold reduction in IL-2 protein levels compared to the 4-1BB^-LAG-3^- population (Figure 3.9A and 4B). As a second approach, we examined $Egr2^{hi}$ TILs (which are also largely 4-1BB^+LAG-3^+) by utilizing the Egr2-GFP reporter mice. Indeed, ex vivo stimulated Egr2-GFP^{hi} $CD8^+$ TILs also exhibited reduced *Il2* transcript compared to Egr2-GFP^{lo} cells (Figure 3.9C). As a final approach, we adoptively transferred congenically marked 2C T cells intravenously into tumor-bearing hosts and recovered the 2C T cells 7 days later from the tumor and TdLN. 2C T cells isolated from tumors exhibited a reduced capacity to produce Il-2 transcripts, at a level equivalent to 4-1BB^+LAG-3^+ TILs, compared to 2C $CD44^+$ T cells isolated from the TdLN (Figure 3.9D). In chronic infection models, expression of PD-1 has been suggested to identify intrinsically dysfunctional or "exhausted" $CD8^+$ T cells. To determine if PD-1 alone might be sufficient to identify cells that lack the capacity to produce IL-2, we isolated $CD8^+$ TILs that lacked expression of LAG-3 and 4-1BB and then tested for the ability of the PD-1^+ fraction to express *Il2*. Approximately 10% of $CD8^+$ TILs were 4-1BB^-LAG-3^-PD-1^+ on day 14 and 21 (Figure 3.9E and F). Upon ex vivo stimulation, this population retained the capacity to produce IL-2 mRNA at a level comparable to the 4-1BB^-LAG-3^- cells (Figure 3.9G). These results indicate that PD-1 expression alone is not sufficient to identify dysfunctional TILs in the tumor microenvironment.

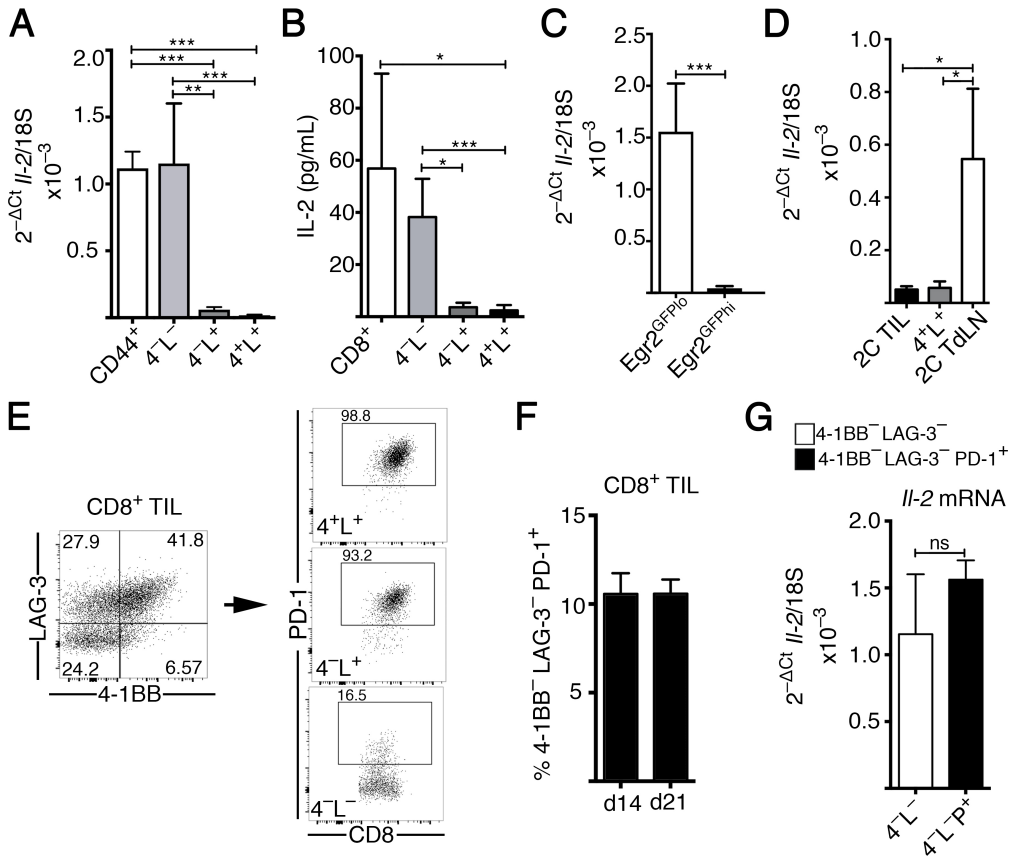

Figure 3.9: Co-expression of 4-1BB and LAG-3 but not PD-1 define dysfunctional CD8$^+$ TILs with diminished IL-2

(A and B) Sorted cells from day 14 B16.SIY tumor bearing mice were stimulated *in vitro* with anti-CD3ε and anti-CD28 for 12 hours and analyzed for (A) *Il2* transcript by qRT-PCR and (B) IL-2 protein by ELISA. Two tumors on opposite flanks pooled per mouse. n=4-5; three independent experiments. (C) Egr2^{hi} and Egr2^{lo} TILs were sorted from day 14 B16.SIY tumor bearing Egr2GFP mice and stimulated *in vitro* for 12 hours and analyzed for *Il2* transcript by qRT-PCR. Two tumors on opposite flanks pooled per mouse. n=5; two independent experiments. (D) On day 7 after tumor inoculation 1x10^6 2C/CD45.1/2 Tg T cells were transferred into mice, 7 days later host 4-1BB$^+$LAG-3$^+$ T cells sorted from the tumor and 2C T cells sorted from the tumor or TdLN were stimulated *in vitro* and analyzed for expression of *Il2* transcript by qRT-PCR. Two tumors on opposite flanks pooled per mouse. n=3; two independent experiments. (E and F) Representative flow analysis of PD-1 expression on 4-1BB/LAG-3 CD8$^+$ TIL subpopulations and (F) summary of the composition of the 4-1BB$^-$LAG-3$^-$PD-1$^+$ subpopulation in the CD8$^+$ TIL compartment on day 14 and 21. n=5; three independent experiments. (G) 4-1BB$^-$LAG-3$^-$PD-1$^+$ and 4-1BB$^+$LAG-3$^+$ CD8$^+$ TILs were sorted from day 14 tumor bearing mice, stimulated *in vitro* and analyzed for *Il2* transcript by qRT-PCR. Two tumors on opposite flanks pooled per mouse. n=3; two independent experiments. All error bars indicate mean SEM. *:P<0.05, **:P<0.01, ***:P<0.001, ****:P<0.0001. A Kruskal-Wallis (non-parametric) test was used for analysis of multiple comparisons (A, B, and D) and a Mann-Whitney test was used for pair-wise comparisons (C and G).

3.8 CD8$^+$ TILs expressing LAG-3 and 4-1BB produce IFN-γ and Treg-recruiting chemokines

To further examine functional alterations during tumor progression we tested for protein levels of IL-2, IFN-γ and TNF-α after TCR stimulation. As the loss of the ability of CD8$^+$ TILs to produce cytokines is suggested to be a temporal process initiated following entry into the tumor microenvironment [102, 21] or progressively after 30 days in the chronic LCMV model [150], we tested for cytokine production on days 7, 14, 21 and 28. The 4-1BB$^+$LAG-3$^+$ population lost the capacity to produce IL-2 as early as day 7 while the 4-1BB$^-$LAG-3$^+$ population lost IL-2 production between day 7 and day 14 (Figure 3.10A). Interestingly, the 4-1BB$^-$LAG-3$^-$ population did not lose the ability to produce IL-2 at any time point tested (Figure 3.10A), supporting the notion that this population is not tumor antigen-specific and that differentiation into the dysfunctional state is an antigen-dependent process [21]. Unexpectedly, the 4-1BB$^+$LAG-3$^+$ population produced more IFN-γ at all time points after day 7 compared to their negative counterparts, albeit with a slight decrease in IFN-γ production over time. While the increase in IFN-γ was maintained until later time points, TNF-α production was lost by day 28 (Figure 3.10A).

We next evaluated production of cytokines directly in the tumor without *in vitro* restimulation, which may more closely reflect which T cells were receiving TCR stimulation *in situ*. Each T cell population was sorted directly *ex vivo* without any culturing and mRNA levels were measured by qRT-PCR. Elevated *Ifnγ* and *Gzmb* transcripts were observed from the 4-1BB$^+$LAG-3$^+$ subpopulation, along with a slight decrease in *Tnfa* levels, compared to the 4-1BB$^-$LAG-3$^-$ cells (Figure 3.10B). As an additional approach, we confirmed production of IFN-γ in primary TILs by injecting tumors with Brefeldin A prior to analysis by intracellular cytokine staining. Consistent with the mRNA expression, the 4-1BB$^+$LAG-3$^+$ population produced significantly greater amounts of IFN-γ protein (Figure 3.10C). Thus, the 4-1BB$^+$LAG-3$^+$ TILs are not completely devoid of functionality, as they continue to

produce IFN-γ despite defective production of IL-2. In fact, this phenotype is consistent with what had been reported previously with *in vitro* T cell anergy models [151].

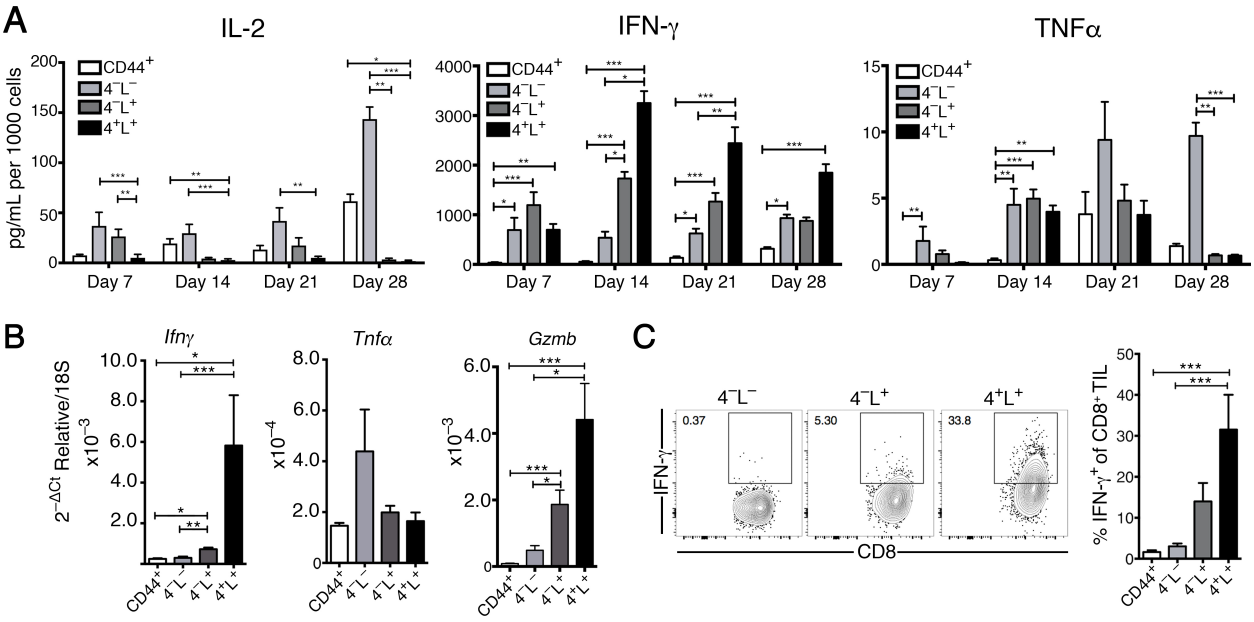

Figure 3.10: Dysfunctional CD8$^+$ TILs retain production of IFN-γ and cytotoxic molecules

(A) Longitudinal analysis CD8$^+$ TIL subpopulation cytokine production capacity. CD8$^+$ TIL subpopulations were sorted and stimulated with anti-CD3ε and anti-CD28 for 10-12 hours and the concentration of IL-2, IFN-γ and TNF-α was measured. Concentration was normalized to cell number. Two tumors on opposite flanks pooled for day 7 and 14. n=4-5; two-independent experiments. (B) *Ifnγ* , *Tnfa* and *Gzmb* transcript levels in the 4-1BB/LAG-3 subpopulations analyzed directly ex vivo. Two tumors on opposite flanks pooled per mouse. n=3-5; three-independent experiments. (C) Representative flow plot and summary of IFN-γ production analyzed directly ex vivo. Briefly, 100 μl of PBS containing 2 mg/mL GolgiPlug was injected intratumorally on day 14 after tumor inoculation. 8 hours later TILs were isolated. All steps were performed on ice with media containing 1 mg/mL GolgiStop until fixation. n=5; two independent experiments. A Kruskal-Wallis (non-parametric) test was used for (A-C) cytokine analysis.

3.9 Dysfunctional TILs retain cytolytic capacity and produce Treg-recruiting chemokines

The high levels of IFN-γ and Gzmb produced by the 4-1BB$^+$LAG-3$^+$ population led us to hypothesize that this population may still retain cytotoxic capacity. To test this possibility we performed re-directed lysis by co-culturing anti-CD3 bound P815 mastocytoma target cells with the different CD8$^+$ TIL subpopulations directly after sorting. 4-1BB$^+$LAG-3$^+$ CD8$^+$ TILs isolated from day 14 tumors were able to lyse target cells at a comparable efficacy to *in vitro* primed OT-I cells. 4-1BB$^+$LAG-3$^+$ TILs isolated from day 21 tumors were still able to lyse target cells, albeit to a lesser extent compared to primed OT-I cells (Figure 3.11A).

We have previously shown that CD8$^+$ T cells in the tumor can be the source of the chemokine CCL22 that recruits FoxP3$^+$ regulatory T (Treg) cells to the tumor microenvironment [63]. In addition, the chemokine Ccl1 was an Egr2 target in anergic T cells [144], and previous work had suggested that CCL1 also could contribute to Treg recruitment in the tumor context *in vivo* [152]. However, whether all CD8$^+$ T cells in the tumor produce these chemokines or if they are only produced by subpopulations of T cells had not been determined. To address this possibility we analyzed the CD8$^+$ TIL phenotypic subpopulations for Ccl1 and Ccl22 mRNA expression directly ex vivo by qRT-PCR. Indeed, the 4-1BB$^+$LAG-3$^+$ TIL population produced substantially greater Ccl1 and Ccl22 compared to their negative counterparts or to splenic CD8$^+$CD44$^+$ T cells (Figure 3.11B). As a control, expression of a distinct chemokine Ccl5 was found not to be differentially expressed (data not shown).

In the light of several negative regulatory aspects of 4-1BB$^+$LAG-3$^+$ TIL, it was of interest to evaluate whether they produced the immune regulatory cytokine IL-10. IL-10 has been reported to be induced upon Egr2 upregulation in CD4$^+$ T cells [145]. In addition, the expression of LAG-3 has been used to identify a population of Foxp3$^-$ CD4$^+$ (Tr1) T

cells that secrete IL-10 and exhibit regulatory properties [153]. To determine if IL-10 is being produced by TILs *in situ* and to explore the phenotypic composition of IL-10$^+$ TILs, we used IL-10^{EGFP} reporter (TIGER) mice. Examination of the CD8$^+$ and CD4$^+$ TIL compartments revealed an increase in the frequency of IL-10-producing TILs in both compartments (Figure 3.11C). Compared to CD4$^+$ TILs, a smaller fraction of CD8$^+$ TILs were positive for IL-10 on day 7, however the frequency of IL-10-producing CD8$^+$ TILs increased significantly by day 21 (Figure 3.11C). Analysis of the different CD8$^+$ subpopulations revealed that the majority of IL-10$^+$ CD8$^+$ TILs fell into the 4-1BB$^+$LAG-3$^+$ or 4-1BB$^-$LAG-3$^+$ subpopulations (Figure 3.11D) and nearly all IL-10$^+$ CD4$^+$ and CD8$^+$ TILs were positive for 4-1BB and/or LAG-3 (Figure 3.11E).

Together, these data show that co-expression of 4-1BB and LAG-3 delineates tumor antigen-specific CD8$^+$ TILs that lack the ability to produce IL-2 yet retain the ability to produce IFN-γ and kill target cells *in vitro*, secrete chemokines capable of Treg recruitment, and produce IL-10. Given the fact that IFN-γ is responsible for the upregulation of PD-L1 and IDO in the tumor microenvironment, chemokines produced by CD8$^+$ TIL contribute to Treg recruitment [63], and IL-10 has known immunomodulatory properties [154], these data suggest the possibility that the 4-1BB$^+$LAG-3$^+$ population might contribute to the network of immune suppressive mechanisms within the tumor microenvironment that limit the efficacy of antitumor immunity.

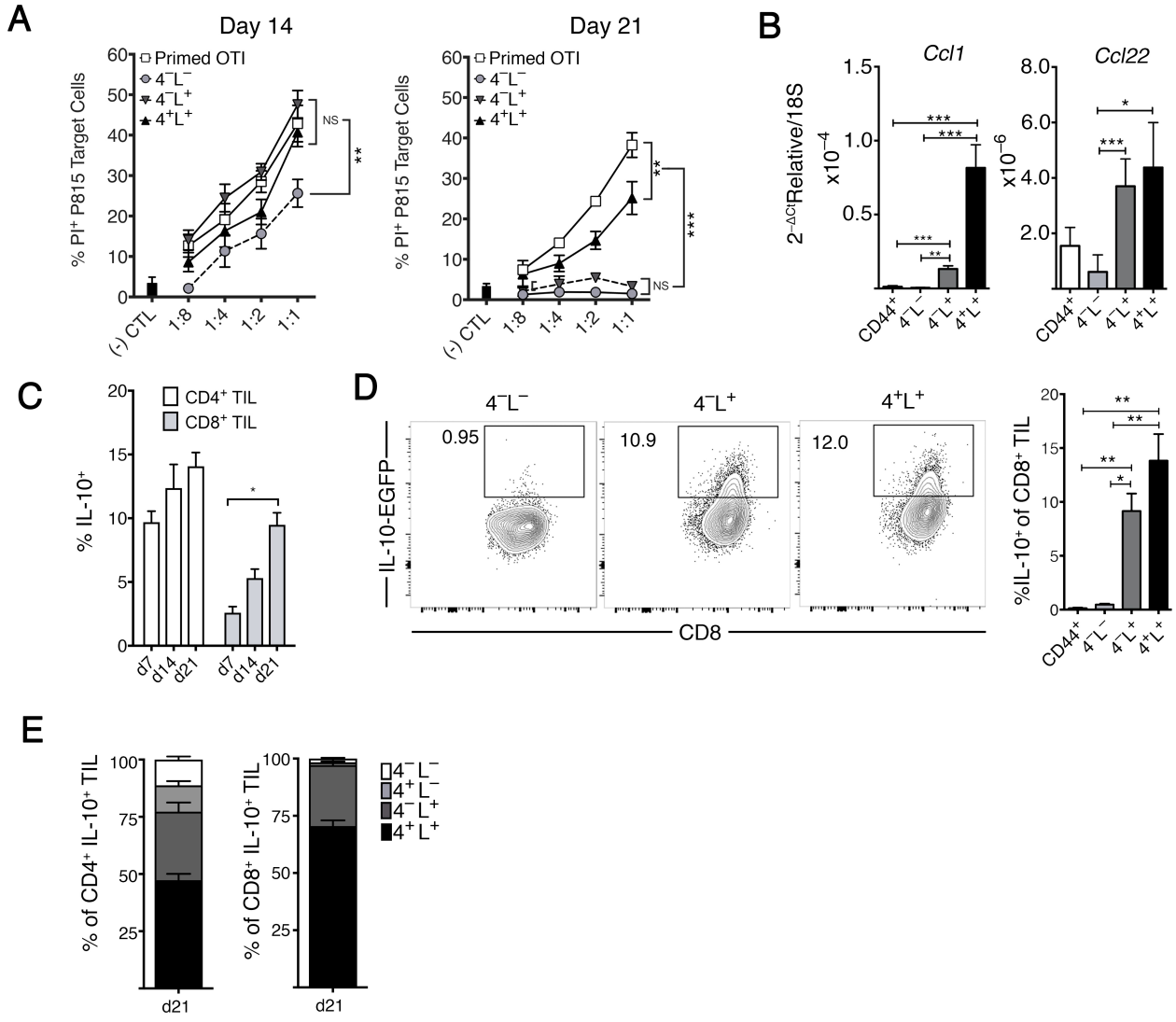

Figure 3.11: Dysfunctional CD8$^+$ TILs retain the capacity to lyse target cells *ex vivo* and produce *ccl1*, *ccl22*, and IL-10.

(A) CD8$^+$ TIL subpopulations at indicated time points were sorted and plated with 50,000 P815 target cells and 1 μg/mL anti-CD3ε. Lysed target cells were measured by positive staining for propidium iodine and/or live/dead fixable viability dye. P815 target cells plated without CTLs were used as a negative control (black bar). Primed OTI cells were used as a positive control. Tumors from 10 mice with 2 tumors on opposite flank were pooled to obtain sufficient quantities of CD8$^+$ TILs. Data are representative of three independent experiments. (B) *Ccl1* and *Ccl22* transcript levels in the 4-1BB/LAG-3 subpopulations analyzed directly ex vivo by qRT-PCR. n=4; two independent experiments. (C) IL-10^{EGFP} (TIGER) reporter mice were inoculated with 2x10^6 B16.SIY cells and IL-10 expresion was tracked over time. n=5; two independent experiments. (D) IL-10 expression by different 4-1BB/LAG-3 CD8$^+$ TIL subsets on day 14. n=5; three independent experiments. (E) Composition of IL-10$^+$ CD4$^+$ and CD8$^+$ TILs on day 21. n=5; two independent experiments. *:P $<$ 0.05, **:P$<$0.01, ***:P$<$0.001, ****:P$<$0.0001. A two-way ANOVA with Bonferroni post-hoc test was used for (A) cytolytic assay and a Kruskal-Wallis (non-parametric) test was used for(B-D) chemokine analysis.

3.10 Dysfunctional CD8$^+$ TILs exhibit suppressive activity *in vitro* and *in vivo*

Because of these phenotypic parallels between dysfunctional CD8$^+$ TILs and Foxp3$^-$CD4$^+$ (Tr1) T cells, we investigated whether CD8$^+$LAG-3$^+$ TILs might have suppressive function. To begin to address this question, an *in vitro* suppression assay was performed using CD4$^+$ T cells as responders. Due to the difficulty to obtain sufficient numbers of 4-1BB$^+$LAG-3$^+$ CD8$^+$ T cells for larger functional assays, we used LAG-3 as the sole marker of dysfunctional CD8$^+$ T cells, as nearly all 4-1BB$^+$ CD8$^+$ TILs co-express LAG-3, and 4-1BB$^-$LAG-3$^+$ CD8$^+$ TILs exhibit a similar functional profile to their 4-1BB$^+$-expressing counterparts. As a control we purified CD4$^+$Foxp3$^+$ Treg cells from the spleens of non-tumor-bearing mice as well as from tumors harvested from tumor-bearing mice. LAG-3$^+$ and LAG-3$^-$ CD8$^+$ TILs were purified from tumors on day 14 by cell sorting and titrated along with cell trace violet (CTV)-labeled CD4$^+$Foxp3$^-$ responder T cells and 300,000 irradiated splenocytes as feeder cells. Co-cultures were stimulated with anti-CD3 mAb for 60 hours. Interestingly, LAG-3$^+$ CD8$^+$ TILs were able to suppress CD4$^+$ T cell proliferation to a comparable level to splenic Treg cells and also to Treg cells isolated from the same tumors (Figure 3.12A and B).

We next sought to address the question whether LAG-3$^+$ CD8$^+$ TILs could exhibit suppressive activity in the context of an antitumor immune response *in vivo*. To do this we developed an adoptive transfer model in which a suppressive cell population dampens an endogenous antitumor T cell response, resulting in increased tumor growth. The model was built upon our laboratory's previous observation that adoptive transfer of Treg-depleted splenocytes (Treg-dep) into Rag2$^{-/-}$ mice can lead to robust tumor control, through the combination of Treg depletion and homeostatic proliferation [155]. Importantly, the tumor control was lost when Treg cells were not depleted, providing an experimental window to examine the effect of regulatory T cell populations. In this model, we adoptively transfer T cell populations i.v. into Rag2$^{-/-}$ mice followed by subcutaneous B16.SIY tumor cell

implantation 5 days later (Figure 3.12C). We have termed this model "tumor rejection reversal" (TRR). To optimize the TRR model we first determined the number of Treg-depleted conventional T cells required to induce tumor control. Using Foxp3^{EGFP} reporter mice, we isolated CD8^{+} and CD4^{+}Foxp3^{-} T cells by FACS and adoptively transferred titrated numbers into Rag2$^{-/-}$ mice. We found that adoptive transfer of 1x10^{6} cells of each CD8^{+} and CD4^{+}Foxp3^{-} T cell populations was sufficient to delay tumor growth compared to non-Treg-depleted cells (data not shown). Using this setup, we co-transferred titrated numbers of FACS-purified CD4^{+}Foxp3^{+} Treg cells to ascertain the minimum number of cells sufficient to reverse tumor control. We found that co-transfer of 50,000 Treg cells was sufficient to reverse the spontaneous control induced by Treg-depleted T cells (data not shown). Next, using the same number of cells, we tested the capacity of LAG-3^{+} and LAG-3^{-} CD8^{+} TILs to blunt tumor control. While LAG-3^{-} CD8^{+} TILs had no impact on tumor growth control by conventional splenic T cells, LAG-3^{+} CD8^{+} TILs were able to blunt tumor growth control to a comparable level seen with splenic Foxp3^{+} Treg cells, as well as increase the weight of tumors at endpoint (Figure 3.12D and E). Together, these results indicate that, despite lacking expression of Foxp3, LAG3^{+} CD8^{+} TILs are in fact immune regulatory and suppress antitumor immunity *in vivo*.

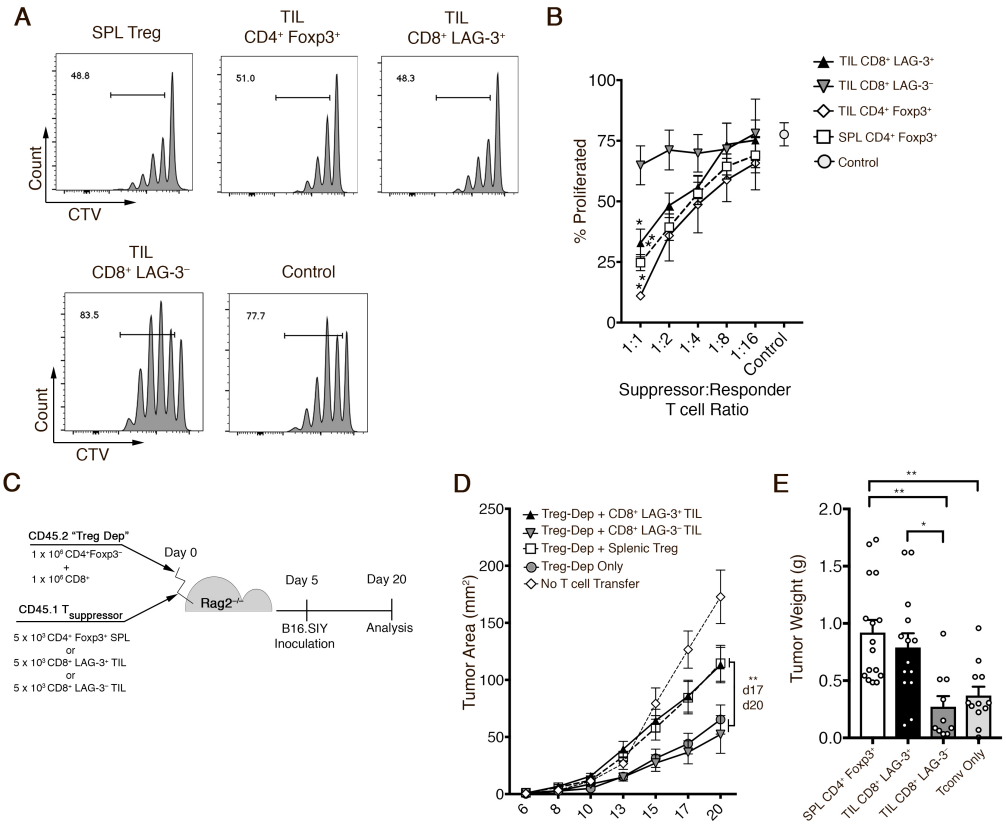

Figure 3.12: Dysfunctional CD8$^+$ TILs exhibit suppressive activity *in vitro* and *in vivo*.

(A) Representative histograms of CD4$^+$Foxp3$^-$ cell proliferation as measured by cell trace violet dilution. Suppressive cell populations were co-cultured at a 1:1 ratio with CD4$^+$Foxp3$^-$ responder cells. (B) Summary of responder cell proliferation with titrated numbers of suppressive cell populations. n=1-2; 5 independent experiments. (C) Diagram of the TRR model to test for suppressive activity *in vivo*. (D) Tumor outgrowth in Rag2$^{-/-}$ after adoptive transfer of populations being tested for suppressive activity and/or Treg-depleted T cells. n=2-5; four independent experiments. *:P < 0.05, **:P$<$0.01, ***:P$<$0.001, ****:P$<$0.0001. (E) Tumor weight (g) at endpoint (day 20-21). n=2-5; four independent experiments. A two-way ANOVA with Bonferroni post-hoc test was used for (B and D) and a Kruskal-Wallis (non-parametric) test was used for (E).

3.11 A more similar molecular program is observed between CD8$^+$ T cells isolated from tumors compared to chronic viral infection

Having in hand surface markers that appeared to define tumor antigen-specific dysfunctional CD8$^+$ TILs, we wanted to compare the gene expression profile of this population to other published profiles of dysfunctional CD8$^+$ T cells to determine genes that may regulate or be used to profile cells in this dysfunctional state. To this end, we conducted a cross-study comparison of the transcriptional profiles of the "dysfunctional" 4-1BB$^+$LAG-3$^+$ CD8$^+$ TILs, "hypofunctional" CD8$^+$ TILs from a study utilizing the murine CT26 tumor model [102] and LCMV "exhausted" GP33 specific CD8$^+$ T cells [156]. We only considered genes with a 2-fold increase over controls from each study independently. Over a 2-fold greater number of genes was found to be shared between our current dysfunctional TIL dataset and the previously published hypofunctional CD8$^+$ TIL data, than with the exhausted T cell profile (Figure 3.14A). In addition, a rank-rank hypergeometric overlap (RRHO) analysis indicated a greater statistically significant overlap (Figure 3.14B) and a greater correlation (Figure 3.14C) between the dysfunctional and hypofunctional CD8$^+$ TIL gene expression profiles compared to the virally-induced exhausted CD8$^+$ T cell profile, suggesting a more similar molecular program between CD8$^+$ T cells isolated from tumors compared to chronic viral infection.

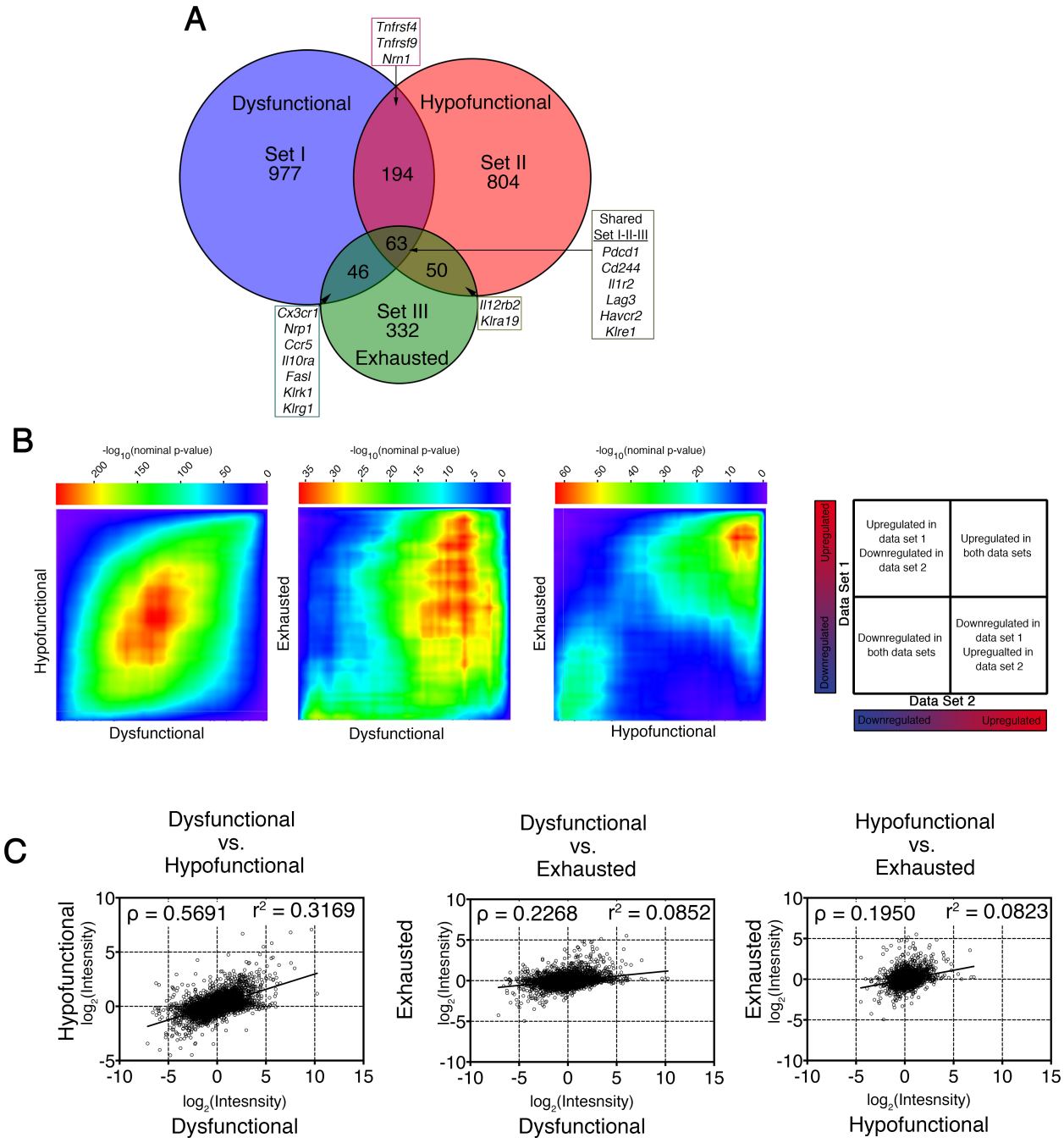

Figure 3.13: Dysfunctional CD8$^+$ TILs share a core genetic program
(A) Differential gene analysis between CD8$^+$ T cells in two tumor models and the chronic LCMV viral model. Probe sets that revealed a 2-fold difference compared to their negative counterpart were considered to be differentially expressed. (B) Statistical analysis of the cross-study comparison of gene expression profiles. Rank-Rank Hypergeometric plots of each pair-wise comparison. (C) Pair-wise correlation of expression values between each data set. Rho (ρ) is the spearman rank correlation coefficient.

3.12 Gene Ontology term analysis between CD8$^+$ T cells from tumor and chronic LCMV models

To investigate the molecular pathways between these three populations we grouped gene ontology networks into nodes and determined the most significant pathways within each node (Figure 3.14A). Interestingly, gene ontology (GO) terms shared between our dysfunctional T cell dataset and the published hypofunctional T cell dataset were greatly enriched in cell cycle genes, consistent with our observation that the dysfunctional population is largely Ki67$^+$. GO terms shared between dysfunctional and exhausted gene sets encompassed effector programs such as regulation of cell killing, chemotaxis, interferon-γ production. GO terms shared between hypofunctional and exhausted gene sets consisted of cell cycle pathways, negative regulation of lymphocytes, and interferon-γ production. These data suggest that while some conserved molecular programs likely exist in these dysfunctional differentiation states, many pathways may be differentially regulated between chronic viral infections and in the tumor context.

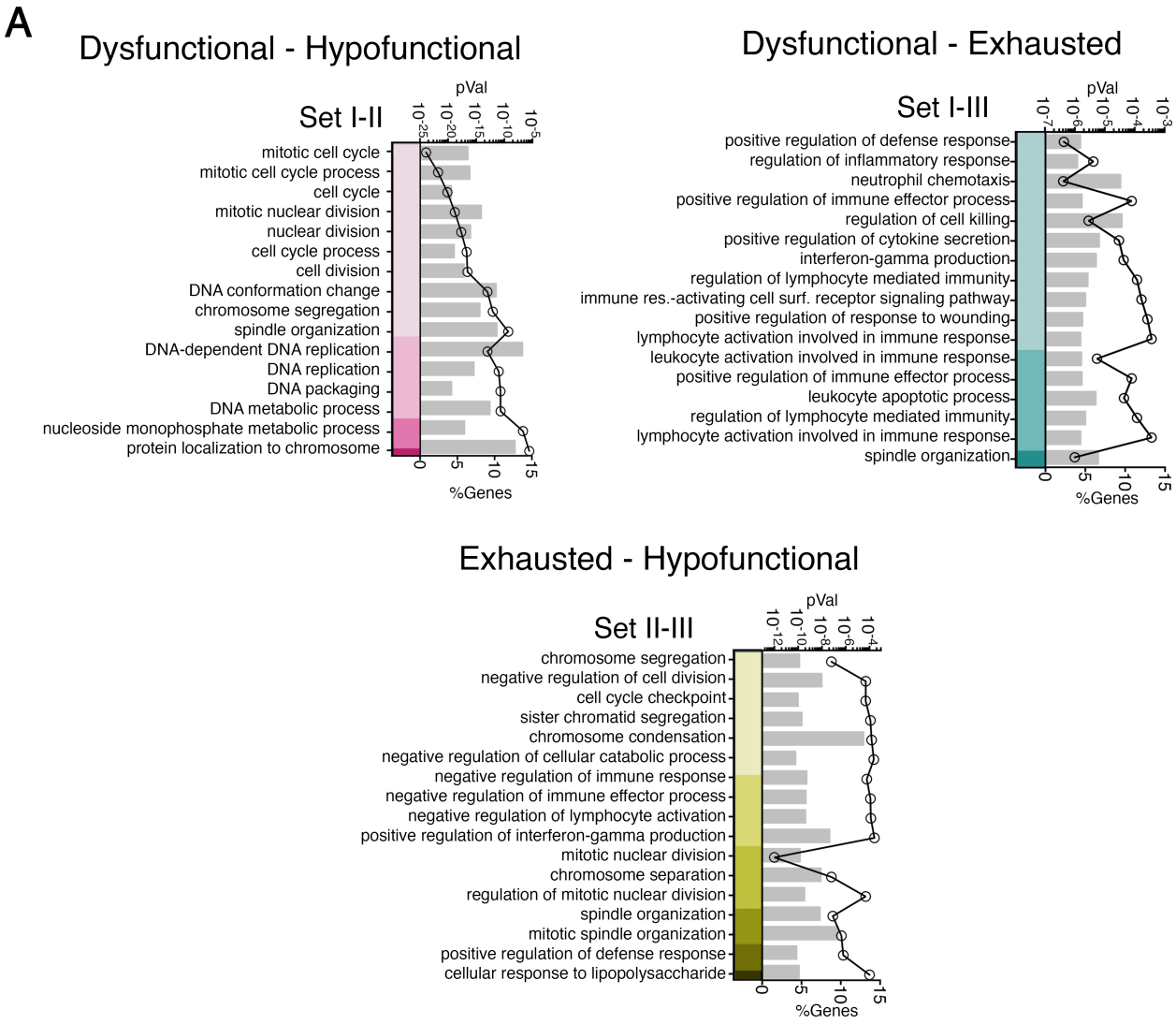

Figure 3.14: Shared gene ontology terms between dysfunctional CD8$^+$ TILs and exhausted CD8$^+$ T cells

(A) In a pair-wise fashion, shared upregulated genes were used as the input for the ClueGO software with the Cytoscape application [130] Stacked bars represent gene term nodes. Top y-axis represents the pVal of terms displayed. Bottom y-axis represents the percent of genes found within the defined term. Only pathways with a Bonferroni step down correction p-value > 0.01 were considered when generating pathway nodes.

3.13 Gene expression profiling reveals that CD8$^+$4-1BB$^+$LAG-3$^+$ TILs express an extensive array of additional co-stimulatory and co-inhibitory receptors

While many inhibitory receptors, including *Pdcd1* (PD-1), *Havcr2* (TIM-3), *Cd244* (2B4), *Klre1*, and *Lag3* were shared between all data sets, the co-stimulatory receptors *Tnfrsf4* (OX-40) and *Tnfrsf9* (4-1BB) were upregulated in dysfunctional and hypofunctional CD8$^+$ TIL data sets. Therefore, to enrich in potential markers and therapeutic targets on tumor specific CD8$^+$ TILs we aimed to characterize the complete cell surface phenotype of the 4-1BB$^+$LAG-3$^+$ CD8$^+$ TIL population. Comparing the different CD8$^+$ TIL subpopulations we found several additional upregulated co-stimulatory receptors: *Tnfrsf18* (GITR), *Nkg2d* (KLRK1) and *Cd27*. The transcript for *Nrp1* (neuropilin-1), which encodes for a cell surface receptor protein implicated in CD4$^+$ Treg function [157], was also highly expressed (Figure 3.17A). We confirmed expression of many of these molecules by flow cytometry at day 7, 14 and 21 after tumor inoculation (Figure 3.17B). We also extended our analysis to include the co-stimulatory molecules ICOS and CD160 and the inhibitory receptor T cell immunoreceptor with Ig and ITIM domains (TIGIT) because ICOS and CD160 were close to the cutoff value and no probe was present for TIGIT in the gene array. In addition, recent reports indicate that targeting these receptors can be therapeutic in murine models of cancer [158, 159]. PD-1, TIGIT, TIM-3, CD27 and NRP1 were expressed the majority of the 4-1BB$^+$LAG-3$^+$ TIL population and expression was maintained over time. 2B4, CD160, CTLA4, OX-40, and GITR subdivided a lesser fraction of the 4-1BB$^+$LAG-3$^+$ population. The expression of several inhibitory receptors, 2B4, TIM3 and CD160 increased over this 3-week time frame while expression of the co-stimulatory receptors, ICOS and OX-40, decreased (Figure 3.17B).

To address if the dysfunctional CD8$^+$ TILs are terminally-differentiated short term effector cells or memory-like cells, we additionally analyzed the expression of KLRG-1 and IL-7Rα [160]. Most of the CD8$^+$ TILs were negative for KLRG-1 expression and there was no differ-

ence between the 4-1BB^{+}LAG-3^{+} and 4-1BB^{-}LAG-3^{-} populations. However, the majority of the 4-1BB^{+}LAG-3^{+} TILs did not express the IL-7 receptor (IL-7Rα) compared to their negative counter parts (Figure 3.17C). These results suggest that the 4-1BB^{-}LAG-3^{-} TIL, which are not apparently specific for antigens expressed in the tumor microenvironment, are more memory-like, yet at the same time the tumor antigen-specific LAG-3^{+}4-1BB^{+} subset has not fully acquired a terminal effector phenotype.

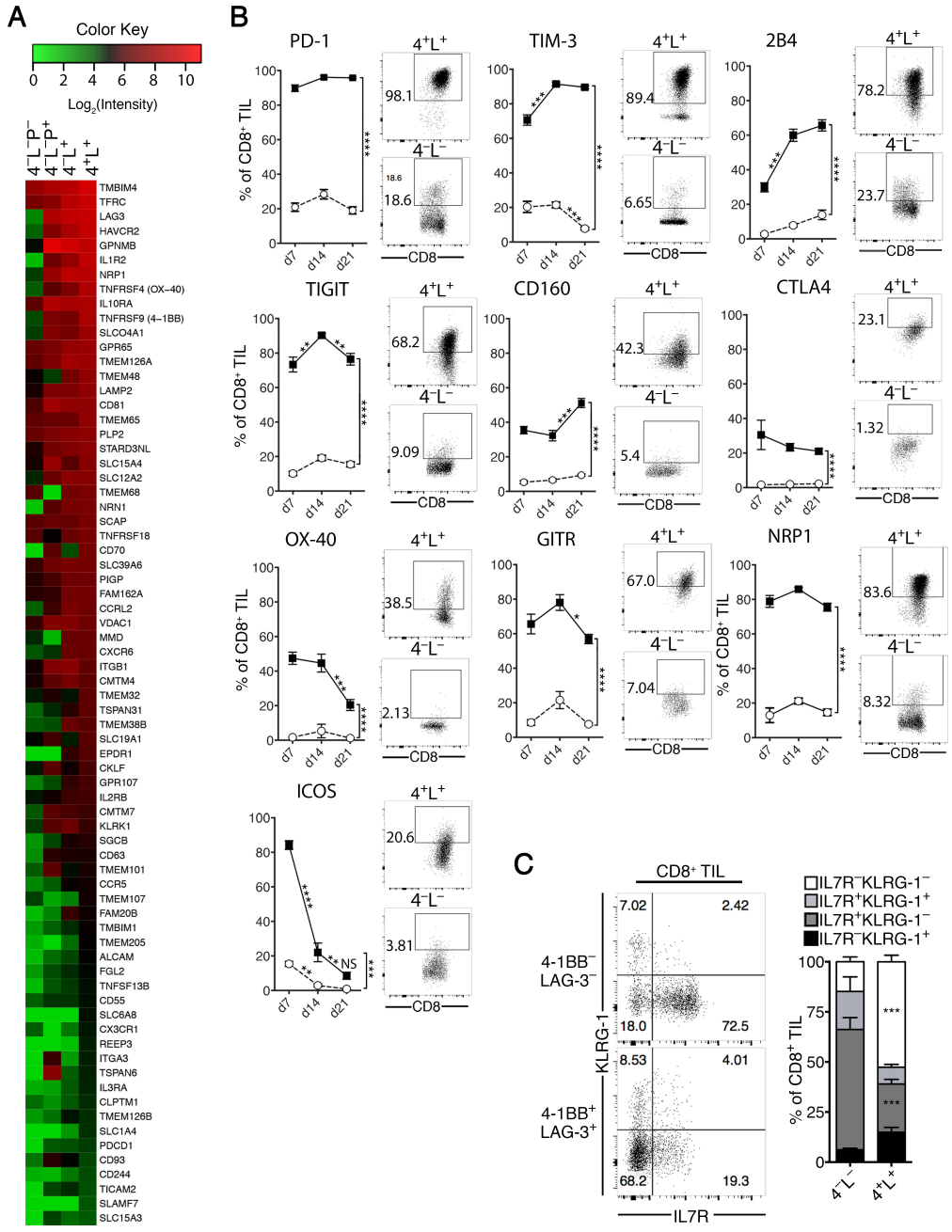

Figure 3.15: Dysfunctional CD8$^+$ TILs express a wide range of co-inhibitory and co-stimulatory receptors

(A) Gene expression profile of cell surface receptors in the 4-1BB/LAG-3 CD8$^+$ TIL subsets. Probe sets that revealed a 1.5-fold increase in the 4-1BB$^+$LAG-3$^+$ population relative to the 4-1BB$^-$LAG-3$^-$PD-1$^-$ population are displayed. Columns show the log2-transformed signal intensity. (B) Longitudinal study of selected up-regulated cell surface receptors. Flow plots are representative of the CD8$^+$ TIL subsets on day 14. n=5; two to five independent experiments for each time point. (C) Representative flow plot and summary of KLRG-1 and IL-7Rα expression among the 4-1BB/LAG-3 subpopulations on day 14 after tumor inoculation. n=5; two independent experiments. *:P $<$ 0.05, **:P$<$0.01, ***:P$<$0.001, ****:P$<$0.0001. A two-way ANOVA with Bonferroni post-hoc test was used for all analyses.

3.14 Targeting 4-1BB and LAG-3 exerts antitumor activity *in vivo*

While it was conceivable that LAG-3 and 4-1BB were just phenotypic markers for dysfunctional tumor antigen-specific CD8$^+$ TIL, it was of interest to assess whether targeting these receptors might have therapeutic utility. To this end, an agonistic anti-4-1BB mAb was administered alone or in combination with a blocking anti-LAG-3 mAb in mice bearing established B16.SIY tumors. While each antibody treatment alone had some therapeutic effect as reflected by slower tumor growth, the combination was particularly potent (Figure 3.17A). Analysis of the tumor microenvironment revealed that improved tumor control with the combination therapy was accompanied by an increase in the number of CD8$^+$ TILs specific for the SIY antigen (Figure 3.17B), consistent with results reported previously with anti-PD-L1 + anti-CTLA-4 mAb [161, 162].

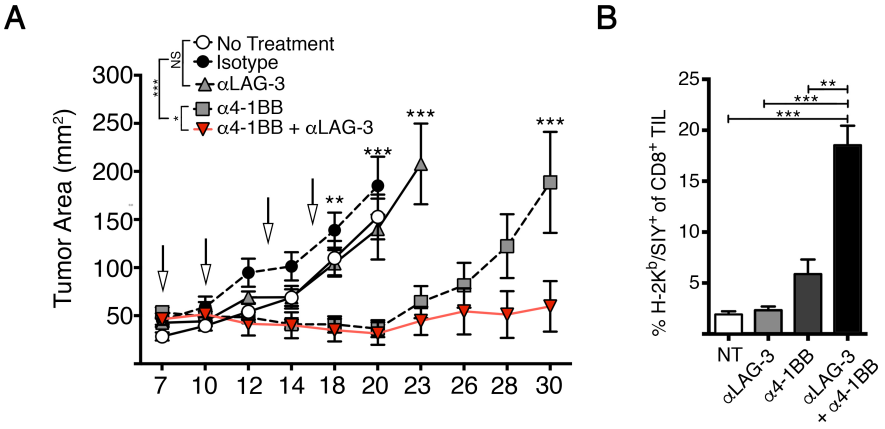

Figure 3.16: Mice treated with anti-4-1BB + anti-LAG-3 antibody exhibit synergistic control of tumor growth
(A) Tumor outgrowth measured in mm^2. Arrows indicate on which days mice received antibody therapy. n=5; two independent experiments. (B) Composition of H-2K^b/SIY$^+$ CD8$^+$ TILs on day 14. Mice received antibody doses (100 µg each) on days 7,10, 13 and 16. n=5; two independent experiments. *:P $<$ 0.05, **:P$<$0.01, ***:P$<$0.001, ****:P$<$0.0001. A two-way ANOVA with Bonferroni post-hoc test was used for all analyses.

3.15 Targeting 4-1BB and LAG-3 normalizes the phenotypic composition of CD8$^+$ TILs

We next examined whether the therapeutic effect of anti-4-1BB + anti-LAG-3 mAbs was associated with a loss of phenotypic markers defining dysfunctional T cells in the steady state. We were concerned that re-analyzing the T cells for expression of LAG-3 and 4-1BB might be problematic, as the administered Abs could theoretically modulate the target receptors from the cell surface. To this end, we took advantage of the coordinate expression of additional receptors as identified above by gene expression profiling. Preliminary analyses of the bulk TIL subpopulations revealed decreased expression of NRP1 and 2B4 following anti-LAG-3 + anti-4-1BB treatment (data not shown). We therefore analyzed co-expression of 2B4 and NRP1 on SIY-reactive CD8$^+$ TILs identified by pentamer staining. Indeed, a 2.7-fold-decrease in the co-expression of 2B4 and NRP1 was observed upon anti-4-1BB + and anti-LAG-3 mAb treatment (Figure 3.17A), indicating a loss of the surface phenotype associated with T cell dysfunction. To determine whether this change was accompanied by a shift towards an effector phenotype, expression of KLGR-1 was examined. Indeed, a marked increase in KLGR-1 expression was observed on the SIY-reactive TILs following treatment, and a 3.7-fold increase in the KLRG-1$^{\text{hi}}$IL-7Rα^{lo} population was observed (Figure 3.17B).

It was conceivable that treatment with anti-LAG-3 + anti-4-1BB mAbs was not altering the phenotype of T cells already within the tumor but rather was supporting recruitment of newly primed functional T cells from secondary lymphoid organs. In order to distinguish these possibilities, we utilized the S1PR inhibitor FTY720, which prevents T cell egress from lymph nodes [163]. We had previously shown that the efficacy of anti-PD-L1-based immunotherapies was preserved in the presence of FTY720, arguing for re-functionalization of TILs as the major mechanism of action [161]. FTY720 administration was started on day 6 after tumor inoculation, 24 hours before the start of anti-LAG-3 + anti-4-1BB treatment, and was continued every day until TIL analysis on day 14. Peripheral blood analyzed at

the same time point revealed marked depletion of circulating T cells (Figure 3.17C). Despite this loss of circulating T cells, the down regulation of 2B4 and NRP1 and the shift towards the KLRG1^{hi}IL-7Rα^{lo} phenotype was nonetheless preserved (Figure 3.17D and E).

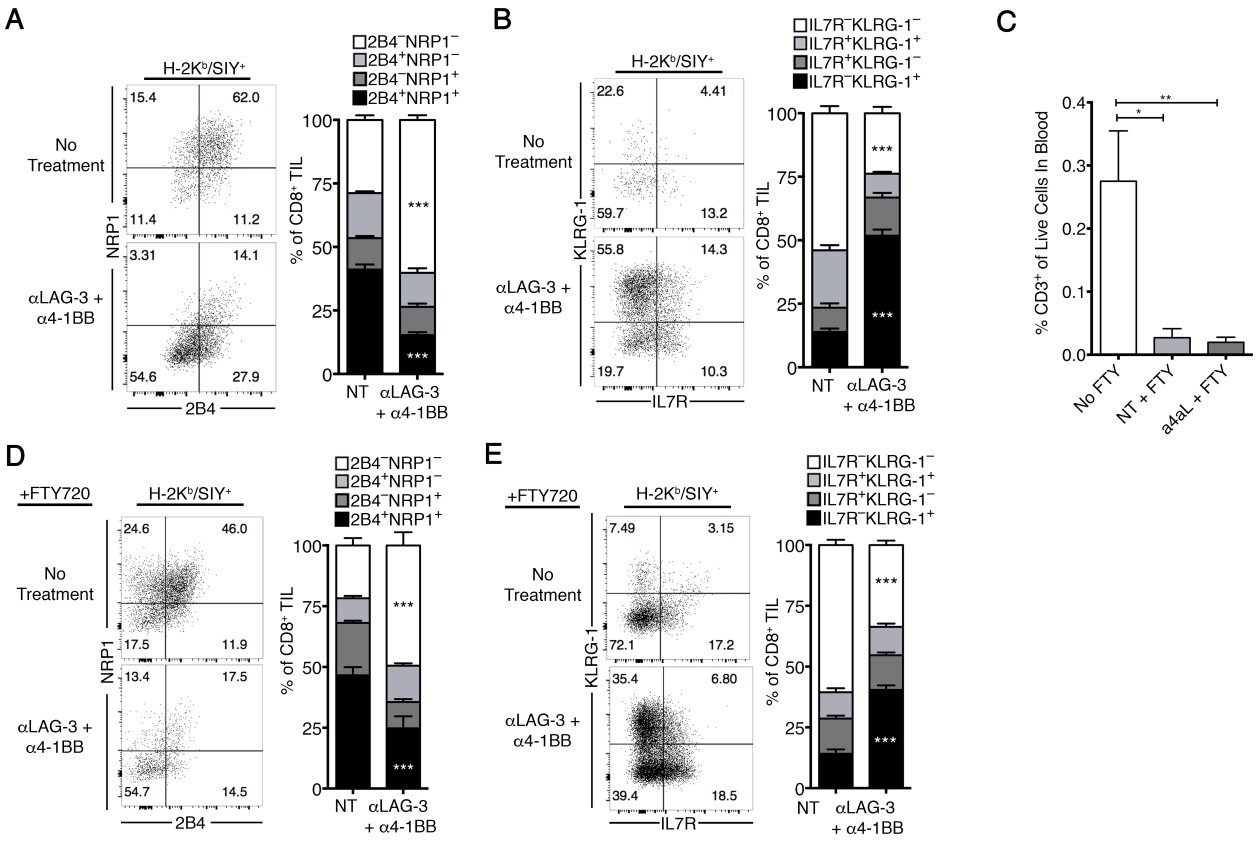

Figure 3.17: Targeting dysfunctional TILs by anti-4-1BB + anti-LAG-3 antibody treatment normalizes phenotypic profile

(A and B) Representative flow plot and summary of (A) NRP1/2B4 and (B) KLRG-1/IL-7Rα expression in H-2K^b/SIY$^+$ CD8$^+$ TILs without FTY720 on day 14 after tumor inoculation. (C) Analysis of T cells found in the blood after FTY720 treatment. (D and E) Representative flow plots after FTY720 administration. Mice received antibody treatment as in (Figure3.17) and FTY720 was administered at a dose of 25 μg/mouse by gavage starting one day before treatment and continuing one dose per day until analysis (day 6 to day 13). n=5; two-independent experiments.*:P $<$ 0.05, **:P$<$0.01, ***:P$<$0.001, ****:P$<$0.0001. A two-way ANOVA with Bonferroni post-hoc test was used for all analyses.

3.16 Targeting 4-1BB and LAG-3 restores the ability of dysfunctional CD8$^+$ TILs to produce IL-2

To examine functional restoration of the TILs, we sorted the KLRG-1^{lo}IL-7Rα^{lo} and KLRG-1^{hi}IL-7Rα^{lo} CD8$^+$ TIL populations from B16.SIY tumors on day 14 following treatment and analyzed for IL-2 after restimulation *in vitro*. Indeed, the KLRG-1^{lo}IL-7Rα^{lo} and KLRG-1^{hi}IL-7Rα^{lo} populations showed an increased capacity to produce IL-2 upon stimulation (Figure 3.18A). The relative level of *Il2* mRNA was comparable between the two CD8$^+$ TIL populations and control CD8$^+$CD44$^+$ TdLN T cells. Collectively, these data suggest that anti-4-1BB/anti-LAG-3 combinatorial treatment induces significant changes in the phenotype profile and promotes functional restoration of tumor antigen-specific CD8$^+$ T cells already present within the tumor microenvironment.

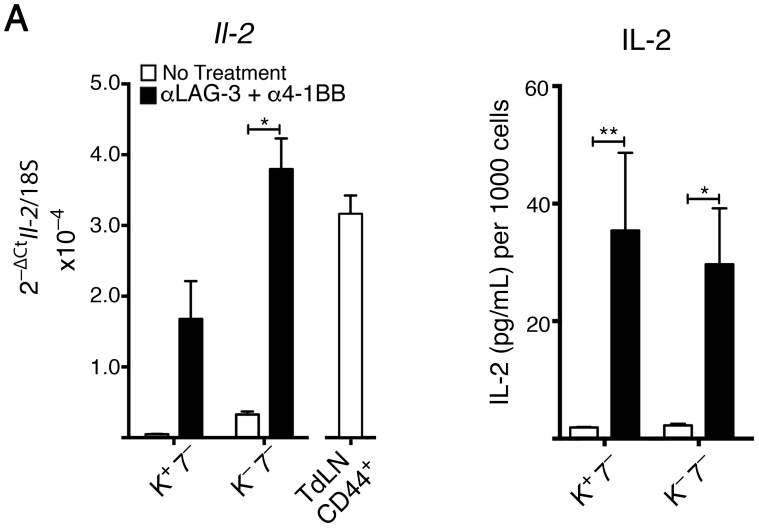

Figure 3.18: Targeting dysfunctional TILs by anti-4-1BB + anti-LAG-3 antibody restores their ability to produce IL-2
(A) IL-2 production after treatment. Sorted cells from treated or untreated day 14 B16.SIY tumor bearing mice were stimulated *in vitro* for 12 hours and analyzed for Il-2 transcript by qRT-PCR. Protein concentration was determined by the bead-based LEGENDplex immunoassay and normalized to cell number. Two tumors on opposite flanks pooled per mouse. n=2-3; two independent experiments. *:P $<$ 0.05, **:P$<$0.01, ***:P$<$0.001, ****:P$<$0.0001. A two-way ANOVA with Bonferroni post-hoc test was used for all analyses.

Vβ Primer Sequences		
Wilson	IMGT	Sequence
Cβ1.1	TRBC1	CTCAAACAAGGAGACCTTGGGTGG
Vβ1	TRVB5	CAGACAGCTCCAAGCTACTTTTAC
Vβ2	TRVB1	ATGAGCCAGGGCAGAACCTTGTAC
Vβ3	TRVB26	GAAATTCAGTCCTCTGAGGCAGGA
Vβ4	TRVB2	CTAAAGCCTGATGACTCGGCCACA
Vβ5.1	TRVB12-2	CTTTGGAGCTAGAGGACTCTGCCG
Vβ5.2	TRVB12-1	CCTTGGAACTGGAGGACTCTGCTA
Vβ6	TRVB19	GCCCAGAAGAACGAGATGGCCGTT
Vβ7	TRVB29	GGATTCTGCTAAAACAAACCAGACATCTGT
Vβ8.1	TRVB13-3	GCTTCCCTTTCTCAGACAGCTGTA
Vβ8.2	TRVB13-2	GCTACCCCCTCTCAGACATCAGTG
Vβ8.3	TRVB13-3	GGCTTCTCCCTCTCAGACATCTT
Vβ9	TRVB17	CTCTCTCTACATTGGCTCTGCAGG
Vβ10	TRVB4	CTTCGAATCAAGTCTGTAGAGCCG
Vβ11	TRVB16	TGAAGATCCAGAGCAGCGGGCCCC
Vβ12	TRVB15	CCACTCTGAAGATTCAACCTACAGAACCC
Vβ13	TRVB14	CAAGATCCAGTCTGCAAAGCAGGG
Vβ14	TRVB31	GCACGGAGAAGCTGCTTCTCAGCC
Vβ15	TRVB20	GCATATCTTGAAGACAGAGGC
Vβ16	TRVB3	CTCTGAAAATCCAACCCACAGCACTGG
Vβ17	TRVB24	TCTGAAGAAGACGACTCAGCACTG
Vβ18	TRVB30	GCAAGGCCTGGAGACAGCAGTATC

Table 3.1: Vβ Primer Sequences

Primer/Probe Sets			
Gene	Primer Forward	Primer Reverse	Roche Probe Number
Lag3	tgctttgggaagctccagt	gctgcagggaagatggac	79
Tnfrsf9	ccggtcttaagcacagacct	gaacggtactggcgtctgtc	108
Egr2	ctacccggtggaagacctc	aatgttgatcatgccatctcc	60
Sema7a	tcaatcggctgcaagatgt	cgcagacagctgagtagttcc	15
Crtam	agatccaacaacgaggagaca	tcatgcaacgcttagactgg	71
Ccl1	tcaccatgaaacccactgc	agcagcagctattggagacc	71
Ngn	caccctagcctaacctcaacc	tgaaaacctcctcccctctt	45
Arl3	ctggcagatccagtcctgtt	acccagttcatgccatcct	100
Exph5	atgagggaggagagcggtat	cagcttgttgtccaaatcgtc	67
Fhl2	agaaaaccatcatgccaggt	acaggtgaagcaggtctcgt	74
Nrn1	atcctcgcggtgcaaata	gcccttaaagactgcatcaca	108
Ptgfrn	ccggggagatctcatcaaa	tcgaaggccatgtcatctg	12
Rankl	gaagacacactacctgactcctg	cccacaatgtgttgcagttc	88
Hif1a	gctgctcactgtgaaggaagt	tggggaatgcattttaccat	2
Egr3	caatctgtaccccgaggaga	ccgatgtccatcacattctct	74
Tnfa	ctgtagcccacgtcgtagc	ttgagatccatgccgttg	25
Gzmb	gctgctcactgtgaaggaagt	tggggaatgcattttaccat	2
Ccl1	tcaccatgaaacccactgc	agcagcagctattggagacc	71
Ccl22	tcttgctgtggcaattcaga	gcagagggtgacggatgtag	74

Table 3.2: Primer/Probe Sets

3.17 Discussion Part I

Recent work has indicated that spontaneous T cell responses against tumors occur frequently, but that infiltrating T cells are functionally impaired by inhibitory mechanisms such as PD-1/PD-L1 interactions. The clinical success of anti-PD-1 mAbs in the treatment of multiple cancers has fueled continued investigation into the biologic properties of dysfunctional tumor-infiltrating T cells *in vivo*. However, the identification and detailed study of the subset of T cells within the tumor microenvironment specific for tumor antigens among the sea of irrelevant T cells has been constrained by a lack of cell surface markers for their identification. Based on our previous work identifying the transcription factor Egr2 as a critical regulator of T cell anergy *in vitro*, we applied knowledge of Egr2 targets to evaluate the applicability of these targets toward understanding dysfunctional TILs *in vivo*.

By using three techniques, CDR3β spectratyping, H-2K^{b}-pentamer staining, and adoptive 2C T cell transfer; we found that 4-1BB and LAG-3 identify the major population of tumor antigen-specific CD8^{+} TILs. By using these markers to isolate and study tumor-specific T cells we avoided techniques frequently used in the literature, namely pentamer staining and TCR transgenic T cells, which may alter the function of T cells or provide limited information due to the use of a single specificity. Therefore, with the discovery of 4-1BB and LAG-3 as markers we were able to isolate minimally altered tumor-specific CD8^{+} TILs to perform detailed functional studies that yielded new and unexpected results.

Using conditional Egr2 KO mice and Egr2 reporter mice, we confirmed a contribution of Egr2 itself in this process. While these T cells also express PD-1, contrary to popular belief, expression of PD-1 alone was not sufficient to define the dysfunctional tumor antigen-specific TIL population. Flow cytometric sorting enabled thorough functional and molecular characterization of these cells. Gene expression profiling revealed the broad collection of additional immunoregulatory molecules expressed, which includes additional novel targets for immunotherapy. Functionally, the bottom line is that these cells were not inert, but rather produced IFN-γ (which induces PD-L1 and IDO), Treg-recruiting chemokines, and IL-10,

arguing that they participate in the immune suppressive nature of the tumor microenvironment. Indeed, we found that the dysfunctional $CD8^+$ TILs can suppress $CD4^+$ proliferation *in vitro*. Moreover, by developing a model to test for *in vivo* suppressive activity, we found that the dysfunctional $CD8^+$ TIL population can impeded the antitumor immune response.

Finally, combinatorial targeting of the dysfunctional $CD8^+$ TIL population through anti-4-1BB and anti-LAG-3 specific Abs was therapeutically synergistic, by a mechanism associated with refunctionalization of T cells already present within the tumor. The reinvigoration was characterized by a regain in the ability to produce IL-2, down regulation of co-inhibitory receptors, and a shift to the $KLRG1^+$ effector phenotype.

Part IV

Tumor intrinsic IFN-γ sensing regulates adaptive immune resistance

Chapter 4

Introduction

A striking and unexpected feature of tumor-specific $CD8^+$ TILs is the retained ability to produce IFN-γ within the tumor microenvironment. Laser capture microdissection from human tumors have revealed the expression of IFN-γ transcripts from $CD8^+$ T cells, particularly from areas showing increased PD-L1 expression [164]. A baseline tumor biopsy IFN-γ-based gene signature, suggestive of active IFN-γ signaling, is a strong predictive biomarker for response to anti-PD-1 therapy [109]. In murine studies, sorted tumor antigen-specific $CD8^+$ T cells from the tumor microenvironment show high basal IFN-γ production, via a technique that enables direct analysis *ex vivo* [19]. Together, these observations argue against a terminally "exhausted" $CD8^+$ T cell differentiation state in the context of cancer in which chronically activated T cells have lost all effector functions, as has been observed in the chronic LCMV mouse model [83]. These observations also raise the question of what functional roles IFN-γ is playing in this context. IFN-γ appears to be necessary for immune-mediated tumor rejection in multiple mouse models *in vivo*, based on studies of IFN-$\gamma^{-/-}$ mice or adoptive transfer of IFN-$\gamma^{-/-}$ T cells [165, 166, 61]. In the B16 melanoma model, it has been reported that the positive action of IFN-γ produced by T cells on tumor control could be either on host cells or on tumor cells, and the effect was correlated with diminished angiogenesis [61]. Studies utilizing overexpression of a dominant-negative IFNγR on tumor cells have indicated that in some circumstances, IFN-γ signaling at the level of tumor cells is required for successful immune-mediated tumor regression [167]. In addition, loss-of-function mutations in genes involved in the IFN-γ signaling pathway were identified in two patients with recurrent tumors following initial response to anti-PD-1 treatment, arguing that loss of IFN-γ signaling can be associated with secondary acquired resistance [168]. IFN-γ has been shown to exert anti-proliferative effects on tumor cells, and also to upregulate expression of class I MHC molecules and components of the antigen-processing machinery [169]. However, at the same time, IFN-γ contributed to negative regulation within the tumor microenvironment, in part

through upregulation of PD-L1 and IDO, on either tumor cells or myeloid cells [63, 170]. A recent report suggested that chronic IFN-γ signaling in tumor cells augmented adaptive resistance by driving STAT1-dependent expression of inhibitory ligands [171]. Consistent with these results, in a mouse model of lung inflammation, elimination of IFN-γ signaling on host cells led to elimination of PD-L1 upregulation and exacerbation of tissue injury [172]. Together, these studies suggest both positive and negative roles for IFN-γ signaling for effective immune-mediated tumor control. A greater understanding of the cellular and molecular events downstream from IFN-γ within tumor cells is critical to understand the mechanistic role for this cytokine in antitumor immunity and immunotherapy efficacy.

In order to identify potential immune escape mechanisms that tumor cells might evolve to avoid T cell-mediated destruction, we have utilized an unbiased CRISPR/Cas9-mutagenesis screen in B16.SIY tumor cells exposed to antigen-specific 2C TCR Tg effector CTLs *in vitro*. Among genes identified in this analysis were the IFNγR signaling components IFNγR2 and Jak1, which appeared to be necessary for T cell-mediated killing of tumor cells *in vitro* Recognizing this cell system as a useful tool for studying the dominant role of IFN-γ signaling on tumor cells *in vivo*, we established an experimental model for addressing this role through construction of single CRISPR/Cas9-directed deletions of these genes and subcutaneous tumor implantation into wildtype C57BL/6 mice.

Chapter 5

Results

5.1 Generation of IFN-γ-insensitive B16.SIY cells by CRISPR/Cas9 mutagenesis of the IFNγR2 and Jak1 genes

To examine the role of tumor-intrinsic IFNγR2 and Jak1 we generated IFNγR2- and Jak1-mutant B16.SIY cells using the same single-guide RNAs (sgRNA) that were effective from the CRISPR-library. We began by first normalizing genomic heterogeneity in our B16.SIY cell line by deriving a founder B16.SIY population by single cell cloning. We selected a subclone that showed similar SIY-dsRed expression compared to the bulk population, exhibited typical progressive tumor growth when transplanted into syngeneic mice, and responded to anti-PD-L1 therapy as did the bulk tumor cell population (Figure 5.1A and B). To mutate the IFNγR2 or Jak1 we stably transduced the sgRNA along with a BFP reporter and transiently transfected with a Cas9 plasmid containing blasticidin resistance. We found that mutagenesis was more efficient when the sgRNA was stably transduced, and the BFP reporter allowed us to more easily identify and isolate tumor cells for subsequent experiments. After single cell sorting we confirmed loss of responsiveness to IFN-γ by the failure to upregulate H-2K^{b} after IFN-γ stimulation *in vitro* (Figure 5.1C).

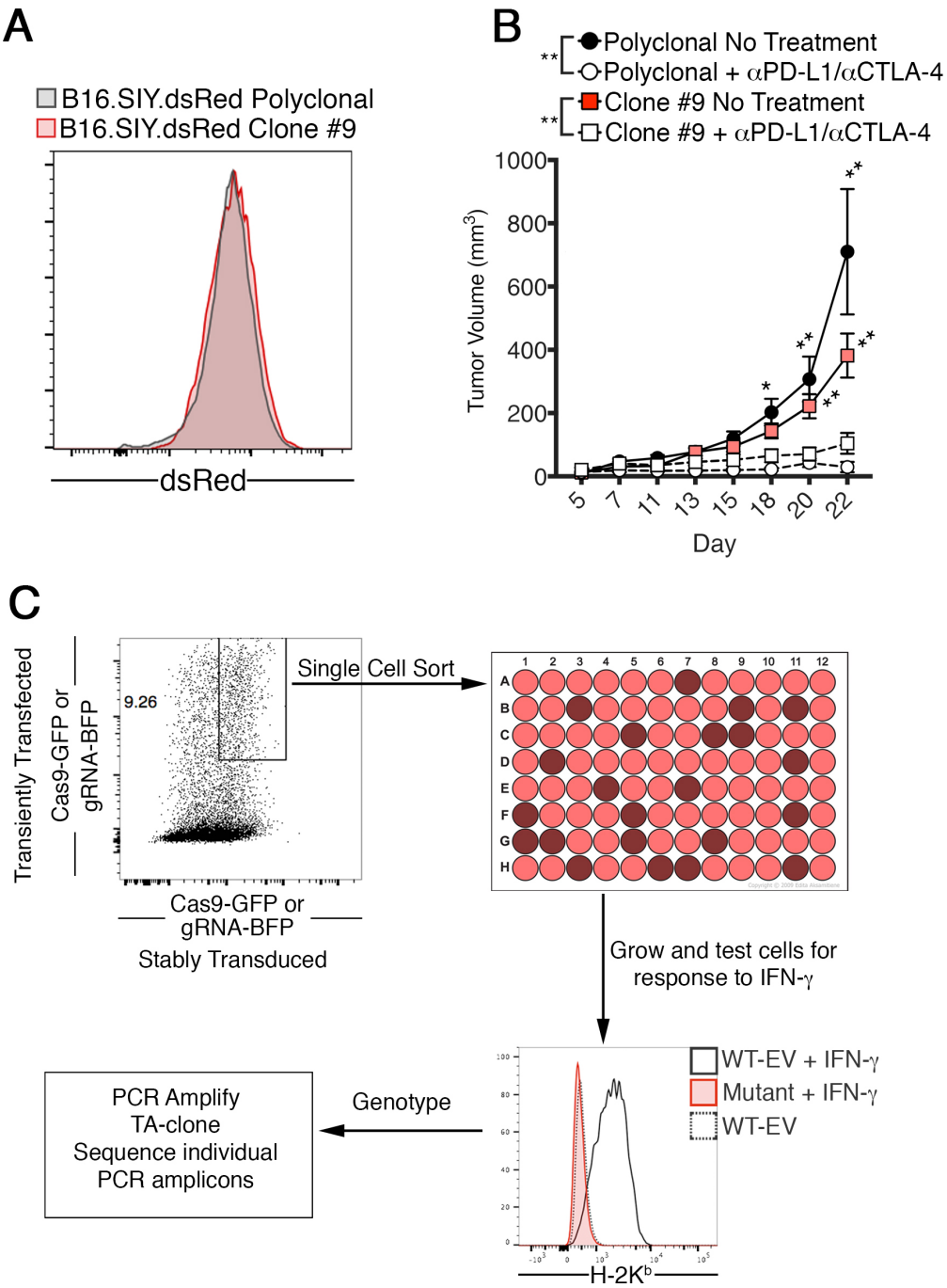

Figure 5.1: Generating IFN-γ insensitive B16.SIY tumor cells
(A) Comparison of dsRed expression between 15 different B16.SIY.dsRed single cell clones. B16.SIY.dsRed tumor cells were single cell sorted into 96-well plates and grown for two weeks. (B) Tumor outgrowth measured in mm (diameter). Treatment groups received 100 μg of anti-PD-L1 + anti-CTLA-4 on days 7, 9, and 12. (C) Schematic of single cell cloning and validation after CRISPR/Cas9-mutagenesis. *:P < 0.05, **:P<0.01. A two-way ANOVA with Bonferroni post-hoc test was used for (B)

5.2 IFNγR2- and Jak1-mutant tumor cells are insensitive to IFN-γ and resistant to *in vitro* mediated T cell killing

We used two different sgRNAs for both genes to control for off-target effects. After single cell sorting we chose 4 subclones (one for each sgRNA) and confirmed disruption of the IFNγR and Jak1 genes (Figure 5.2A). DNA was extracted from these subclones and the genotype was determined by sequencing (Figure 5.2B). CRISPR/Cas9-targeted mutagenesis induced a premature stop codon in all alleles in all clones, with the exception of Jak1.37 allele 2, which obtained an in-frame 6 base pair deletion (Figure 5.2B). To control for any additional epitopes from the BFP protein, we transduced the WT B16.SIY subclone with an empty-BFP reporter. To validate our initial *in vitro* CRISPR/Cas9 screen we used the same killing assay with the IFNγR2- and Jak1-mutant B16.SIY cells and found that these mutant subclones were indeed relatively resistant to *in vitro* 2C-mediated cytolysis *in vitro*, confirming our initial genome-wide screen results (Figure 5.2C).

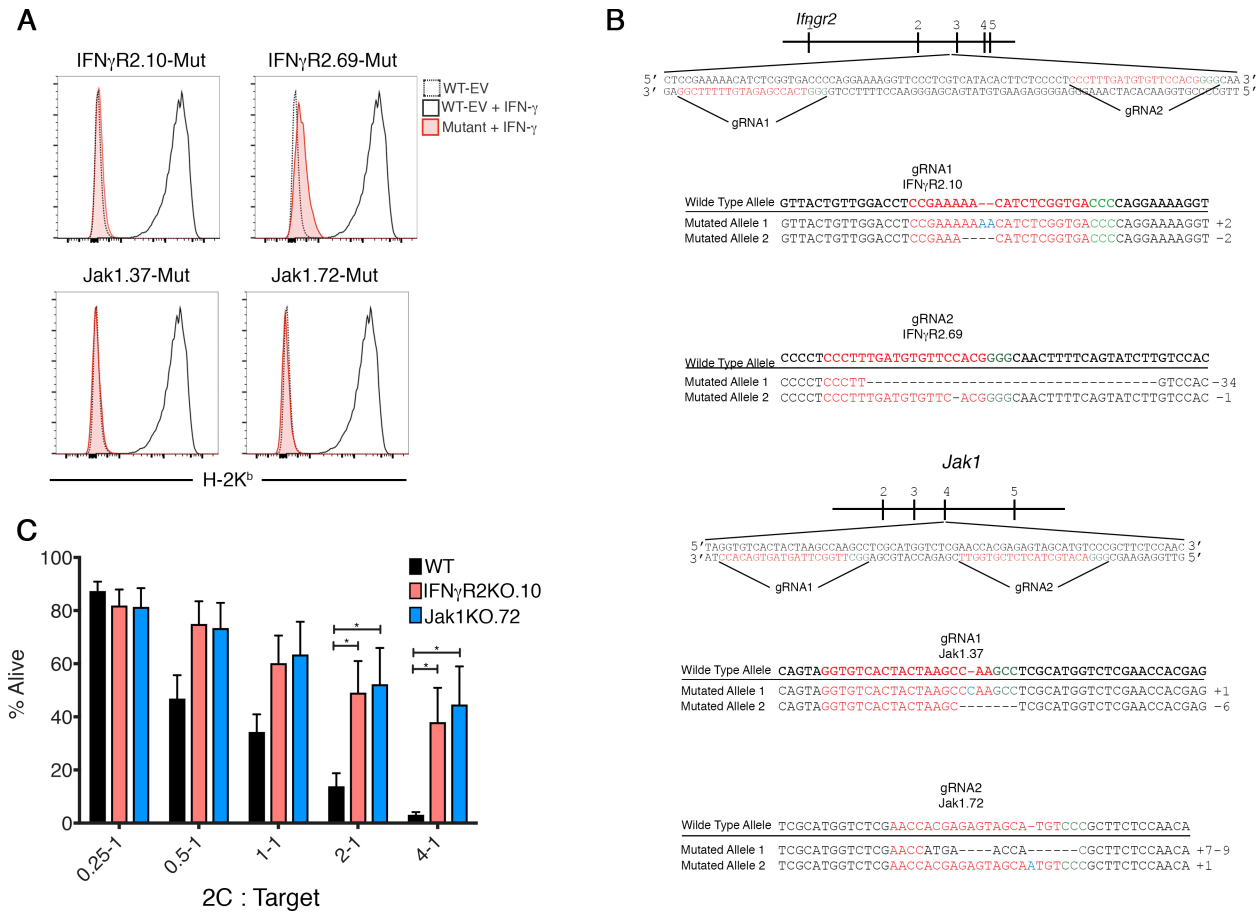

Figure 5.2: Generating IFN-γ insensitive B16.SIY tumor cells
(A) H-2K^{b} expression after IFN-γ stimulation of WT and IFNγR2- and Jak1-mutant subclone populations *in vitro*. (B) Genotype of the IFNγR2- and Jak1-mutant subclones. (C) 2C-mediated *in vitro* killing of WT or IFNγR2- and Jak1-mutant subclones. *:P < 0.05. A Kruskal-Wallis (non-parametric) test was used for (C).

5.3 IFN-γ-insensitive tumors are paradoxically spontaneously controlled *in vivo* in multiple tumor models

In order to assess the behavior of IFNγR2- and Jak1-mutant tumor cells *in vivo*, they were transplanted subcutaneously into C57BL/6 mice. Unexpectedly, both IFNγR2- and Jak1-mutant B16 tumors were spontaneously rejected by day 14. This was not due to increased immunogenicity from BFP expression as WT-BFP B16.SIY tumors grew progressively (Figure 5.3A). To be certain that loss of IFN-γ signaling was responsible for the spontaneous control of the IFNγR2-mutant tumor, we retrovirally re-introduced IFNγR2 and Jak1 into IFNγR2- and Jak1-mutant cells respectively, and confirmed successful IFN-γ signaling by H-2K^{b} upregulation after IFN-γ stimulation and *in vivo* (Figure 5.3B and C and data not shown for Jak1). These IFNγR2- and Jak1-mutant tumors with restored IFN-γ signaling exhibited similar progressive growth kinetics compared to wild type tumors in B6 mice (Figure 5.3D and data not shown). This restoration of tumor growth kinetics indicates that on- or off-target mutations from CRISPR/Cas9-mutagenesis, which could lead to increased immunogenecity through generation of neoantigens, was not responsible for the spontaneous control of IFN-γ-insensitive tumors.

It was desirable to assess whether a similar effect would be seen in another tumor system beyond B16.SIY melanoma. Therefore, we generated MC38 IFNγR2- and Jak1-mutant tumors using a similar CRISPR/Cas9 method and confirmed loss of IFN-γ signaling *in vitro* (Figure 5.3E). As we observed with the B16.SIY model, MC38 IFNγR2- and Jak1-mutant tumors exhibited markedly slowed tumor growth *in vivo* (Figure 5.3F). Next, since B16.SIY and MC38 are known to be antigenic, we tested whether this phenotype was observed in a less antigenic model, B16F10. To test this, we mutated IFNγR2- and Jak1 and confirmed successful disruption of IFN-γ signaling (Figure 5.3G). Because B16F10 tumors are highly aggressive, we decreased the number of tumor cells inoculated to 100,0000 to allow for more time for the immune system to mount a response. While the difference in tumor growth was

minor, the IFNγR2- and Jak1-mutant B16F10 tumors trended towards slower tumor growth (Figure 5.3H). These data indicate that the antigenicity of the tumor likely is a contributing factor to the growth kinetics if IFN-γ-insensitive tumors.

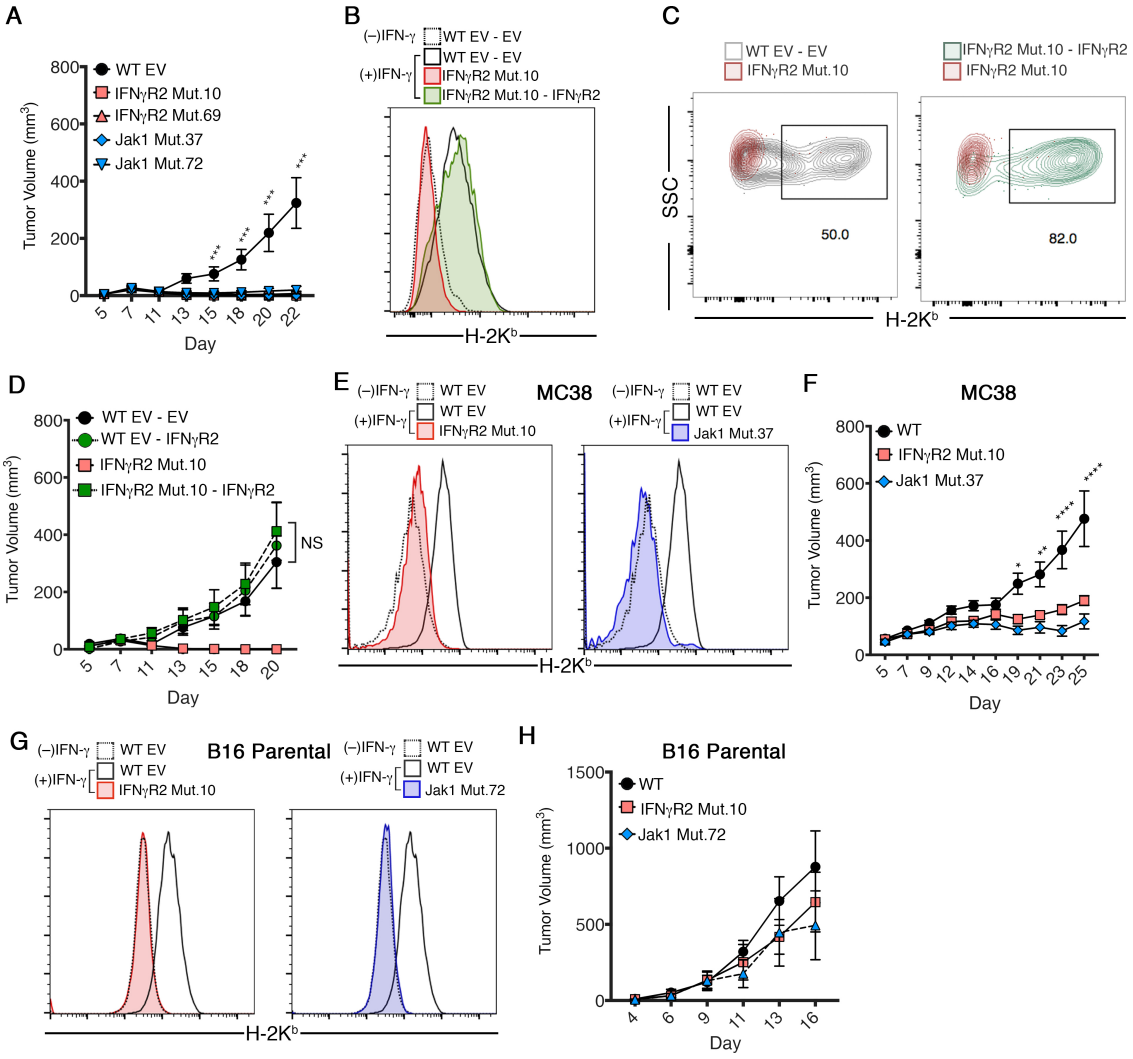

Figure 5.3: IFN-γ-insensitive tumors are spontaneously controlled *in vivo*
(A) Outgrowth kinetics of IFNγR2- and Jak1-mutant tumors measured in mm^3. Mice were inoculated with $2x10^6$ of indicated tumor cell populations. n=5; two independent experiments. (B) Representative histogram of H-$2K^b$ expression after IFN-γ stimulation *in vitro*. 50,000 tumor cells were incubated for 16-20 hours with 2 μg/mL IFN-γ. (C) Representative flow plot of H-$2K^b$ expression on tumor cells from B16.SIY WT tumors (left) or IFNγR2 Mut.10-IFNγR2 (right) tumor isolated on day 7. H-$2K^b$ expression is compared to tumor cells isolated from B16.SIY IFNγR2 Mut.10 tumors. n=5; two independent experiments. (D) Tumor outgrowth kinetics of B16.SIY IFNγR-Mut.10-IFNγR2. n=5; three independent experiments. (E) H-$2K^b$ expression of MC38 IFNγR2- and Jak1-mutant tumors cells after IFN-γ stimulation as in (B). Two independent experiments. (F) Tumor outgrowth kinetics of MC38 IFNγR2- and Jak1-mutant tumors. n=5; two independent experiments. (G) H-$2K^b$ expression of B16F10 IFNγR2- and Jak1-mutant tumors cells after IFN-γ stimulation as in (B). (H) Tumor outgrowth kinetics of B16F10 IFNγR2- and Jak1-mutant tumors in B6 mice. Mice were inoculated with 100,000 of the indicated tumor cells. n=5; two independent experiments. *:$P < 0.05$, **:$P<0.01$, ***:$P<0.001$, ****:$P<0.0001$. A two-way ANOVA with Bonferroni post-hoc test was used for all analyses.

5.4 Spontaneous tumor control is dependent on CD8$^+$ T cells

B16 melanoma is an example of a tumor that shows low expression of class I MHC at baseline, which is upregulated by IFN-γ thereby increasing recognition by CD8$^+$ T cells. As such, it was conceivable that IFN-γ-insensitive tumors became controlled by a distinct immunologic mechanism *in vivo*, such as by NK cells. To address the cellular requirements for this acquired rejection, Rag2$^{-/-}$ mice were engrafted with WT or mutant tumor cells and tumor growth was assessed over time. Both IFNγR2- and Jak1-mutant tumors grew progressively in Rag2$^{-/-}$ mice indicating the observed tumor control is dependent on the adaptive immune system (Figure 5.4A). Next, to investigate which immune cell population was required for tumor control we depleted CD8$^+$ T cells, CD4$^+$ T cells or NK cells with depleting antibodies in C57BL/6 mice before tumor engraftment. While tumor growth in CD4$^+$- and NK-depleted mice was comparable to non-treated mice (Figure 5.4C and D), CD8-depleted mice failed to control IFNγR2- and Jak1-mutant tumors (Figure 5.4B). These data indicate that CD8$^+$ T cells are required for rejection of the IFN-γ-insensitive tumors.

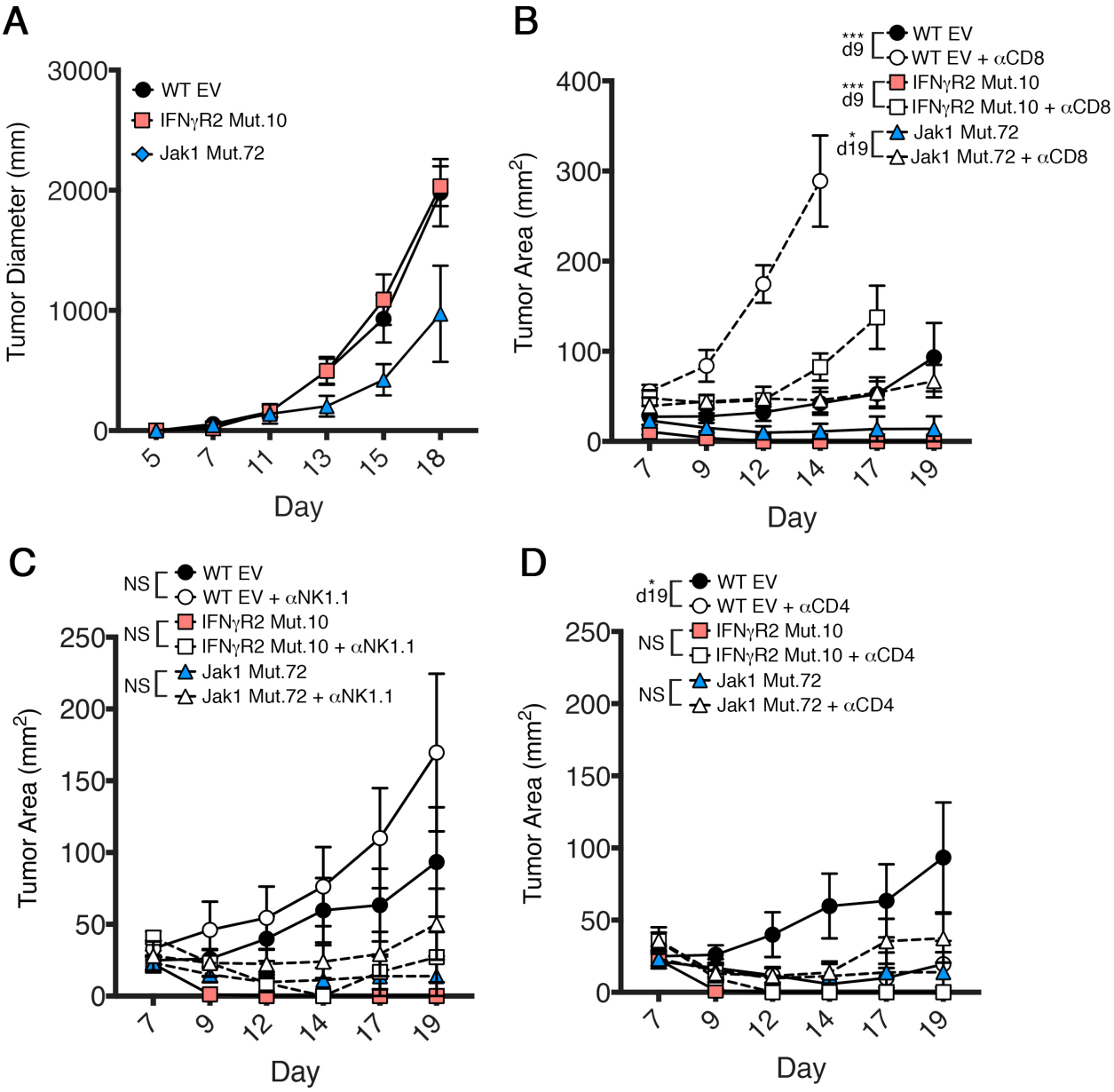

Figure 5.4: CD8^{+} T cells are required to control IFNγR2- and Jak1-mutant tumors

(A) Outgrowth kinetics of IFNγR2- and Jak1-mutant tumors in Rag2$^{-/-}$ mice. n=5; two independent experiments. (B-D) Tumor outgrowth kinetics in mice treated with depleting antibodies against (B) anti-CD8α, (C) anti-NK1.1, or (D) anti-CD4. n=5; two independent experiments. *:P $<$ 0.05, **:P$<$0.01, ***:P$<$0.001, ****:P$<$0.0001. A two-way ANOVA with Bonferroni post-hoc test was used for all analyses.

5.5 The antitumor response against Jak1- and IFNγR2-mutant B16.SIY tumors is augmented and dependent on reduced tumor intrinsic IFN-γ sensing

Next we characterized the antitumor T cell response against IFNγR2 and Jak1-mutant tumors. First, we measured the frequency of SIY-reactive $CD8^+$ T cells in the spleens of mice by an IFN-γ ELISPOT assay. On day 7 after tumor inoculation, we observed a modest increase in the frequency of IFN-γ producing effector cells in response to the SIY antigen (Figure 5.5A). Next, we measured the frequency of tumor antigen-specific $CD8^+$ T cells in the tumor by H-$2K^b$/SIY pentamer staining. Strikingly, on day 7 after tumor challenge, we observed a 3-fold increase in the frequency of H-$2K^b$/SIY^+ $CD8^+$ TILs in IFNγR2- and Jak1-mutant tumors compared to WT tumors. (Figure 5.5B). It was conceivable that off-target mutations were responsible for the increase in H-$2K^b$/SIY^+ $CD8^+$ TIL. We thought this unlikely as tumor outgrowth was returned to normal when IFN-γ signaling was restored (Figure 5.3D). However, it remained possible that the spontaneous tumor control and increase in H-$2K^b$/SIY^+ $CD8^+$ TILs were unrelated to the lack of IFN-γ signaling in tumor cells, with the latter being driven by off-target mutations. To address this possibility, we measured the frequency of antigen-specific $CD8^+$ TILs in IFNγR2-mutant tumors with reintroduced IFNγR2 or Jak1. An analysis of H-$2K^b$/SIY-specific $CD8^+$ TILs on day 7 after tumor inoculations revealed that reintroduction of IFNγR2 and Jak1 reverted the frequency of antigen-specific $CD8^+$ TILs to WT levels (Figure 5.5C and D). Together, these data indicate that priming of SIY-specific $CD8^+$ T cells was slightly augmented against IFNγR2- and Jak1-mutant tumors 5.5A), but it is unlikely that this fully explains the 3-fold increase in SIY-reactive cells in the tumor. Three possibilities remain to explain the increase in H-$2K^b$/SIY^+ $CD8^+$ TILs: first, it could be that T cell recruitment to the tumor site is increased; second, expansion of SIY-reactive TILs is augmented; and third, $CD8^+$ TIL cell death is diminished.

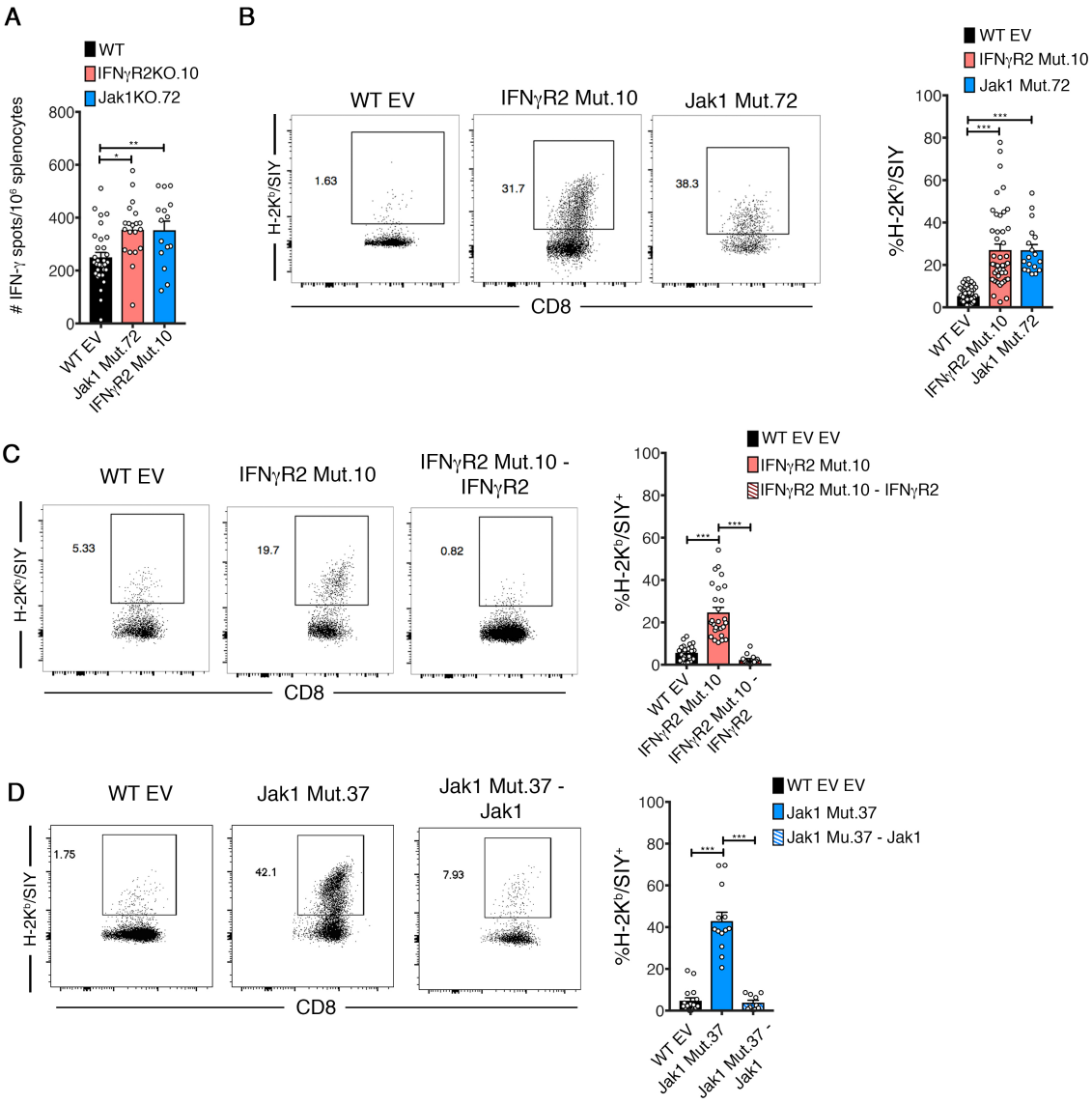

Figure 5.5: CD8$^+$ T cells are required to control IFNγR2- and Jak1-mutant tumors

(A) ELISPOT measuring IFN-γ production in response to soluble SIY. C57BL/6 mice were inoculated s.c. with the indicated tumor cell lines, splenocytes were harvested on day 7 and restimulated with SIY (1.6 nM) for 16 h. n=5; two independent experiments. (B) Representative flow plots and summary of the frequency of H-2K^b/SIY$^+$ CD8$^+$ TILs isolated from WT, IFNγR2- and Jak1-mutant tumors. n=4-5; 4-5 independent experiments. (C and D) Representative flow plots and summary of the frequency of H-2K^b/SIY$^+$ CD8$^+$ TILs isolated from WT, IFNγR2-mutant, IFNγR2-mutant with reintroduced IFNγR2, Jak1-mutant and Jak1-mutant with reintroduced Jak1. *:P $<$ 0.05, **:P$<$0.01, ***:P$<$0.001, ****:P$<$0.0001. A Kruskal-Wallis (non-parametric) test was used for all analyses.

5.6 CD8$^+$ TILs express similar levels of effector molecules against wild-type and IFN-γ-insensitive tumors

Knowing that CD8$^+$ T cells were the imperative immune cell population mediating tumor control we next sought to determine whether CD8$^+$ TILs exhibited heightened cytokine expression against IFNγR2- or Jak1-mutant tumors, as this may help explain why these tumors are spontaneous rejected. To do this, we isolated CD8$^+$ TILs on day 7 after tumor engraftment and measured for expression of *Ifng*, *Gzmb*, *Tnfa*, *Prf1*, and *Il2* by qRT-PCR. We did not observe any major differences in expression of these cytokines among CD8$^+$ TILs isolated from WT, IFNγR2-, and Jak1-mutant tumors (Figure 5.6A). These data indicate that the CD8$^+$ TIL compartment contains the necessary cytotoxic functions to eradicate IFNγR2- and Jak1-mutant tumors but not WT tumors, suggesting another aspect of CD8$^+$ TILs may be responsible for tumor control.

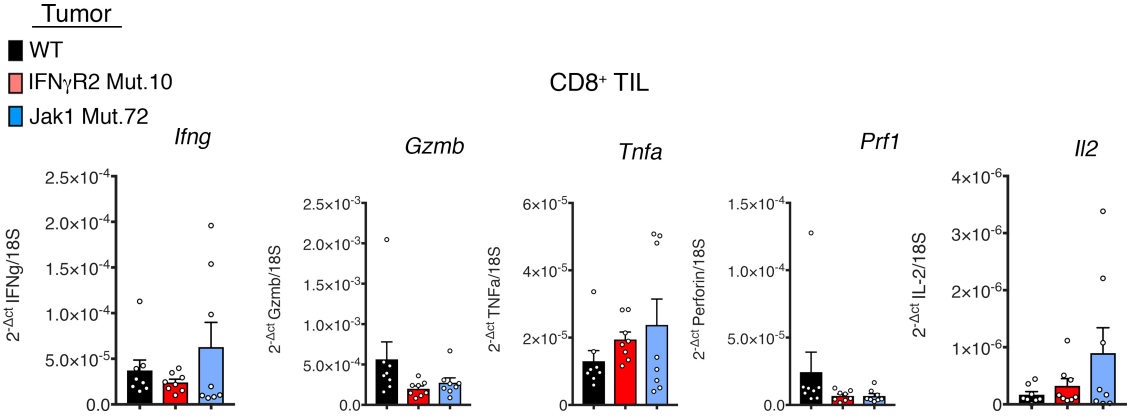

Figure 5.6: Effector gene expression against WT and IFN-γ-insensitive tumors are expressed at similar levels
(A) CD8$^+$ TILs were isolated on day 7 after engraftment of indicated tumors by cell sorting. n=4; two independent experiments.*:P $<$ 0.05, **:P$<$0.01, ***:P$<$0.001, ****:P$<$0.0001. A Kruskal-Wallis (non-parametric) test was used for all analyses.

5.7 Restored expression of PD-L1 re-establishes progressive tumor growth of IFN-γ-insensitive tumors

The augmented antitumor T cell response in the absence of IFNγR2 on tumor cells led us to hypothesize that a negative regulatory pathway dependent on IFN-γ sensing might have been eliminated, enabling improved T cell-mediated tumor rejection. The obvious candidates were PD-L1 and IDO. With WT B16.SIY tumors analyzed at day 7 *ex vivo*, we found that very little IDO mRNA was expressed by the tumor cells themselves; rather, high levels of expression were observed among non-tumor immune cells (Figure 5.7A). In contrast, very high expression of PD-L1 was observed by the tumor cells and host APCs directly (Figure 5.7B and C), as we had reported previously [63]. Therefore, we analyzed expression of PD-L1 by IFN-γ-insensitive tumors following *in vivo* growth for 7 days. In fact, IFNγR2 and Jak1-mutant tumor cells showed a marked reduction of PD-L1 expression compared to WT tumor cells (Figure 5.7B and D). This was confirmed by qRT-PCR analysis on sorted tumor cells (Figure 5.7E). These results suggested the possibility that reduced PD-L1 expression might be responsible for improved tumor control. To test this notion, we retrovirally restored expression of PD-L1 in IFNγR2- and Jak1-mutant B16.SIY cells (Figure 5.7F). Interestingly, restored expression of PD-L1 in IFNγR2- and Jak1-mutant tumor cells re-established the progressive growth kinetics seen with WT tumors (Figure 5.7G) but did not substantially decrease the frequency of H-2K^{b}/SIY^{+} CD8^{+} TILs (Figure 5.7H). These results suggested that PD-L1 may be acting directly at the T cell:tumor cell interface to inhibit CD8^{+} T cell cytotoxicity. If this were true, by removing tumor recognition by CD8^{+} T cells, IFN-γ-insensitive tumors should not be spontaneously rejected. To test this, we deleted H-2K^{b} in the IFNγR2-mutant tumor and tracked tumor growth. Indeed, IFN-γ-insensitive tumors lacking H-2K^{b} grew progressively (Figure 5.7I). These results indicate that IFNγR2- and Jak1-mutant tumors are better controlled immunologically through defective expression of PD-L1, in a manner dependent on direct tumor recognition by CD8^{+} TILs.

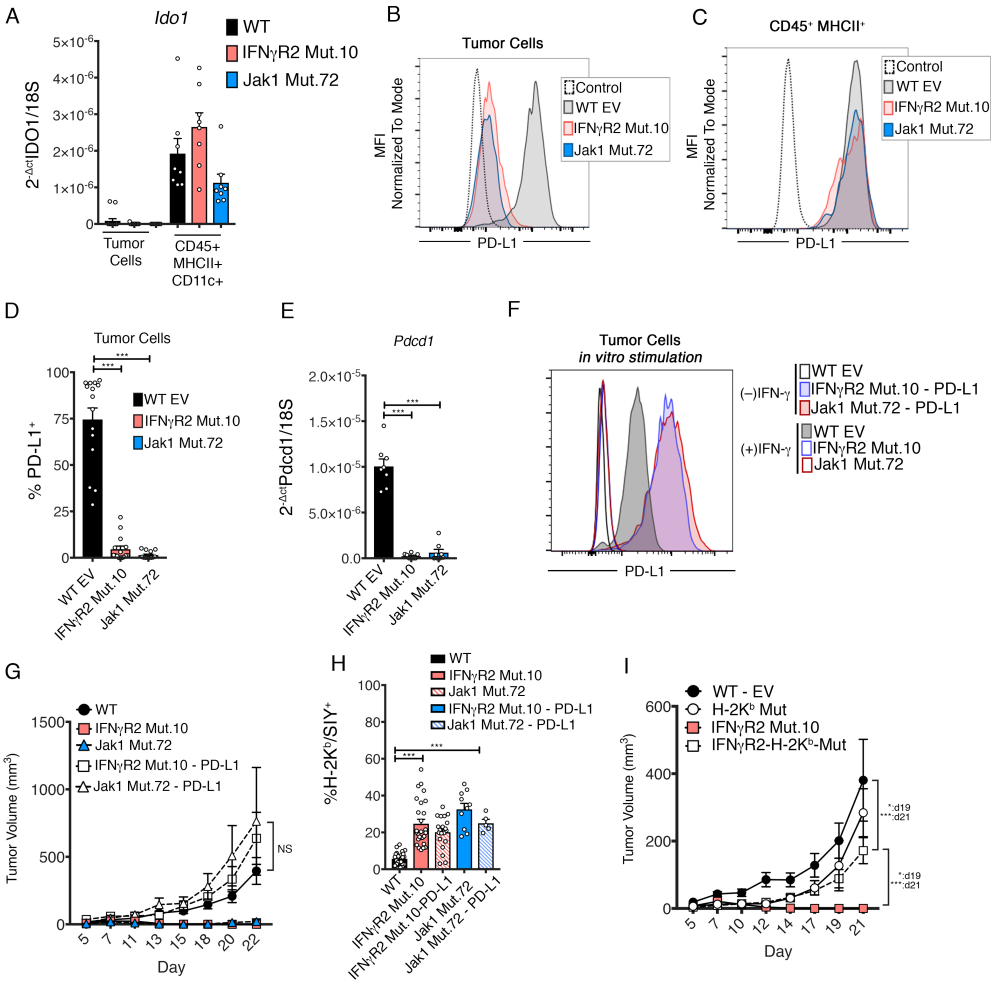

Figure 5.7: Restored expression of PD-L1 re-establishes progressive tumor growth of IFN-γ insensitive tumors

(A) *Ido* mRNA levels in tumor cells and host APCs from WT, IFNγR2-, and Jak1-mutant tumors. n=5; 2 independent experiments. (B) Representative histogram of PD-L1 MFI on indicated tumor cell populations. n=5; 5 independent experiments. (C) Representative histogram of PD-L1 MFI on $CD45^{+}MHCII^{+}$ cells isolated from indicated tumors. n=5; two independent experiments. (D) Percent of indicated tumor cell populations positive for PD-L1. n=5; 3 independent experiments. (E) *Pdl1* mRNA levels in indicated tumor cell populations. n=5; two independent experiments. (A-D) All cell isolations occurred on day 7. (F) Representative histogram of PD-L1 expression *in vitro* after retroviral transduction of PD-L1. n=3; two independent experiments. (G) Outgrowth kinetics of IFNγR2- and Jak1-mutant tumors when PD-L1 is re-expressed. n=5; two independent experiments. (H) Summary of the frequency of $H\text{-}2K^{b}/SIY^{+}$ $CD8^{+}$ TILs isolated from WT, IFNγ-insensitive tumors, and IFNγ-insensitive tumors with retroviral re-expression of PD-L1. (I) Outgrowth kinetics of IFNγR2 $H\text{-}2K^{2}$-double mutant tumors. n=5; two independent experiments. *:$P < 0.05$, **:$P<0.01$, ***:$P<0.001$. A Kruskal-Wallis (non-parametric) test was used for A,D, and E, and a two-way ANOVA with Bonferroni post-hoc test was used for G, H, and I

Guide RNA Sequences		
Gene Target	sgRNA1	sgRNA2
IFNγR2	TCACCGAGATGTTTTTCGG	CCCTTTGATGTGTTCCACG
Jak1	CCACAGTGATGATTCGGTT	TTGGTGCTCTCATCGTACA
H-2K^{b}	ACCAGCAGTACGCCTACGA	
PD-L1	GTAGAAAACATCATTCGCTG	GCTTCCCACTCACGGGTTGG

Table 5.1: Single-guide RNA sequences

5.8 Discussion Part II

An IFN-γ gene signature has been observed in many cancer types and is associated with improved clinical response to immunotherapy [173, 174, 175]. While, IFN-γ has many well-known antitumor properties, IFN-γ signaling can be co-opted by tumor cells to induce the expression of negative regulatory receptors and molecules. Early studies dissecting the effects of IFN-γ on tumor cells used a dominant negative IFNγR1 or tumor cells generated in IFNγR1$^{-/-}$. These studies pointed to the effects of IFN-γ as solely antitumor, mainly through the upregulation of antigen presentation machinery. Therefore, it was not surprising that disruption of the IFNγR2 gene rendered tumor cells resistant to T cell mediated killing *in vitro*. However, contrary to our initial hypothesis, IFN-γ-insensitive tumors were spontaneously rejected when implanted into mice. When IFNγR2 and Jak1 expression was restored, tumor growth was normalized, indicating that IFN-γ-insensitive tumors were not more immunogenic, which may occur during the Cas9 mutagenesis process. Moreover, in another tumor model, MC38, tumor growth was also delayed in IFN-γ-insensitive tumors. However, both the B16.SIY and MC38 models are generally considered to be immunogenic. Which may explain why no significant difference in tumor growth was observed in IFN-γ-insensitive B16F10 tumors.

Depletion of CD8$^+$ T cells, NK cells, and CD4$^+$ T cells, revealed a necessary role for CD8$^+$ T cells for the rejection of IFN-γ-insensitive tumors. In line with this observation was the necessity of H-2K^b expression by tumor cells from the CD8$^+$ T cell mediated tumor control. Functional profiling of CD8$^+$ TILs directly *ex vivo* did not reveal any differences in the expression of cytotoxic genes, indicating that the CD8$^+$ TIL compartment contained the necessary components to mediate tumor rejection. By using H-2K^b/SIY-pentamer staining we were able to track the tumor antigen-specific CD8$^+$ T cell response against IFN-γ-insensitive tumors. This analysis revealed a marked increase in the frequency of H-2K^b/SIY$^+$ CD8$^+$ TILs. This augmentation was reverted when IFNγR2 or Jak1 was reintroduced, suggesting that some negative regulators may not be upregulated due to the inability of tumor cells to

sense IFN-γ.

The most well-known and well defined example of an IFN-γ-inducible negative regulator is PD-L1. In fact, in several murine models of cancer [63, 176] and in some human cancer cell lines [170], IFN-γ seems to be the main driver of PD-L1 expression. Flow cytometric and transcript analysis of IFN-γ-insensitive tumor cells revealed a lack of PD-L1 expression. Reintroduction of PD-L1 in these tumors restored tumor growth but did not substantially decrease the frequency of H-2K^{b}/SIY^{+} CD8^{+} TILs. We believe that PD-L1 may be acting directly at the T cell:tumor cell interface to inhibit CD8^{+} T cell cytotoxicity. In line with this hypothesis, PD-L1-deficient tumors did not exhibit an increase in the frequency of H-2K^{b}/SIY^{+} CD8^{+} TILs, indicating that other IFN-γ-regulated genes are responsible for this accumulation. It will be important to determine the complete IFN-γ-driven negative regulatory pathways, as this may lead to the development of new and novel immunotherapies.

Part V

Discussion

Chapter 6

Identifying and describing dysfunctional antigen-specific CD8$^+$ TILs and their role in the endogenous antitumor T cell response

6.1 From *in vitro* anergy to *in vivo* dysfunction

Dysfunction of tumor antigen-specific TILs is characteristic of the T cell-inflamed tumor microenvironment phenotype, and likely explains the paradox of progressing tumors in the face of ongoing immunity (Figure 6.1). However, identifying tumor antigen-specific TILs among the background of passively trafficking irrelevant T cells, and understanding this phenotype as a differentiation state, had been hampered by a lack of accurate surface markers. Based on previous work identifying the transcription factor Egr2 as a critical regulator of T cell anergy under reductionist conditions *in vitro*, we applied knowledge of Egr2 targets to evaluate applicability of these markers toward understanding dysfunctional T cells within tumors *in vivo*. Our current data indeed confirm that co-expression of LAG-3 and 4-1BB is sufficient to identify the majority of tumor antigen-specific CD8$^+$ T cells within the tumor microenvironment. Co-expression of these markers was not observed within peripheral lymphoid organs in tumor-bearing mice, suggesting that a property unique to the tumor context drives 4-1BB and LAG-3 expression. In addition, acquisition of LAG-3 and 4-1BB expression was not observed within tumors that were undergoing successful rejection, arguing that the acquisition of this phenotype occurs under conditions of incomplete antigen clearance.

While the molecular characterization of anergic CD4$^+$ T cells *in vitro* provided the foundational information that enabled the study of dysfunctional CD8$^+$ TILs *in vivo*, it is clear that these two T cell states are not identical and only partially overlapping. Egr2 was expressed in a subpopulation of CD8$^+$ TILs and this population was enriched in several Egr2 target genes, including 4-1BB and LAG-3. However, Egr2 expression did not define the entire population of 4-1BB$^+$LAG-3$^+$ TIL. In addition, conditional deletion of Egr2 in T cells only showed a partial functional role of Egr2 in regulating 4-1BB and LAG-3 expression suggest-

ing that other factors such as HIF-1α and Egr3 might compensate in the regulation of these receptors. In addition, NF-κB and NFAT/AP-1 have been implicated in 4-1BB expression after TCR stimulation [177, 178]. It will be of interest to elucidate the full transcription factor network that mediates the dysfunctional state of $CD8^+$ TILs *in vivo*, as inhibiting these pathways may lead to novel immunotherapeutics.

6.2 Describing dysfunctional $CD8^+$ TILs and possible immune regulatory functions

The induction of T cell exhaustion during chronic infection is thought to be a mechanism to limit collateral damage to the host [179], and IFN-γ has been implicated in both pro-inflammatory and immune-regulatory roles in chronic infection [180, 181]. Therefore, dysfunctional antigen-specific $CD8^+$ TILs may contribute to the overall immune suppressive network within the tumor microenvironment (Figure 6.1). IFN-γ produced by antigen-specific $CD8^+$ TILs results in upregulation of PD-L1 on tumors cells and IDO expression by infiltrating myeloid cells [63]. In addition, the production of the chemokines CCL22 and CCL1 by these T cells likely contributes to Treg recruitment into the tumor microenvironment. Our laboratory had previously shown that PD-L1 and IDO upregulation, as well as Treg accumulation within the tumor, all depend on $CD8^+$ T cells [63], and our current work has indicated that the 4-1BB$^+$LAG-3$^+$ subset is the major source of IFN-γ and chemokines mediating these effects. Thus, the dysfunctional $CD8^+$ TILs might be viewed as part of the regulatory network from this perspective. Further work will be needed to understand the full functional contribution of these cells to immune regulation within the tumor microenvironment.

Significant effort has been aimed at understanding the molecular mechanisms of T cell dysfunction using various model systems, both *in vitro* and *in vivo*. The term T cell anergy was originally applied to describe a hyporesponsive state resulting from TCR ligation in the

absence of co-stimulation in $CD4^+$ Th1 clones [182]. However, the term T cell anergy has since been used to describe many different types of tolerance phenomena [28]. T cell exhaustion was originally described in models of chronic viral infection, particularly the LCMV clone 13 model [183]. It has been assumed that the similarities between chronic infection and progressing tumors, such as persistent antigen exposure and involvement of negative regulatory pathways, implied an identical or similar dysfunctional state in these two disease contexts [184]. Indeed, many of the co-inhibitory receptors expressed on $CD8^+$ TILs and exhausted virus-specific T cells are shared as well as a component of the gene expression network (Figure 3.14) [185, 90]. However, the mechanisms inducing and maintaining $CD8^+$ TIL dysfunction are likely regulated by additional factors that differ between chronic infections and cancer, such as the balance between metabolic provision and demands on the T cells [186], as well as the tissue localization of the effects. In addition, T cells in different tumor microenvironments could differentiate into unique dysfunctional states. Therefore, it may be preferable to describe this phenotype more descriptively, as "T cell dysfunction within the tumor microenvironment" rather than "anergy" or "exhaustion". Furthermore, our current work emphasizes that the term dysfunction does not imply complete lack of function. Indeed, cytolytic capacity of the 4-1BB$^+$LAG-3$^+$ population was retained as analyzed directly *ex vivo*. Therefore, the failure of the endogenous immune response to eliminate the tumor does not appear to be attributable to a lack of intrinsic cytolytic activity by antigen-specific T cells.

6.3 A range of co-inhibitory and co-stimulatory receptor expression on antigen-specific dysfunctional $CD8^+$ TILs

The use of 4-1BB and LAG-3 as markers of dysfunctional tumor-reactive T cells enabled flow cytometric sorting for gene expression profiling without altering transcript levels that could be caused by TCR ligation through MHC/multimer binding. Comparison of two tumor-

specific dysfunctional $CD8^+$ TIL gene expression profiles to the LCMV-specific exhausted profile indicated a greater overlap of the genetic signature in the tumor context. In addition, pathways regulating the cell cycle were enriched among the $CD8^+$ TIL profiles suggesting that unchecked proliferation may be an additional characteristic of the dysfunctional state within the tumor microenvironment. Gene expression analysis also revealed upregulated transcripts encoding additional co-inhibitory receptors, but also several co-stimulatory receptors. This latter observation was unexpected based on the phenotype of dysfunctional $CD8^+$ T cells in chronic infection models [185, 187]. Observations in these models suggest that co-stimulatory receptors on exhausted $CD8^+$ T cells are expressed at low levels or wane over time [188, 187, 150], on the contrary, dysfunctional $CD8^+$ TILs continually expressed several co-stimulatory receptors (4-1BB, OX-40 and GITR). These data suggest a scenario in which persistently activated $CD8^+$ TILs are in a state of chronic activation and are awaiting engagement by co-stimulatory ligands, which might be inadequately available within the tumor microenvironment. This notion is consistent with the therapeutic effect of combined 4-1BB ligation added to LAG-3 blockade, which might be viewed as rescuing TILs from a paucity of 4-1BB signaling. The net composition of ligands for co-stimulatory versus co-inhibitory receptors within the tumor could contribute to the ultimately functional phenotype of tumor antigen-specific TILs and will be an interesting question to pursue in future studies.

6.4 Phenotypic and functional changes after therapeutic targeting of dysfunctional TILs by anti-4-1BB + anti-LAG-3 antibody treatment

Our gene expression profiling of the dysfunctional $CD8^+$ TIL population allowed us to determine additional cell surface receptors co-expressed by this population and track these markers during antibody therapy. While the significant decrease in NRP1 and 2B4 and in-

crease in KLRG-1 expression in the tumor-specific H-2K^{b}/SIY^{+} cells suggest a phenotypic response in the 4-1BB^{+}LAG-3^{+} TIL subset, it remains possible that a precursor population found in the 4-1BB^{-}LAG-3^{-} subset could be a source of cells for the observed changes in the CD8^{+} TIL population overall. We believe this is unlikely due to several observations. First, approximately 17% of H-2K^{b}/SIY^{+} CD8^{+} TILs are found in the 4-1BB^{-}LAG-3^{-} subpopulation and since transcript levels of *Tnfrsf9* (4-1BB) and *Lag3* do not change upon treatment (unpublished data), it remains likely that the phenotypic changes occur in the 4-1BB^{+}LAG-3^{+} subpopulation. Second, the 4-1BB^{-}LAG-3^{-} population displays a phenotype closely resembling memory precursor effector cells (MPEC; KLRG-1^{lo}IL-7Rα^{hi}CD44^{+}, which are thought not to give rise to short-lived effector cells (SLEC; KLRG-1^{hi}IL-7Rα^{lo}) [189, 190]. While we do not formally prove a direct causal relationship between antibody treatment and phenotypic changes in the 4-1BB^{+}LAG-3^{+} population, indirect evidence suggests that this is the case.

Our previous work had suggested that restoration of IL-2 production in the CD8^{+} TIL compartment strongly correlated with the therapeutic efficacy of anti-CTLA-4 + anti-PD-L1 or combined with an IDO inhibitor [161]. Our current results also identified restored IL-2 production by tumor antigen-specific CD8^{+} TILs in response to anti-4-1BB + anti-LAG-3 therapy. Thus, restoration of IL-2 might be a useful pharmacodynamic biomarker to be measured in post-treatment biopsies in patients participating in immunotherapy clinical trials. However, it is not yet known if restored IL-2 production is functionally important for antitumor T cell efficacy or serves as a correlate to refunctionalized CD8^{+} TILs, a possibility that should be investigated in future studies.

Both anti-4-1BB and anti-LAG-3 mAbs are being tested in early phase clinical trials, and it is attractive to consider a combination study in human cancer patients. The ability of CD8^{+} TILs to upregulate KLRG-1 and downregulate 2B4 and NRP1 expression could be additional translational biomarkers. As some patients do not respond to anti-PD-1-based therapies, novel combinations may have utility in such individuals. Moreover, the additional

co-stimulatory and co-inhibitory receptors identified in our current work could represent functionally relevant targets for new immunotherapy strategies.

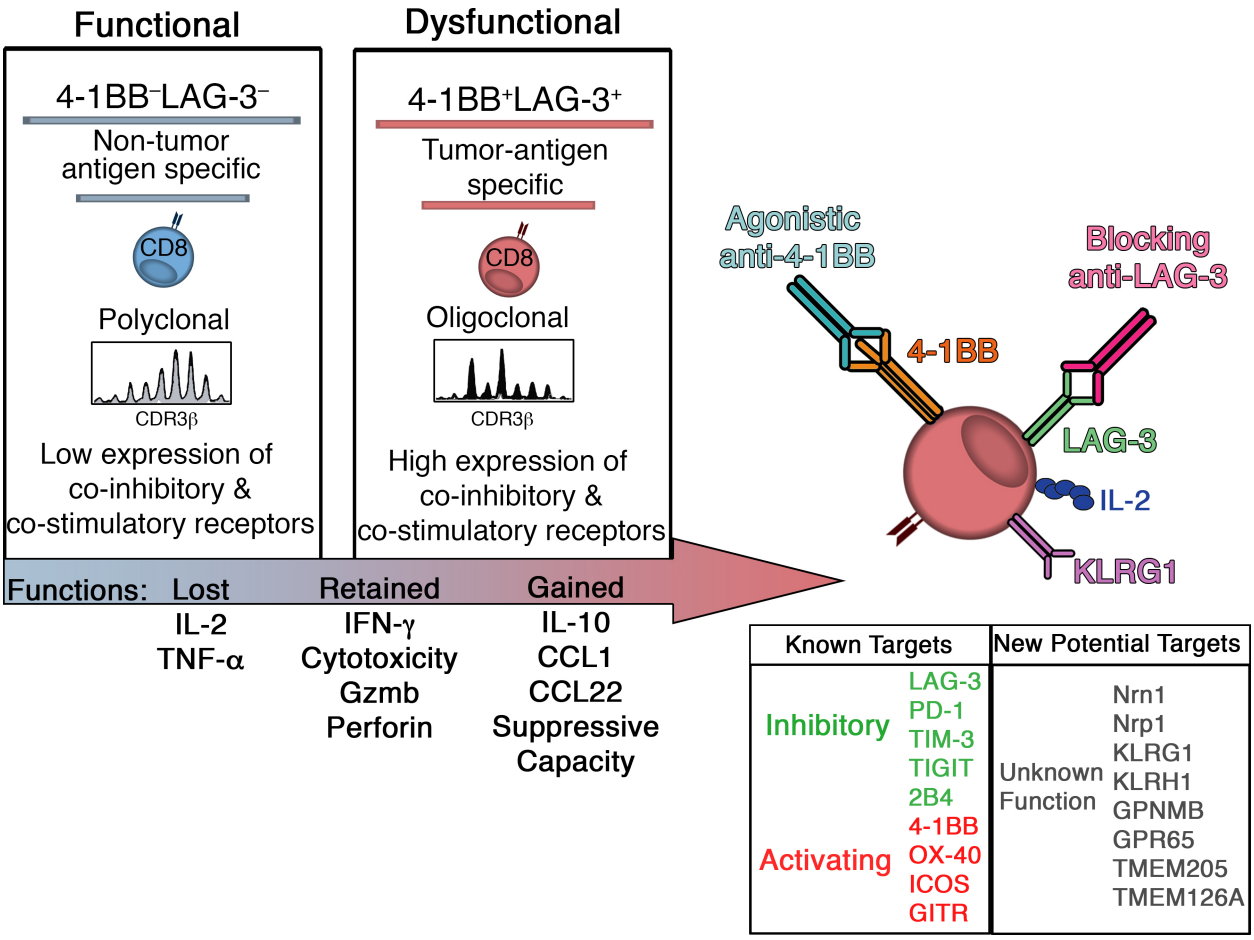

Figure 6.1: Phenotypic and functional characterization of dysfunctional CD8$^+$ TILs and new potential therapeutic targets.
After entering the tumor microenvironment, antigen-specific CD8$^+$ T cells upregulate both co-inhibitory and co-stimulatory receptors. As the tumor progresses, they lose the ability to produce IL-2 and TNF-α, retain the production of IFN-γ and the ability to lyse target cells, and begin to produce CCL1, CCL22, IL-10 and exhibit suppressive activity. Targeting of these now dysfunctional antigen-specific CD8$^+$ TILs by means of agonizing 4-1BB and blocking LAG-3, restores the restores the function of these cells and drives them into an effector memory T cell phenotype.

Chapter 7

Tumor intrinsic IFN-γ sensing regulates adaptive resistance

7.1 Centering on the IFN-γ pathway as a critical regulator of adaptive and acquired resistance

Based on our observation that dysfunctional $CD8^+$ TILs produce abundant amounts of IFN-γ in the tumor microenvironment, we became interested on what role IFN-γ was playing during the different phases of tumor progression. While it is well known that IFN-γ is generally necessary for T cell-mediated tumor rejection in vivo, IFN-γ can also induce expression of negative regulatory factors when secreted within the tumor microenvironment [176, 170, 175]. The extent and relative contribution of this process among tumor cells versus host cells during the different phases of tumorigenesis had been incompletely elucidated. Our current data indicate that, at least in some tumor models, IFN-γ signaling at the level of the tumor cell can drive a dominant immune-regulatory process, through upregulation of PD-L1 expression.

The functional contribution of PD-L1 on tumor cells versus host APCs in engaging PD-1 on TILs and inhibiting T cell function has been controversial but likely varies with the tumor type and degree of antigenicity. In human cancer patients, T cell-infiltrated tumors can show PD-L1 upregulation on either tumor cells or myeloid cells, and each can be associated with anti-PD-1 therapeutic efficacy in defined contexts [191]. In mouse models, $PD\text{-}L1^{-/-}$ hosts have been reported to show improved antitumor immunity in some model systems [192, 193], but in other models CRISPR-Cas9-mediated disruption of the PD-L1 gene in tumor cells can be sufficient for improved tumor control [194]. In our current work, we utilized the B16.SIY and MC38 models, which have high antigenicity and prime strong $CD8^+$ T cell responses, even though the tumors eventually grow progressively. It seems clear now that a major mechanism for that ultimate tumor growth is through PD-L1 upregulation on tumor cells via persistent IFN-γ production in the tumor microenvironment (Figure 7.1).

7.2 Discrepancies between *in vitro* and *in vivo* models systems

Our *in vitro* CRISPR screen led us to the hypothesis that tumor cell-intrinsic IFN-γ signaling pathway was necessary for T cell-mediated tumor cell killing *in vitro*. These results are consistent with other recently published CRISPR screens that similarly identified IFN-γ signaling mutants using *in vitro* T cell selection systems [195, 196]. We validated that loss of IFNγR2 and Jak1 rendered tumor cells resistance to T cell-mediated lysis *in vitro*. Yet, the opposite result was observed when these tumor cells were implanted into mice *in vivo*. These discrepant phenomena are likely explained by differing requirements for tumor cell killing and for class I MHC upregulation *in vitro* versus *in vivo*. Short-term *in vitro* lysis assays are highly sensitive to the level of class I MHC expression by target cells, and cultured B16 melanoma cells show undetectable expression of H-2K^{b} by flow cytometry *in vitro*. However, following implantation subcutaneously into mice, class I MHC upregulation is observed. While most of this upregulation is IFN-γ-dependent, a component is likely IFN-γ-independent. In order to prove whether the low levels of class I MHC on IFN-γ-insensitive B16.SIY cells were sufficient for T cell recognition *in vivo*, we utilized CRISPR/Cas9 to delete H-2K^{b} and indeed found reversion to a progressively growing tumor phenotype. IFNγR2-H-2K^{b}-double-mutant tumors grew progressively *in vivo*. Together, these results make an argument for directly using *in vivo* tumor model systems for screening strategies aiming to identify candidate immune evasion mechanisms mediating immunotherapy resistance.

7.3 IFN-γ driven immune suppressive mechanisms regulating the magnitude of the antitumor CD8^{+} T cell response

Our results revealed that an increased frequency of antigen-specific CD8^{+} T cells was detected in the setting of IFN-γ-insensitive tumors. While it is conceivable that PD-L1 expression on tumor cells limits T cell expansion in the tumor microenvironment, it is worth considering broader potential mechanisms by which lack of IFN-γ signaling on tumor cells

might translate into increased accumulation of tumor antigen-specific $CD8^+$ TILs. In general, IFN-γ drives a significant transcriptional program in host cells that promotes increased antigen processing, antigen presentation, and secretion of immune cell-recruiting chemokines. It is conceivable that absence of IFN-γ responsiveness on tumor cells liberates additional IFN-γ that can have positive effects on host APCs. But it is also possible that IFN-γ induces upregulation of additional ligands that are inhibitory for T cells. IFN-γ has been shown to upregulate expression of FasL, which has recently been reported to contribute to TIL apoptosis *in vivo* [197]. In addition, IFN-γ upregulates expression of class II MHC, which in addition to presenting peptides to $CD4^+$ T cells also is a ligand for the inhibitory receptor LAG-3 [198, 199], which we also have reported is expressed by tumor antigen-specific $CD8^+$ TILs [19]. Some of these considerations also may help to explain why previous reports found that tumor cells expressing a dominant negative IFNγR1 exhibited increased tumor growth, as this dominant negative receptor can still bind IFN-γ and sequester it from the tumor microenvironment. Future work will be required to continue to dissect the additional complexities of IFN-γ signaling within the tumor microenvironment.

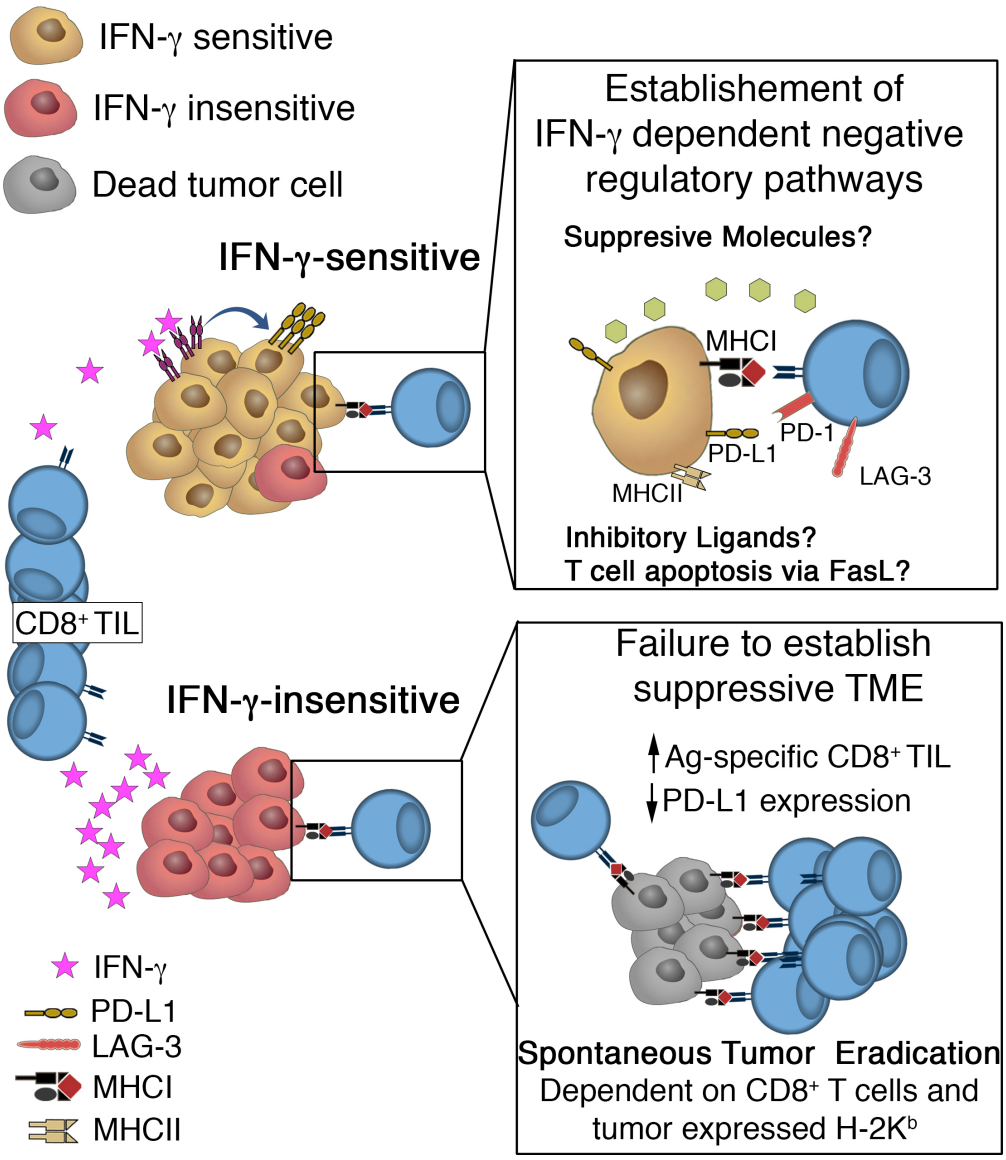

Figure 7.1: IFN-γ drives immune suppressive mechanisms in the tumor microenvironment.
After entering the tumor microenvironment, antigen-specific $CD8^+$ T cells produce IFN-γ which is sensed by tumor cells resulting in the upregulation of immune regulatory pathways. While the full extent of the IFN-γ driven negative regulatory network is not fully elucidated, such pathways include the upregulation of inhibitory ligands, secretion of immune suppressive molecules and upregulation of FasL, which may directly induce T cell apoptosis. If tumor cells cannot sense IFN-γ, these negative regulatory pathways are not upregulated and the tumor is eradicated.

REFERENCES

[1] Matthew D Vesely, Michael H Kershaw, Robert D Schreiber, and Mark J Smyth. Natural Innate and Adaptive Immunity to Cancer. *Annu. Rev. Immunol.*, 29(1):235–271, April 2011.

[2] Thomas F Gajewski, Hans Schreiber, and Yang-Xin Fu. Innate and adaptive immune cells in the tumor microenvironment. *Nat Immunol*, 14(10):1014–1022, October 2013.

[3] Helena Harlin, Yuru Meng, Amy C Peterson, Yuanyuan Zha, Maria Tretiakova, Craig Slingluff, Mark McKee, and Thomas F Gajewski. Chemokine expression in melanoma metastases associated with CD8+ T-cell recruitment. *Cancer Res.*, 69(7):3077–3085, April 2009.

[4] Mercedes B Fuertes, Aalok K Kacha, Justin Kline, Seng-Ryong Woo, David M Kranz, Kenneth M Murphy, and Thomas F Gajewski. Host type I IFN signals are required for antitumor CD8+ T cell responses through CD8alpha+ dendritic cells. *J. Exp. Med.*, 208(10):2005–2016, September 2011.

[5] Franck Pagès, Anne Berger, Matthieu Camus, Fatima Sanchez-Cabo, Anne Costes, Robert Molidor, Bernhard Mlecnik, Amos Kirilovsky, Malin Nilsson, Diane Damotte, Tchao Meatchi, Patrick Bruneval, Paul-Henri Cugnenc, Zlatko Trajanoski, Wolf Herman Fridman, and Jérôme Galon. Effector memory T cells, early metastasis, and survival in colorectal cancer. *New England Journal of Medicine*, 353(25):2654–2666, December 2005.

[6] Jérôme Galon, J Galon, Anne Costes, Fatima Sanchez-Cabo, Amos Kirilovsky, Bernhard Mlecnik, Christine Lagorce-Pagès, Marie Tosolini, Matthieu Camus, Anne Berger, Philippe Wind, Franck Zinzindohoué, Patrick Bruneval, Paul-Henri Cugnenc, Zlatko Trajanoski, Wolf Herman Fridman, and Franck Pagès. Type, density, and location of immune cells within human colorectal tumors predict clinical outcome. *Science*, 313(5795):1960–1964, September 2006.

[7] Wolf Herman Fridman, Franck Pagès, Catherine Sautès-Fridman, and Jérôme Galon. The immune contexture in human tumours: impact on clinical outcome. *Nat. Rev. Cancer*, 12(4):298–306, March 2012.

[8] Jérôme Galon, Franck Pagès, Francesco M Marincola, Helen K Angell, Magdalena Thurin, Alessandro Lugli, Inti Zlobec, Anne Berger, Carlo Bifulco, Gerardo Botti, Fabiana Tatangelo, Cedrik M Britten, Sebastian Kreiter, Lotfi Chouchane, Paolo Delrio, Hartmann Arndt, Martin Asslaber, Michele Maio, Giuseppe V Masucci, Martin Mihm, Fernando Vidal-Vanaclocha, James P Allison, Sacha Gnjatic, Leif Hakansson, Christoph Huber, Harpreet Singh-Jasuja, Christian Ottensmeier, Heinz Zwierzina, Luigi Laghi, Fabio Grizzi, Pamela S Ohashi, Patricia A Shaw, Blaise A Clarke, Bradly G Wouters, Yutaka Kawakami, Shoichi Hazama, Kiyotaka Okuno, Ena Wang, Jill O'Donnell-Tormey, Christine Lagorce, Graham Pawelec, Michael I Nishimura, Robert Hawkins, Réjean Lapointe, Andreas Lundqvist, Samir N Khleif, Shuji Ogino,

Peter Gibbs, Paul Waring, Noriyuki Sato, Toshihiko Torigoe, Kyogo Itoh, Prabhu S Patel, Shilin N Shukla, Richard Palmqvist, Iris D Nagtegaal, Yili Wang, Corrado D'Arrigo, Scott Kopetz, Frank A Sinicrope, Giorgio Trinchieri, Thomas F Gajewski, Paolo A Ascierto, and Bernard A Fox. Cancer classification using the Immunoscore: a worldwide task force. *J Transl Med*, 10(1):205, October 2012.

[9] Thomas F Gajewski and T F Gajewski. Failure at the Effector Phase: Immune Barriers at the Level of the Melanoma Tumor Microenvironment. *Clin. Cancer Res.*, 13(18):5256–5261, September 2007.

[10] Drew M Pardoll. The blockade of immune checkpoints in cancer immunotherapy. *Nat. Rev. Cancer*, 12(4):1–13, April 2012.

[11] Thomas F Gajewski, Yuru Meng, Christian Blank, Ian E Brown, Aalok K Kacha, Justin Kline, and Helena Harlin. Immune resistance orchestrated by the tumor microenvironment. *Immunological Reviews*, pages 1–15, September 2006.

[12] Lieping Chen and Dallas B Flies. Molecular mechanisms of T cell co-stimulation and co-inhibition. *Nat Rev Immunol*, 13(4):227–242, April 2013.

[13] Thomas F Gajewski. The expanding universe of regulatory T cell subsets in cancer. *Immunity*, 27(2):185–187, August 2007.

[14] Vinit Kumar, Sima Patel, Evgenii Tcyganov, and Dmitry I Gabrilovich. The Nature of Myeloid-Derived Suppressor Cells in the Tumor Microenvironment. *Trends in Immunology*, 37(3):208–220, March 2016.

[15] Xiangdong Liu, Niu Shin, Holly K Koblish, Gengjie Yang, Qian Wang, Kathy Wang, Lynn Leffet, Michael J Hansbury, Beth Thomas, Mark Rupar, Paul Waeltz, Kevin J Bowman, Padmaja Polam, Richard B Sparks, Eddy W Yue, Yanlong Li, Richard Wynn, Jordan S Fridman, Timothy C Burn, Andrew P Combs, Robert C Newton, and Peggy A Scherle. Selective inhibition of IDO1 effectively regulates mediators of antitumor immunity. *Blood*, 115(17):3520–3530, April 2010.

[16] Silvia Deaglio, Karen M Dwyer, Wenda Gao, David Friedman, Anny Usheva, Anna Erat, Jiang-Fan Chen, Keiichii Enjyoji, Joel Linden, Mohamed Oukka, Vijay K Kuchroo, Terry B Strom, and Simon C Robson. Adenosine generation catalyzed by CD39 and CD73 expressed on regulatory T cells mediates immune suppression. *Journal of Experimental Medicine*, 204(6):1257–1265, June 2007.

[17] Ivan D Mascanfroni, Ada Yeste, Silvio M Vieira, Evan J Burns, Bonny Patel, Ido Sloma, Yan Wu, Lior Mayo, Rotem Ben-Hamo, Sol Efroni, Vijay K Kuchroo, Simon C Robson, and Francisco J Quintana. IL-27 acts on DCs to suppress the T cell response and autoimmunity by inducing expression of the immunoregulatory molecule CD39. *Nature Publishing Group*, 14(10):1054–1063, October 2013.

[18] Yan Zheng, Yuanyuan Zha, and Thomas F Gajewski. Molecular regulation of T-cell anergy. *EMBO Rep.*, 9(1):50–55, January 2008.

[19] Jason B Williams, Brendan L Horton, Yan Zheng, Yukan Duan, Jonathan D Powell, and Thomas F Gajewski. The EGR2 targets LAG-3 and 4-1BB describe and regulate dysfunctional antigen-specific CD8+ T cells in the tumor microenvironment. *J. Exp. Med.*, 214(2):381–400, January 2017.

[20] Meromit Singer, Chao Wang, Le Cong, Nemanja D Marjanovic, Monika S Kowalczyk, Huiyuan Zhang, Jackson Nyman, Kaori Sakuishi, Sema Kurtulus, David Gennert, Junrong Xia, John Y H Kwon, James Nevin, Rebecca H Herbst, Itai Yanai, Orit Rozenblatt-Rosen, Vijay K Kuchroo, Aviv Regev, and Ana C Anderson. A Distinct Gene Module for Dysfunction Uncoupled from Activation in Tumor-Infiltrating T Cells. *Cell*, 166(6):1500–1511.e9, September 2016.

[21] Andrea Schietinger, Mary Philip, Varintra E Krisnawan, Edison Y Chiu, Jeffrey J Delrow, Ryan S Basom, Peter Lauer, Dirk G Brockstedt, Sue E Knoblaugh, Günter J Hämmerling, Todd D Schell, Natalio Garbi, and Philip D Greenberg. Tumor-Specific T Cell Dysfunction Is a Dynamic Antigen-Driven Differentiation Program Initiated Early during Tumorigenesis. *Immunity*, August 2016.

[22] M M Davis and P J Bjorkman. T-cell antigen receptor genes and T-cell recognition. *Nature*, 334(6181):395–402, August 1988.

[23] M R Lieber. Site-specific recombination in the immune system. *FASEB J*, 5(14):2934–2944, November 1991.

[24] T Petteri Arstila, Armanda Casrouge, Véronique Baron, Jos Even, Jean Kanellopoulos, and Philippe Kourilsky. A Direct Estimate of the Human $\alpha\beta$ T Cell Receptor Diversity. *Science*, 286(5441):958–961, October 1999.

[25] Armanda Casrouge, Emmanuel Beaudoing, Sophie Dalle, Christophe Pannetier, Jean Kanellopoulos, and Philippe Kourilsky. Size Estimate of the $\alpha\beta$ TCR Repertoire of Naive Mouse Splenocytes. *Journal of Immunology (Baltimore, Md. : 1950)*, 164(11):5782–5787, June 2000.

[26] Daniel L Mueller. Mechanisms maintaining peripheral tolerance. *Nat Immunol*, 11(1):21–27, January 2010.

[27] Jeong M Kim, Jeffrey P Rasmussen, and Alexander Y Rudensky. Regulatory T cells prevent catastrophic autoimmunity throughout the lifespan of mice. *Nat Immunol*, 8(2):191–197, November 2006.

[28] Ronald H Schwartz. T C ELLA NERGY. *Annu. Rev. Immunol.*, 21(1):305–334, April 2003.

[29] Pierre G Coulie, Benoît J Van den Eynde, Pierre van der Bruggen, and Thierry Boon. Tumour antigens recognized by T lymphocytes: at the core of cancer immunotherapy. *Nat. Rev. Cancer*, 14(2):135–146, February 2014.

[30] Ludmil B Alexandrov, Serena Nik-Zainal, David C Wedge, Samuel A J R Aparicio, Sam Behjati, Andrew V Biankin, Graham R Bignell, Niccolò Bolli, Ake Borg, Anne-Lise Børresen-Dale, Sandrine Boyault, Birgit Burkhardt, Adam P Butler, Carlos Caldas, Helen R Davies, Christine Desmedt, Roland Eils, Jórunn Erla Eyfjörd, John A Foekens, Mel Greaves, Fumie Hosoda, Barbara Hutter, Tomislav Ilicic, Sandrine Imbeaud, Marcin Imielinski, Marcin Imielinsk, Natalie Jäger, David T W Jones, David Jones, Stian Knappskog, Marcel Kool, Sunil R Lakhani, Carlos López-Otín, Sancha Martin, Nikhil C Munshi, Hiromi Nakamura, Paul A Northcott, Marina Pajic, Elli Papaemmanuil, Angelo Paradiso, John V Pearson, Xose S Puente, Keiran Raine, Manasa Ramakrishna, Andrea L Richardson, Julia Richter, Philip Rosenstiel, Matthias Schlesner, Ton N Schumacher, Paul N Span, Jon W Teague, Yasushi Totoki, Andrew N J Tutt, Rafael Valdés-Mas, Marit M van Buuren, Laura van 't Veer, Anne Vincent-Salomon, Nicola Waddell, Lucy R Yates, Australian Pancreatic Cancer Genome Initiative, ICGC Breast Cancer Consortium, ICGC MMML-Seq Consortium, ICGC PedBrain, Jessica Zucman-Rossi, P Andrew Futreal, Ultan McDermott, Peter Lichter, Matthew Meyerson, Sean M Grimmond, Reiner Siebert, Elías Campo, Tatsuhiro Shibata, Stefan M Pfister, Peter J Campbell, and Michael R Stratton. Signatures of mutational processes in human cancer. *Nature*, 500(7463):415–421, August 2013.

[31] Mark Yarchoan, Burles A Johnson III, Eric R Lutz, Daniel A Laheru, and Elizabeth M Jaffee. Targeting neoantigens to augment antitumour immunity. *Nat. Rev. Cancer*, 17(4):209–222, April 2017.

[32] Ignacio Melero, Gustav Gaudernack, Winald Gerritsen, Christoph Huber, Giorgio Parmiani, Suzy Scholl, Nicholas Thatcher, John Wagstaff, Christoph Zielinski, Ian Faulkner, and Håkan Mellstedt. Therapeutic vaccines for cancer: an overview of clinical trials. *Nature Publishing Group*, 11(9):509–524, July 2014.

[33] Richard A Morgan, James C Yang, Mio Kitano, Mark E Dudley, Carolyn M Laurencot, and Steven A Rosenberg. Case report of a serious adverse event following the administration of T cells transduced with a chimeric antigen receptor recognizing ERBB2. *Mol. Ther.*, 18(4):843–851, April 2010.

[34] Richard A Morgan, Nachimuthu Chinnasamy, Daniel Abate-Daga, Alena Gros, Paul F Robbins, Zhili Zheng, Mark E Dudley, Steven A Feldman, James C Yang, Richard M Sherry, Giao Q Phan, Marybeth S Hughes, Udai S Kammula, Akemi D Miller, Crystal J Hessman, Ashley A Stewart, Nicholas P Restifo, Martha M Quezado, Meghna Alimchandani, Avi Z Rosenberg, Avindra Nath, Tongguang Wang, Bibiana Bielekova, Simone C Wuest, Nirmala Akula, Francis J McMahon, Susanne Wilde, Barbara Mosetter, Dolores J Schendel, Carolyn M Laurencot, and Steven A Rosenberg. Cancer regression and neurological toxicity following anti-MAGE-A3 TCR gene therapy. *J. Immunother.*, 36(2):133–151, February 2013.

[35] P A Monach, S C Meredith, C T Siegel, and H Schreiber. A unique tumor antigen produced by a single amino acid substitution. *Immunity*, 2(1):45–59, January 1995.

[36] T Wölfel, M Hauer, J Schneider, M Serrano, C Wölfel, E Klehmann-Hieb, E De Plaen, T Hankeln, K H Meyer zum Büschenfelde, and D Beach. A p16INK4a-insensitive CDK4 mutant targeted by cytolytic T lymphocytes in a human melanoma. *Science*, 269(5228):1281–1284, September 1995.

[37] Volker Lennerz, Martina Fatho, Chiara Gentilini, Roy A Frye, Alexander Lifke, Dorothea Ferel, Catherine Wölfel, Christoph Huber, and Thomas Wölfel. The response of autologous T cells to a human melanoma is dominated by mutated neoantigens. *PNAS*, 102(44):16013–16018, November 2005.

[38] Alena Gros, Maria R Parkhurst, Eric Tran, Anna Pasetto, Paul F Robbins, Sadia Ilyas, Todd D Prickett, Jared J Gartner, Jessica S Crystal, Ilana M Roberts, Kasia Trebska-McGowan, John R Wunderlich, James C Yang, and Steven A Rosenberg. Prospective identification of neoantigen-specific lymphocytes in the peripheral blood of melanoma patients. *Nature Medicine*, 22(4):433–438, April 2016.

[39] Juhua Zhou, Mark E Dudley, Steven A Rosenberg, and Paul F Robbins. Persistence of Multiple Tumor-Specific T-Cell Clones Is Associated with Complete Tumor Regression in a Melanoma Patient Receiving Adoptive Cell Transfer Therapy. *Journal of Immunotherapy*, 28(1):53–62, January 2005.

[40] Matthew M Gubin, Xiuli Zhang, Heiko Schuster, Etienne Caron, Jeffrey P Ward, Takuro Noguchi, Yulia Ivanova, Jasreet Hundal, Cora D Arthur, Willem-Jan Krebber, Gwenn E Mulder, Mireille Toebes, Matthew D Vesely, Samuel S K Lam, Alan J Korman, James P Allison, Gordon J Freeman, Arlene H Sharpe, Erika L Pearce, Ton N Schumacher, Ruedi Aebersold, Hans-Georg Rammensee, Cornelis J M Melief, Elaine R Mardis, William E Gillanders, Maxim N Artyomov, and Robert D Schreiber. Checkpoint blockade cancer immunotherapy targets tumour-specific mutant antigens. *Nature*, 515(7528):577–581, November 2014.

[41] Naiyer A Rizvi, Matthew D Hellmann, Alexandra Snyder, Pia Kvistborg, Vladimir Makarov, Jonathan J Havel, William Lee, Jianda Yuan, Phillip Wong, Teresa S Ho, Martin L Miller, Natasha Rekhtman, Andre L Moreira, Fawzia Ibrahim, Cameron Bruggeman, Billel Gasmi, Roberta Zappasodi, Yuka Maeda, Chris Sander, Edward B Garon, Taha Merghoub, Jedd D Wolchok, Ton N Schumacher, and Timothy A Chan. Mutational landscape determines sensitivity to PD-1 blockade in non–small cell lung cancer. *Science*, 348(6230):124–128, April 2015.

[42] Melvyn T Chow and Andrew D Luster. Chemokines in cancer. *Cancer Immunology Research*, 2(12):1125–1131, December 2014.

[43] Stefani Spranger, Riyue Bao, and Thomas F Gajewski. Melanoma-intrinsic β-catenin signalling prevents anti-tumour immunity. *Nature*, 523(7559):231–235, July 2015.

[44] Laura van 't Veer, L Van'T Veer, D M Wolf, M E Lenburg, C Yau, A Boudreau, and L J van. Gene Co-Expression Modules as Clinically Relevant Hallmarks of Breast Cancer Diversity. *PLoS ONE*, February 2014.

[45] Mark S Diamond, Michelle Kinder, Hirokazu Matsushita, Mona Mashayekhi, Gavin P Dunn, Jessica M Archambault, Hsiaoju Lee, Cora D Arthur, J Michael White, Ulrich Kalinke, Kenneth M Murphy, and Robert D Schreiber. Type I interferon is selectively required by dendritic cells for immune rejection of tumors. *J. Exp. Med.*, 208(10):1989–2003, September 2011.

[46] Kai Hildner, Brian T Edelson, Whitney E Purtha, Mark Diamond, Hirokazu Matsushita, Masako Kohyama, Boris Calderon, Barbara U Schraml, Emil R Unanue, Michael S Diamond, Robert D Schreiber, Theresa L Murphy, and Kenneth M Murphy. Batf3 deficiency reveals a critical role for CD8alpha+ dendritic cells in cytotoxic T cell immunity. *Science*, 322(5904):1097–1100, November 2008.

[47] Lionel Apetoh, François Ghiringhelli, Antoine Tesniere, Michel Obeid, Carla Ortiz, Alfredo Criollo, Grégoire Mignot, M Chiara Maiuri, Evelyn Ullrich, Patrick Saulnier, Huan Yang, Sebastian Amigorena, Bernard Ryffel, Franck J Barrat, Paul Saftig, Francis Levi, Rosette Lidereau, Catherine Nogues, Jean-Paul Mira, Agnès Chompret, Virginie Joulin, Françoise Clavel-Chapelon, Jean Bourhis, Fabrice André, Suzette Delaloge, Thomas Tursz, Guido Kroemer, and Laurence Zitvogel. Toll-like receptor 4–dependent contribution of the immune system to anticancer chemotherapy and radiotherapy. *Nature Medicine*, 13(9):1050–1059, August 2007.

[48] François Ghiringhelli, Lionel Apetoh, Antoine Tesniere, Laetitia Aymeric, Yuting Ma, Carla Ortiz, Karim Vermaelen, Theocharis Panaretakis, Grégoire Mignot, Evelyn Ullrich, Jean-Luc Perfettini, Frédéric Schlemmer, Ezgi Tasdemir, Martin Uhl, Pierre Génin, Ahmet Civas, Bernhard Ryffel, Jean Kanellopoulos, Jürg Tschopp, Fabrice André, Rosette Lidereau, Nicole M McLaughlin, Nicole M Haynes, Mark J Smyth, Guido Kroemer, and Laurence Zitvogel. Activation of the NLRP3 inflammasome in dendritic cells induces IL-1beta-dependent adaptive immunity against tumors. *Nature Medicine*, 15(10):1170–1178, October 2009.

[49] Seng-Ryong Woo, Mercedes B Fuertes, Leticia Corrales, Stefani Spranger, Michael J Furdyna, Michael Y K Leung, Ryan Duggan, Ying Wang, Glen N Barber, Katherine A Fitzgerald, Maria-Luisa Alegre, and Thomas F Gajewski. STING-dependent cytosolic DNA sensing mediates innate immune recognition of immunogenic tumors. *Immunity*, 41(5):830–842, November 2014.

[50] J N Mandl, R Liou, F Klauschen, N Vrisekoop, J P Monteiro, A J Yates, A Y Huang, and R N Germain. Quantification of lymph node transit times reveals differences in antigen surveillance strategies of naive CD4+ and CD8+ T cells. *PNAS*, 109(44):18036–18041, October 2012.

[51] Hai Qi, Wolfgang Kastenmüller, and Ronald N Germain. Spatiotemporal basis of innate and adaptive immunity in secondary lymphoid tissue. *Annu. Rev. Cell Dev. Biol.*, 30(1):141–167, 2014.

[52] Reinhard Obst. The Timing of T Cell Priming and Cycling. *Front Immunol*, 6:239, November 2015.

[53] Marc K Jenkins and James J Moon. The role of naive T cell precursor frequency and recruitment in dictating immune response magnitude. *The Journal of Immunology*, 188(9):4135–4140, May 2012.

[54] Hiroaki Musha, Haruo Ohtani, Takayuki Mizoi, Makoto Kinouchi, Takashi Nakayama, Kennichi Shiiba, Kikuo Miyagawa, Hiroshi Nagura, Osamu Yoshie, and Iwao Sasaki. Selective infiltration of CCR5+CXCR3+ T lymphocytes in human colorectal carcinoma. *Int. J. Cancer*, 116(6):949–956, 2005.

[55] Anna Marie Mulligan, Irene Raitman, Linda Feeley, Dushanthi Pinnaduwage, Linh T Nguyen, Frances P O'Malley, Pamela S Ohashi, and Irene L Andrulis. Tumoral Lymphocytic Infiltration and Expression of the Chemokine CXCL10 in Breast Cancers from the Ontario Familial Breast Cancer Registry. *Clin. Cancer Res.*, 19(2):336–346, January 2013.

[56] M E Mikucki, D T Fisher, J Matsuzaki, J J Skitzki, N B Gaulin, J B Muhitch, A W Ku, J G Frelinger, K Odunsi, T F Gajewski, A D Luster, and S S Evans. Non-redundant requirement for CXCR3 signalling during tumoricidal T-cell trafficking across tumour vascular checkpoints. *Nature Communications*, 6(1):298, June 2015.

[57] Joanna R Groom and Andrew D Luster. CXCR3 ligands: redundant, collaborative and antagonistic functions. *Immunol Cell Biol*, 89(2):207–215, February 2011.

[58] Michelle Hong, Anne-Laure Puaux, Caleb Huang, Laure Loumagne, Charlene Tow, Charles Mackay, Masashi Kato, Armelle Prévost-Blondel, Marie-Françoise Avril, Alessandra Nardin, and Jean-Pierre Abastado. Chemotherapy Induces Intratumoral Expression of Chemokines in Cutaneous Melanoma, Favoring T-cell Infiltration and Tumor Control. *Cancer Res.*, 71(22):6997–7009, November 2011.

[59] Stefani Spranger, Daisy Dai, Brendan Horton, and Thomas F Gajewski. Tumor-Residing Batf3 Dendritic Cells Are Required for Effector T Cell Trafficking and Adoptive T Cell Therapy. *Cancer Cell*, 31(5):711–723.e4, May 2017.

[60] Rebecca Berlant Liu, Boris Engels, Karin Schreiber, Cezary Ciszewski, Andrea Schietinger, Hans Schreiber, and Bana Jabri. IL-15 in tumor microenvironment causes rejection of large established tumors by T cells in a noncognate T cell receptor-dependent manner. *PNAS*, 110(20):8158–8163, May 2013.

[61] Justin Kline, Long Zhang, Lauren Battaglia, Kenneth S Cohen, and Thomas F Gajewski. Cellular and molecular requirements for rejection of B16 melanoma in the setting of regulatory T cell depletion and homeostatic proliferation. *The Journal of Immunology*, 188(6):2630–2642, March 2012.

[62] Stefani Spranger, Jason J Luke, Riyue Bao, Yuanyuan Zha, Kyle M Hernandez, Yan Li, Alexander P Gajewski, Jorge Andrade, and Thomas F Gajewski. Density of immunogenic antigens does not explain the presence or absence of the T-cell–inflamed tumor microenvironment in melanoma. *PNAS*, 113(48):E7759–E7768, November 2016.

[63] Stefani Spranger, Robbert M Spaapen, Yuanyuan Zha, Jason Williams, Yuru Meng, Thanh T Ha, and Thomas F Gajewski. Up-regulation of PD-L1, IDO, and T(regs) in the melanoma tumor microenvironment is driven by CD8(+) T cells. *Science Translational Medicine*, 5(200):200ra116–200ra116, August 2013.

[64] Daniel E Speiser, Ping-Chih Ho, and Grégory Verdeil. Regulatory circuits of T cell function in cancer. *Nat Rev Immunol*, 16(10):599–611, August 2016.

[65] Soumaya Kouidhi, Amel Benammar Elgaaied, and Salem Chouaib. Impact of Metabolism on T-Cell Differentiation and Function and Cross Talk with Tumor Microenvironment. *Front Immunol*, 8(1):270, 2017.

[66] Candace M Cham, Gregory Driessens, James P O'Keefe, and Thomas F Gajewski. Glucose deprivation inhibits multiple key gene expression events and effector functions in CD8+ T cells. *Eur. J. Immunol.*, 38(9):2438–2450, September 2008.

[67] Chih-Hao Chang, Jing Qiu, David O'Sullivan, Michael D Buck, Takuro Noguchi, Jonathan D Curtis, Qiongyu Chen, Mariel Gindin, Matthew M Gubin, Gerritje J W van der Windt, Elena Tonc, Robert D Schreiber, Edward J Pearce, and Erika L Pearce. Metabolic Competition in the Tumor Microenvironment Is a Driver of Cancer Progression. *Cell*, 162(6):1229–1241, September 2015.

[68] David H Munn and Vincenzo Bronte. Immune suppressive mechanisms in the tumor microenvironment. *Curr. Opin. Immunol.*, 39:1–6, April 2016.

[69] Bin Shang, Yao Liu, Shu-juan Jiang, and Yi Liu. Prognostic value of tumor-infiltrating FoxP3+ regulatory T cells in cancers: a systematic review and meta-analysis. *Sci Rep*, 5(1):15179, October 2015.

[70] S Onizuka, I Tawara, J Shimizu, S Sakaguchi, T Fujita, and E Nakayama. Tumor rejection by in vivo administration of anti-CD25 (interleukin-2 receptor alpha) monoclonal antibody. *Cancer Res.*, 59(13):3128–3133, July 1999.

[71] David Coe, Shaima Begom, Caroline Addey, Matthew White, Julian Dyson, and Jian-Guo Chai. Depletion of regulatory T cells by anti-GITR mAb as a novel mechanism for cancer immunotherapy. *Cancer Immunol Immunother*, 59(9):1367–1377, September 2010.

[72] Paula D Bos, George Plitas, Dipayan Rudra, Sue Y Lee, and Alexander Y Rudensky. Transient regulatory T cell ablation deters oncogene-driven breast cancer and enhances radiotherapy. *Journal of Experimental Medicine*, 210(11):2435–2466, October 2013.

[73] Yannick Bulliard, Rose Jolicoeur, Jimin Zhang, Glenn Dranoff, Nicholas S Wilson, and Jennifer L Brogdon. OX40 engagement depletes intratumoral Tregs via activating FcγRs, leading to antitumor efficacy. *Immunol Cell Biol*, 92(6):475–480, July 2014.

[74] Frederick Arce Vargas, Andrew J S Furness, Isabelle Solomon, Kroopa Joshi, Leila Mekkaoui, Marta H Lesko, Enrique Miranda Rota, Rony Dahan, Andrew Georgiou,

Anna Sledzinska, Assma Ben Aissa, Dafne Franz, Mariana Werner Sunderland, Yien Ning Sophia Wong, Jake Y Henry, Tim O'Brien, David Nicol, Ben Challacombe, Stephen A Beers, Melanoma TRACERx Consortium, Renal TRACERx Consortium, Lung TRACERx Consortium, Samra Turajlic, Martin Gore, James Larkin, Charles Swanton, Kerry A Chester, Martin Pule, Jeffrey V Ravetch, Teresa Marafioti, Karl S Peggs, and Sergio A Quezada. Fc-Optimized Anti-CD25 Depletes Tumor-Infiltrating Regulatory T Cells and Synergizes with PD-1 Blockade to Eradicate Established Tumors. *Immunity*, 46(4):577–586, April 2017.

[75] Joannes F M Jacobs, Cornelis J A Punt, W Joost Lesterhuis, Roger P M Sutmuller, H Mary-Lène H Brouwer, Nicole M Scharenborg, Ina S Klasen, Luuk B Hilbrands, Carl G Figdor, I Jolanda M de Vries, and Gosse J Adema. Dendritic cell vaccination in combination with anti-CD25 monoclonal antibody treatment: a phase I/II study in metastatic melanoma patients. *Clin. Cancer Res.*, 16(20):5067–5078, October 2010.

[76] Andrew J Rech, Rosemarie Mick, Sunil Martin, Adri Recio, Nicole A Aqui, Daniel J Powell, Theresa A Colligon, Jennifer A Trosko, Leah I Leinbach, Charles H Pletcher, Carol K Tweed, Angela DeMichele, Kevin R Fox, Susan M Domchek, James L Riley, and Robert H Vonderheide. CD25 Blockade Depletes and Selectively Reprograms Regulatory T Cells in Concert with Immunotherapy in Cancer Patients. *Science Translational Medicine*, 4(134):134ra62–134ra62, May 2012.

[77] Jason J Luke, Yuanyuan Zha, Karen Matijevich, and Thomas F Gajewski. Single dose denileukin diftitox does not enhance vaccine-induced T cell responses or effectively deplete Tregs in advanced melanoma: immune monitoring and clinical results of a randomized phase II trial. *J Immunother Cancer*, 4(1):15, June 2016.

[78] Emanuela Romano, Monika Kusio-Kobialka, Periklis G Foukas, Petra Baumgaertner, Christiane Meyer, Pierluigi Ballabeni, Olivier Michielin, Benjamin Weide, Pedro Romero, and Daniel E Speiser. Ipilimumab-dependent cell-mediated cytotoxicity of regulatory T cells ex vivo by nonclassical monocytes in melanoma patients. *Proc. Natl. Acad. Sci. U.S.A.*, 112(19):6140–6145, May 2015.

[79] Greg M Delgoffe, Seng-Ryong Woo, Meghan E Turnis, David M Gravano, Cliff Guy, Abigail E Overacre, Matthew L Bettini, Peter Vogel, David Finkelstein, Jody Bonnevier, Creg J Workman, and Dario A A Vignali. Stability and function of regulatory T cells is maintained by a neuropilin-1-semaphorin-4a axis. *Nature*, 501(7466):252–256, September 2013.

[80] Qi Pan, Yvan Chanthery, Wei-Ching Liang, Scott Stawicki, Judy Mak, Nisha Rathore, Raymond K Tong, Joe Kowalski, Sharon Fong Yee, Glenn Pacheco, Sarajane Ross, Zhiyong Cheng, Jennifer Le Couter, Greg Plowman, Franklin Peale, Alexander W Koch, Yan Wu, Anil Bagri, Marc Tessier-Lavigne, and Ryan J Watts. Blocking Neuropilin-1 Function Has an Additive Effect with Anti-VEGF to Inhibit Tumor Growth. *Cancer Cell*, 11(1):53–67, January 2007.

[81] Abigail E Overacre-Delgoffe, Maria Chikina, Rebekah E Dadey, Hiroshi Yano, Erin A Brunazzi, Gulidanna Shayan, William Horne, Jessica M Moskovitz, Jay K Kolls, Cindy Sander, Yongli Shuai, Daniel P Normolle, John M Kirkwood, Robert L Ferris, Greg M Delgoffe, Tullia C Bruno, Creg J Workman, and Dario A A Vignali. Interferon-γ Drives Treg Fragility to Promote Anti-tumor Immunity. *Cell*, 169(6):1130–1141.e11, June 2017.

[82] Matthew A Williams and Michael J Bevan. Effector and Memory CTL Differentiation. *Annu. Rev. Immunol.*, 25(1):171–192, April 2007.

[83] E John Wherry, Joseph N Blattman, Kaja Murali-Krishna, Robbert van der Most, and Rafi Ahmed. Viral persistence alters CD8 T-cell immunodominance and tissue distribution and results in distinct stages of functional impairment. *J. Virol.*, 77(8):4911–4927, April 2003.

[84] E John Wherry. T cell exhaustion. *Nature Publishing Group*, 131(6):492–499, June 2011.

[85] John C Riches, Jeffrey K Davies, Fabienne McClanahan, Rewas Fatah, Sameena Iqbal, Samir Agrawal, Alan G Ramsay, and John G Gribben. T cells from CLL patients exhibit features of T-cell exhaustion but retain capacity for cytokine production. *Blood*, 121(9):1612–1621, February 2013.

[86] Mojgan Ahmadzadeh, Laura A Johnson, Bianca Heemskerk, John R Wunderlich, Mark E Dudley, Donald E White, and Steven A Rosenberg. Tumor antigen-specific CD8 T cells infiltrating the tumor express high levels of PD-1 and are functionally impaired. *Blood*, 114(8):1537–1544, August 2009.

[87] C Yee, J A Thompson, D Byrd, S R Riddell, P Roche, E Celis, and P D Greenberg. Adoptive T cell therapy using antigen-specific CD8+ T cell clones for the treatment of patients with metastatic melanoma: in vivo persistence, migration, and antitumor effect of transferred T cells. *PNAS*, 99(25):16168–16173, December 2002.

[88] Virginie Vignard, Brigitte Lemercier, Annick Lim, Marie-Christine Pandolfino, Yannick Guilloux, Amir Khammari, Catherine Rabu, Klara Echasserieau, François Lang, Marie-Lise Gougeon, Brigitte Dreno, Francine Jotereau, and Nathalie Labarrière. Adoptive Transfer of Tumor-Reactive Melan-A-Specific CTL Clones in Melanoma Patients Is Followed by Increased Frequencies of Additional Melan-A-Specific T Cells. *Journal of Immunology (Baltimore, Md. : 1950)*, 175(7):4797–805, November 2005.

[89] Nicholas P Restifo, Mark E Dudley, and Steven A Rosenberg. Adoptive immunotherapy for cancer: harnessing the T cell response. *Nature Publishing Group*, 12(4):269–281, April 2012.

[90] Lukas Baitsch, Petra Baumgaertner, Estelle Devêvre, Sunil K Raghav, Amandine Legat, Leticia Barba, Sébastien Wieckowski, Hanifa Bouzourene, Bart Deplancke, Pedro Romero, Nathalie Rufer, and Daniel E Speiser. Exhaustion of tumor-specific CD8

T cells in metastases from melanoma patients. *J. Clin. Invest.*, 121(6):2350–2360, June 2011.

[91] Anusha-Preethi Ganesan, James Clarke, Oliver Wood, Eva M Garrido-Martin, Serena J Chee, Toby Mellows, Daniela Samaniego-Castruita, Divya Singh, Grégory Seumois, Aiman Alzetani, Edwin Woo, Peter S Friedmann, Emma V King, Gareth J Thomas, Tilman Sanchez-Elsner, Pandurangan Vijayanand, and Christian H Ottensmeier. Tissue-resident memory features are linked to the magnitude of cytotoxic T cell responses in human lung cancer. *Nature Publishing Group*, 122:3491, June 2017.

[92] Anusha-Preethi Ganesan, James Clarke, Oliver Wood, Eva M Garrido-Martin, Serena J Chee, Toby Mellows, Daniela Samaniego-Castruita, Divya Singh, Grégory Seumois, Aiman Alzetani, Edwin Woo, Peter S Friedmann, Emma V King, Gareth J Thomas, Tilman Sanchez-Elsner, Pandurangan Vijayanand, and Christian H Ottensmeier. Tissue-resident memory features are linked to the magnitude of cytotoxic T cell responses in human lung cancer. *Nat Immunol*, 18(8):940–950, August 2017.

[93] Yuanyuan Zha, Reinhard Marks, Allen W Ho, Amy C Peterson, Sujit Janardhan, Ian Brown, Kesavannair Praveen, Stacey Stang, James C Stone, and Thomas F Gajewski. T cell anergy is reversed by active Ras and is regulated by diacylglycerol kinase-alpha. *Nat Immunol*, 7(11):1166–1173, November 2006.

[94] Patrice M Dubois, Maria Pihlgren, Martine Tomkowiak, Marcelle Van Mechelen, and Jacqueline Marvel. Tolerant CD8 T Cells Induced by Multiple Injections of Peptide Antigen Show Impaired TCR Signaling and Altered Proliferative Responses In Vitro and In Vivo. *Journal of Immunology (Baltimore, Md. : 1950)*, 161(10):5260–5267, November 1998.

[95] CD4(+) T cell anergy prevents autoimmunity and generates regulatory T cell precursors. *Nat Immunol*, 17(3):304–314, March 2016.

[96] Jo Marie Tran Janco, Purushottam Lamichhane, Lavakumar Karyampudi, and Keith L Knutson. Tumor-Infiltrating Dendritic Cells in Cancer Pathogenesis. *Journal of Immunology (Baltimore, Md. : 1950)*, 194(7):2985–2991, April 2015.

[97] S E Townsend and J P Allison. Tumor rejection after direct costimulation of CD8+ T cells by B7-transfected melanoma cells. *Science*, 259(5093):368–370, January 1993.

[98] T F Gajewski. B7-1 but not B7-2 efficiently costimulates CD8+ T lymphocytes in the P815 tumor system in vitro. *Journal of Immunology (Baltimore, Md. : 1950)*, 156(2):465–472, January 1996.

[99] Gregory Driessens, Justin Kline, and Thomas F Gajewski. Costimulatory and coinhibitory receptors in anti-tumor immunity. *Immunological Reviews*, 229(1):126–144, May 2009.

[100] Ana C Anderson, Nicole Joller, and Vijay K Kuchroo. Lag-3, Tim-3, and TIGIT: Co-inhibitory Receptors with Specialized Functions in Immune Regulation. *Immunity*, 44(5):989–1004, May 2016.

[101] Shawn D Blackburn, Haina Shin, W Nicholas Haining, Tao Zou, Creg J Workman, Creg J Workman, Antonio Polley, Michael R Betts, Gordon J Freeman, Dario A A Vignali, and E John Wherry. Coregulation of CD8+ T cell exhaustion by multiple inhibitory receptors during chronic viral infection. *Nature Publishing Group*, 10(1):29–37, January 2009.

[102] Molecular Profile of Tumor-Specific CD8+ T Cell Hypofunction in a Transplantable Murine Cancer Model. *The Journal of Immunology*, 197(4):1477–1488, August 2016.

[103] Hashem O Alsaab, Samaresh Sau, Rami Alzhrani, Katyayani Tatiparti, Ketki Bhise, Sushil K Kashaw, and Arun K Iyer. PD-1 and PD-L1 Checkpoint Signaling Inhibition for Cancer Immunotherapy: Mechanism, Combinations, and Clinical Outcome. *Front Pharmacol*, 8:561, 2017.

[104] Paul C Tumeh, Christina L Harview, Jennifer H Yearley, I Peter Shintaku, Emma J M Taylor, Lidia Robert, Bartosz Chmielowski, Marko Spasic, Gina Henry, Voicu Ciobanu, Alisha N West, Manuel Carmona, Christine Kivork, Elizabeth Seja, Grace Cherry, Antonio J Gutierrez, Tristan R Grogan, Christine Mateus, Gorana Tomasic, John A Glaspy, Ryan O Emerson, Harlan Robins, Robert H Pierce, David A Elashoff, Caroline Robert, and Antoni Ribas. PD-1 blockade induces responses by inhibiting adaptive immune resistance. *Nature*, 515(7528):568–571, November 2014.

[105] Dung T Le, Jennifer N Uram, Hao Wang, Bjarne R Bartlett, Holly Kemberling, Aleksandra D Eyring, Andrew D Skora, Brandon S Luber, Nilofer S Azad, Dan Laheru, Barbara Biedrzycki, Ross C Donehower, Atif Zaheer, George A Fisher, Todd S Crocenzi, James J Lee, Steven M Duffy, Richard M Goldberg, Albert de la Chapelle, Minori Koshiji, Feriyl Bhaijee, Thomas Huebner, Ralph H Hruban, Laura D Wood, Nathan Cuka, Drew M Pardoll, Nickolas Papadopoulos, Kenneth W Kinzler, Shibin Zhou, Toby C Cornish, Janis M Taube, Robert A Anders, James R Eshleman, Bert Vogelstein, and Luis A Diaz. PD-1 Blockade in Tumors with Mismatch-Repair Deficiency. *New England Journal of Medicine*, 372(26):2509–2520, June 2015.

[106] Nienke van Rooij, Marit M van Buuren, Daisy Philips, Arno Velds, Mireille Toebes, Bianca Heemskerk, Laura J A van Dijk, Sam Behjati, Henk Hilkmann, Dris el Atmioui, Marja Nieuwland, Michael R Stratton, Ron M Kerkhoven, Can Keşmir, John B Haanen, Pia Kvistborg, and Ton N Schumacher. Tumor Exome Analysis Reveals Neoantigen-Specific T-Cell Reactivity in an Ipilimumab-Responsive Melanoma. *J. Clin. Oncol.*, 31(32):e439–e442, November 2013.

[107] Yong-Chen Lu, Xin Yao, Jessica S Crystal, Yong F Li, Mona El-Gamil, Colin Gross, Lindy Davis, Mark E Dudley, James C Yang, Yardena Samuels, Steven A Rosenberg, and Paul F Robbins. Efficient Identification of Mutated Cancer Antigens Recognized by T Cells Associated with Durable Tumor Regressions. *Clin. Cancer Res.*, 20(13):3401–3410, July 2014.

[108] Eric Tran, Mojgan Ahmadzadeh, Yong-Chen Lu, Alena Gros, Simon Turcotte, Paul F Robbins, Jared J Gartner, Zhili Zheng, Yong F Li, Satyajit Ray, John R Wunderlich,

Robert P Somerville, and Steven A Rosenberg. Immunogenicity of somatic mutations in human gastrointestinal cancers. *Science*, 350(6266):1387–1390, December 2015.

[109] Mark Ayers, Jared Lunceford, Michael Nebozhyn, Erin Murphy, Andrey Loboda, David R Kaufman, Andrew Albright, Jonathan D Cheng, S Peter Kang, Veena Shankaran, Sarina A Piha-Paul, Jennifer Yearley, Tanguy Y Seiwert, Antoni Ribas, and Terrill K McClanahan. IFN-γ–related mRNA profile predicts clinical response to PD-1 blockade. *J. Clin. Invest.*, 127(8):2930–2940, August 2017.

[110] Daniel S Chen and Ira Mellman. Elements of cancer immunity and the cancer–immune set point. *Nature*, 541(7637):321–330, January 2017.

[111] Stefani Spranger, Jason J Luke, Riyue Bao, Yuanyuan Zha, Kyle M Hernandez, Yan Li, Alexander P Gajewski, Jorge Andrade, and Thomas F Gajewski. Density of immunogenic antigens does not explain the presence or absence of the T-cell-inflamed tumor microenvironment in melanoma. *Proc. Natl. Acad. Sci. U.S.A.*, 113(48):E7759–E7768, November 2016.

[112] James Larkin, F Stephen Hodi, and Jedd D Wolchok. Combined Nivolumab and Ipilimumab or Monotherapy in Untreated Melanoma. *New England Journal of Medicine*, 373(13):1270–1271, September 2015.

[113] Creg J Workman, Kari J Dugger, and Dario A A Vignali. Cutting edge: molecular analysis of the negative regulatory function of lymphocyte activation gene-3. *Journal of Immunology (Baltimore, Md. : 1950)*, 169(10):5392–5395, November 2002.

[114] Seng-Ryong Woo, Meghan E Turnis, Meghan E Turnis, Monica V Goldberg, Monica V Goldberg, Jaishree Bankoti, Jaishree Bankoti, Mark Selby, Mark Selby, Christopher J Nirschl, Christopher J Nirschl, Matthew L Bettini, David M Gravano, David M Gravano, Peter Vogel, Peter Vogel, Chih Long Liu, Chih Long Liu, Stephanie Tangsombatvisit, Stephanie Tangsombatvisit, Joseph F Grosso, Joseph F Grosso, George Netto, George Netto, Matthew P Smeltzer, Matthew P Smeltzer, Alcides Chaux, Alcides Chaux, Paul J Utz, Paul J Utz, Creg J Workman, Creg J Workman, Drew M Pardoll, Alan J Korman, Charles G Drake, Charles G Drake, and Dario A A Vignali. Immune inhibitory molecules LAG-3 and PD-1 synergistically regulate T-cell function to promote tumoral immune escape. *Cancer Res.*, 72(4):917–927, February 2012.

[115] Linh T Nguyen and Pamela S Ohashi. Clinical blockade of PD1 and LAG3 - potential mechanisms of action. *Nat Rev Immunol*, 15(1):45–56, December 2014.

[116] Lawrence P Andrews, Ariel E Marciscano, Charles G Drake, and Dario A A Vignali. LAG3 (CD223) as a cancer immunotherapy target. *Immunological Reviews*, 276(1):80–96, March 2017.

[117] Cariad Chester, Miguel F Sanmamed, Jun Wang, and Ignacio Melero. Immunotherapy targeting 4-1BB: mechanistic rationale, clinical results, and future strategies. *Blood*, pages blood–2017–06–741041, November 2017.

[118] Deborah A Knee, Becker Hewes, and Jennifer L Brogdon. Rationale for anti-GITR cancer immunotherapy. *Eur. J. Cancer*, 67:1–10, November 2016.

[119] Sandrine Aspeslagh, Sophie Postel-Vinay, Sylvie Rusakiewicz, Jean-Charles Soria, Laurence Zitvogel, and Aurélien Marabelle. Rationale for anti-OX40 cancer immunotherapy. *European Journal of Cancer*, 52:50–66, January 2016.

[120] Enfu Hui, Jeanne Cheung, Jing Zhu, Xiaolei Su, Marcus J Taylor, Heidi A Wallweber, Dibyendu K Sasmal, Jun Huang, Jeong M Kim, Ira Mellman, and Ronald D Vale. T cell costimulatory receptor CD28 is a primary target for PD-1-mediated inhibition. *Science*, 355(6332):1428–1433, March 2017.

[121] Alice O Kamphorst, Andreas Wieland, Tahseen Nasti, Shu Yang, Ruan Zhang, Daniel L Barber, Bogumila T Konieczny, Candace Z Daugherty, Lydia Koenig, Ke Yu, Gabriel L Sica, Arlene H Sharpe, Gordon J Freeman, Bruce R Blazar, Laurence A Turka, Taofeek K Owonikoko, Rathi N Pillai, Suresh S Ramalingam, Koichi Araki, and Rafi Ahmed. Rescue of exhausted CD8 T cells by PD-1–targeted therapies is CD28-dependent. *Science*, 355(6332):1423–1427, March 2017.

[122] Yan Zheng, Yuanyuan Zha, Gregory Driessens, Frederick Locke, and Thomas F Gajewski. Transcriptional regulator early growth response gene 2 (Egr2) is required for T cell anergy in vitro and in vivo. *J. Exp. Med.*, 209(12):2157–2163, November 2012.

[123] Ian E Brown, Christian Blank, Justin Kline, Aalok K Kacha, and Thomas F Gajewski. Homeostatic proliferation as an isolated variable reverses CD8+ T cell anergy and promotes tumor rejection. *Journal of Immunology (Baltimore, Md. : 1950)*, 177(7):4521–4529, October 2006.

[124] Long Zhang, Thomas F Gajewski, and Justin Kline. PD-1/PD-L1 interactions inhibit antitumor immune responses in a murine acute myeloid leukemia model. *Blood*, 114(8):1545–1552, August 2009.

[125] Michael T Spiotto, Ping Yu, Donald A Rowley, Michael I Nishimura, Stephen C Meredith, Thomas F Gajewski, Yang-Xin Fu, and Hans Schreiber. Increasing Tumor Antigen Expression Overcomes "Ignorance" to Solid Tumors via Crosspresentation by Bone Marrow-Derived Stromal Cells. *Immunity*, 17(6):737–747, December 2002.

[126] Matthew Kearse, Richard Moir, Amy Wilson, Steven Stones-Havas, Matthew Cheung, Shane Sturrock, Simon Buxton, Alex Cooper, Sidney Markowitz, Chris Duran, Tobias Thierer, Bruce Ashton, Peter Meintjes, and Alexei Drummond. Geneious Basic: an integrated and extendable desktop software platform for the organization and analysis of sequence data. *Bioinformatics*, 28(12):1647–1649, June 2012.

[127] Jeffrey R Currier and Mary Ann Robinson. *Spectratype/Immunoscope Analysis of the Expressed TCR Repertoire*. John Wiley & Sons, Inc., Hoboken, NJ, USA, 2001.

[128] S B Plaisier, R Taschereau, J A Wong, and T G Graeber. Rank-rank hypergeometric overlap: identification of statistically significant overlap between gene-expression signatures. *Nucl. Acids Res.*, 38(17):e169–e169, September 2010.

[129] Jonathan D Rosenblatt and Jason L Stein. *RRHO: Test overlap using the Rank-Rank Hypergeometric test*, 2014.

[130] Paul Shannon, Andrew Markiel, Owen Ozier, Nitin S Baliga, Jonathan T Wang, Daniel Ramage, Nada Amin, Benno Schwikowski, and Trey Ideker. Cytoscape: a software environment for integrated models of biomolecular interaction networks. *Genome Res.*, 13(11):2498–2504, November 2003.

[131] Hiroko Koike-Yusa, Yilong Li, E-Pien Tan, Martin Del Castillo Velasco-Herrera, and Kosuke Yusa. Genome-wide recessive genetic screening in mammalian cells with a lentiviral CRISPR-guide RNA library. *Nat. Biotechnol.*, 32(3):267–273, March 2014.

[132] Daniel L Barber, E John Wherry, David Masopust, Baogong Zhu, James P Allison, Arlene H Sharpe, Gordon J Freeman, and Rafi Ahmed. Restoring function in exhausted CD8 T cells during chronic viral infection. *Nature*, 439(7077):682–687, February 2006.

[133] Mary E Keir, Manish J Butte, Gordon J Freeman, and Arlene H Sharpe. PD-1 and Its Ligands in Tolerance and Immunity. *Annu. Rev. Immunol.*, 26(1):677–704, April 2008.

[134] Shawn D Blackburn, Haina Shin, Gordon J Freeman, and E John Wherry. Selective expansion of a subset of exhausted CD8 T cells by alphaPD-L1 blockade. *Proc. Natl. Acad. Sci. U.S.A.*, 105(39):15016–15021, September 2008.

[135] Takashi Inozume, Ken-Ichi Hanada, Qiong J Wang, Mojgan Ahmadzadeh, John R Wunderlich, Steven A Rosenberg, and James C Yang. Selection of CD8+PD-1+ lymphocytes in fresh human melanomas enriches for tumor-reactive T cells. *J. Immunother.*, 33(9):956–964, November 2010.

[136] Julien Fourcade, Zhaojun Sun, Mourad Benallaoua, Philippe Guillaume, Immanuel F Luescher, Cindy Sander, John M Kirkwood, Vijay Kuchroo, and Hassane M Zarour. Upregulation of Tim-3 and PD-1 expression is associated with tumor antigen-specific CD8+ T cell dysfunction in melanoma patients. *J. Exp. Med.*, 207(10):2175–2186, September 2010.

[137] Lukas Baitsch, Amandine Legat, Leticia Barba, Silvia A Fuertes Marraco, Jean-Paul Rivals, Petra Baumgaertner, Céline Christiansen-Jucht, Hanifa Bouzourene, Donata Rimoldi, Hanspeter Pircher, Nathalie Rufer, Maurice Matter, Olivier Michielin, and Daniel E Speiser. Extended co-expression of inhibitory receptors by human CD8 T-cells depending on differentiation, antigen-specificity and anatomical localization. *PLoS ONE*, 7(2):e30852, 2012.

[138] Alena Gros, Paul F Robbins, Xin Yao, Yong F Li, Simon Turcotte, Eric Tran, John R Wunderlich, Arnold Mixon, Shawn Farid, Mark E Dudley, Ken-Ichi Hanada, Jorge R Almeida, Sam Darko, Daniel C Douek, James C Yang, and Steven A Rosenberg. PD-1 identifies the patient-specific CD8 tumor-reactive repertoire infiltrating human tumors. *J. Clin. Invest.*, 124(5):2246–2259, May 2014.

[139] Qunrui Ye, De-Gang Song, Mathilde Poussin, Tori Yamamoto, Andrew Best, Chunsheng Li, George Coukos, and Daniel J Powell. CD137 accurately identifies and enriches for naturally occurring tumor-reactive T cells in tumor. *Clin. Cancer Res.*, 20(1):44–55, January 2014.

[140] Junko Matsuzaki, Sacha Gnjatic, Paulette Mhawech-Fauceglia, Amy Beck, Austin Miller, Takemasa Tsuji, Cheryl Eppolito, Feng Qian, Shashikant Lele, Protul Shrikant, Lloyd J Old, and Kunle Odunsi. Tumor-infiltrating NY-ESO-1–specific CD8 +T cells are negatively regulated by LAG-3 and PD-1 in human ovarian cancer. *PNAS*, 107(17):7875–7880, April 2010.

[141] Kaori Sakuishi, Lionel Apetoh, Jenna M Sullivan, Bruce R Blazar, Vijay K Kuchroo, and Ana C Anderson. Targeting Tim-3 and PD-1 pathways to reverse T cell exhaustion and restore anti-tumor immunity. *J. Exp. Med.*, 207(10):2187–2194, September 2010.

[142] Roberta Mortarini, Adriano Piris, Andrea Maurichi, Alessandra Molla, Ilaria Bersani, Aldo Bono, Cesare Bartoli, Mario Santinami, Claudia Lombardo, Fernando Ravagnani, Natale Cascinelli, Giorgio Parmiani, and Andrea Anichini. Lack of terminally differentiated tumor-specific CD8+ T cells at tumor site in spite of antitumor immunity to self-antigens in human metastatic melanoma. *Cancer Res.*, 63(10):2535–2545, May 2003.

[143] Adil I Daud, Kimberly Loo, Mariela L Pauli, Robert Sanchez-Rodriguez, Priscila Munoz Sandoval, Keyon Taravati, Katy Tsai, Adi Nosrati, Lorenzo Nardo, Michael D Alvarado, Alain P Algazi, Miguel H Pampaloni, Iryna V Lobach, Jimmy Hwang, Robert H Pierce, Iris K Gratz, Matthew F Krummel, and Michael D Rosenblum. Tumor immune profiling predicts response to anti-PD-1 therapy in human melanoma. *J. Clin. Invest.*, 126(9):3447–3452, September 2016.

[144] Yan Zheng, Yuanyuan Zha, Robbert M Spaapen, Rebecca Mathew, Kenneth Barr, Albert Bendelac, and Thomas F Gajewski. Egr2-dependent gene expression profiling and ChIP-Seq reveal novel biologic targets in T cell anergy. *Mol. Immunol.*, 55(3-4):283–291, October 2013.

[145] Shuji Sumitomo, Keishi Fujio, Tomohisa Okamura, and Kazuhiko Yamamoto. Egr2 and Egr3 are the unique regulators for systemic autoimmunity. *JAKSTAT*, 2(2):e23952, April 2013.

[146] Suling Li, Tizong Miao, Meera Sebastian, Punamdip Bhullar, Emma Ghaffari, Mengya Liu, Alistair L J Symonds, and Ping Wang. The transcription factors Egr2 and Egr3 are essential for the control of inflammation and antigen-induced proliferation of B and T cells. *Immunity*, 37(4):685–696, October 2012.

[147] Meredith Safford, Samuel Collins, Michael A Lutz, Amy Allen, Ching-Tai Huang, Jeanne Kowalski, Amanda Blackford, Maureen R Horton, Charles Drake, Ronald H Schwartz, and Jonathan D Powell. Egr-2 and Egr-3 are negative regulators of T cell activation. *Nat Immunol*, 6(5):472–480, April 2005.

[148] Asís Palazón, Iván Martínez-Forero, Alvaro Teijeira, Aizea Morales-Kastresana, Carlos Alfaro, Miguel F Sanmamed, Jose Luis Perez-Gracia, Iván Peñuelas, Sandra Hervás-Stubbs, Ana Rouzaut, Manuel Ortiz de Landázuri, Maria Jure-Kunkel, Julian Aragonés, and Ignacio Melero. The HIF-1α hypoxia response in tumor-infiltrating T lymphocytes induces functional CD137 (4-1BB) for immunotherapy. *Cancer Discov*, 2(7):608–623, July 2012.

[149] Helena Harlin, Todd V Kuna, Amy C Peterson, Yuru Meng, and Thomas F Gajewski. Tumor progression despite massive influx of activated CD8(+) T cells in a patient with malignant melanoma ascites. *Cancer Immunol Immunother*, 55(10):1185–1197, October 2006.

[150] E John Wherry, Sang-Jun Ha, Susan M Kaech, W Nicholas Haining, Surojit Sarkar, Vandana Kalia, Shruti Subramaniam, Joseph N Blattman, Daniel L Barber, and Rafi Ahmed. Molecular signature of CD8+ T cell exhaustion during chronic viral infection. *Immunity*, 27(4):670–684, October 2007.

[151] M K Jenkins, D M Pardoll, J Mizuguchi, T M Chused, and R H Schwartz. Molecular events in the induction of a nonresponsive state in interleukin 2-producing helper T-lymphocyte clones. *PNAS*, 84(15):5409–5413, August 1987.

[152] D B Hoelzinger, S E Smith, N Mirza, A L Dominguez, S Z Manrique, and J Lustgarten. Blockade of CCL1 Inhibits T Regulatory Cell Suppressive Function Enhancing Tumor Immunity without Affecting T Effector Responses. *The Journal of Immunology*, 184(12):6833–6842, June 2010.

[153] Nicola Gagliani, Chiara F Magnani, Samuel Huber, Monica E Gianolini, Mauro Pala, Paula Licona-Limon, Binggege Guo, De'Broski R Herbert, Alessandro Bulfone, Filippo Trentini, Clelia Di Serio, Rosa Bacchetta, Marco Andreani, Leonie Brockmann, Silvia Gregori, Richard A Flavell, and Maria-Grazia Roncarolo. Coexpression of CD49b and LAG-3 identifies human and mouse T regulatory type 1 cells. *Nature Medicine*, 19(6):739–746, April 2013.

[154] M Oft. IL-10: Master Switch from Tumor-Promoting Inflammation to Antitumor Immunity. *Cancer Immunology Research*, 2(3):194–199, March 2014.

[155] Justin Kline, Ian E Brown, Yuan-Yuan Zha, Christian Blank, John Strickler, Harald Wouters, Long Zhang, and Thomas F Gajewski. Homeostatic proliferation plus regulatory T-cell depletion promotes potent rejection of B16 melanoma. *Clin. Cancer Res.*, 14(10):3156–3167, May 2008.

[156] Travis A Doering, Alison Crawford, Jill M Angelosanto, Michael A Paley, Carly G Ziegler, and E John Wherry. Network analysis reveals centrally connected genes and pathways involved in CD8+ T cell exhaustion versus memory. *Immunity*, 37(6):1130–1144, December 2012.

[157] Milka Sarris, Kristian G Andersen, Felix Randow, Luzia Mayr, and Alexander G Betz. Neuropilin-1 Expression on Regulatory T Cells Enhances Their Interactions with Dendritic Cells during Antigen Recognition. *Immunity*, 28(3):402–413, March 2008.

[158] Robert J Johnston, Laetitia Comps-Agrar, Jason Hackney, Xin Yu, Mahrukh Huseni, Yagai Yang, Summer Park, Vincent Javinal, Henry Chiu, Bryan Irving, Dan L Eaton, and Jane L Grogan. The immunoreceptor TIGIT regulates antitumor and antiviral CD8(+) T cell effector function. *Cancer Cell*, 26(6):923–937, December 2014.

[159] Xiaozhou Fan, Sergio A Quezada, Manuel A Sepulveda, Padmanee Sharma, and James P Allison. Engagement of the ICOS pathway markedly enhances efficacy of CTLA-4 blockade in cancer immunotherapy. *J. Exp. Med.*, 211(4):715–725, April 2014.

[160] Nikhil S Joshi, Weiguo Cui, Anmol Chandele, Heung Kyu Lee, David R Urso, James Hagman, Laurent Gapin, and Susan M Kaech. Inflammation Directs Memory Precursor and Short-Lived Effector CD8+ T Cell Fates via the Graded Expression of T-bet Transcription Factor. *Immunity*, 27(2):281–295, August 2007.

[161] Stefani Spranger, Holly K Koblish, Brendan Horton, Peggy A Scherle, Robert Newton, and Thomas F Gajewski. Mechanism of tumor rejection with doublets of CTLA-4, PD-1/PD-L1, or IDO blockade involves restored IL-2 production and proliferation of CD8(+) T cells directly within the tumor microenvironment. *J Immunother Cancer*, 2(1):3, 2014.

[162] Christina Twyman-Saint Victor, Andrew J Rech, Amit Maity, Ramesh Rengan, Kristen E Pauken, Erietta Stelekati, Joseph L Benci, Bihui Xu, Hannah Dada, Pamela M Odorizzi, Ramin S Herati, Kathleen D Mansfield, Dana Patsch, Ravi K Amaravadi, Lynn M Schuchter, Hemant Ishwaran, Rosemarie Mick, Daniel A Pryma, Xiaowei Xu, Michael D Feldman, Tara C Gangadhar, Stephen M Hahn, E John Wherry, Robert H Vonderheide, and Andy J Minn. Radiation and dual checkpoint blockade activate non-redundant immune mechanisms in cancer. *Nature*, 520(7547):373–377, April 2015.

[163] Cornelia Halin, M Lucila Scimone, Roberto Bonasio, Jean-Marc Gauguet, Thorsten R Mempel, Elizabeth Quackenbush, Richard L Proia, Suzanne Mandala, and Ulrich H von Andrian. The S1P-analog FTY720 differentially modulates T-cell homing via HEV: T-cell-expressed S1P1 amplifies integrin activation in peripheral lymph nodes but not in Peyer patches. *Blood*, 106(4):1314–1322, August 2005.

[164] Janis M Taube, Robert A Anders, Geoffrey D Young, Haiying Xu, Rajni Sharma, Tracee L McMiller, Shuming Chen, Alison P Klein, Drew M Pardoll, Suzanne L Topalian, and Lieping Chen. Colocalization of inflammatory response with B7-h1 expression in human melanocytic lesions supports an adaptive resistance mechanism of immune escape. *Science Translational Medicine*, 4(127):127ra37–127ra37, March 2012.

[165] S E A Street. Perforin and interferon-gamma activities independently control tumor initiation, growth, and metastasis. *Blood*, 97(1):192–197, January 2001.

[166] Shayna E A Street, Joseph A Trapani, Duncan MacGregor, and Mark J Smyth. Suppression of lymphoma and epithelial malignancies effected by interferon gamma. *Journal of Experimental Medicine*, 196(1):129–134, July 2002.

[167] D H Kaplan, V Shankaran, A S Dighe, E Stockert, M Aguet, L J Old, and R D Schreiber. Demonstration of an interferon gamma-dependent tumor surveillance system in immunocompetent mice. *PNAS*, 95(13):7556–7561, June 1998.

[168] Jesse M Zaretsky, Angel Garcia-Diaz, Daniel S Shin, Helena Escuin-Ordinas, Willy Hugo, Siwen Hu-Lieskovan, Davis Y Torrejon, Gabriel Abril-Rodriguez, Salemiz Sandoval, Lucas Barthly, Justin Saco, Blanca Homet Moreno, Riccardo Mezzadra, Bartosz Chmielowski, Kathleen Ruchalski, I Peter Shintaku, Phillip J Sanchez, Cristina Puig-Saus, Grace Cherry, Elizabeth Seja, Xiangju Kong, Jia Pang, Beata Berent-Maoz, Begoña Comin-Anduix, Thomas G Graeber, Paul C Tumeh, Ton N M Schumacher, Roger S Lo, and Antoni Ribas. Mutations Associated with Acquired Resistance to PD-1 Blockade in Melanoma. *New England Journal of Medicine*, 375(9):NEJMoa1604958–829, July 2016.

[169] Interferons, immunity and cancer immunoediting. *Nat Rev Immunol*, 6(11):836–848, November 2006.

[170] Angel Garcia-Diaz, Daniel Sanghoon Shin, Blanca Homet Moreno, Justin Saco, Helena Escuin-Ordinas, Gabriel Abril Rodriguez, Jesse M Zaretsky, Lu Sun, Willy Hugo, Xiaoyan Wang, Giulia Parisi, Cristina Puig Saus, Davis Y Torrejon, Thomas G Graeber, Begonya Comin-Anduix, Siwen Hu-Lieskovan, Robert Damoiseaux, Roger S Lo, and Antoni Ribas. Interferon Receptor Signaling Pathways Regulating PD-L1 and PD-L2 Expression. *Cell Rep*, 19(6):1189–1201, May 2017.

[171] Joseph L Benci, Bihui Xu, Yu Qiu, Tony J Wu, Hannah Dada, Christina Twyman-Saint Victor, Lisa Cucolo, David S M Lee, Kristen E Pauken, Alexander C Huang, Tara C Gangadhar, Ravi K Amaravadi, Lynn M Schuchter, Michael D Feldman, Hemant Ishwaran, Robert H Vonderheide, Amit Maity, E John Wherry, and Andy J Minn. Tumor Interferon Signaling Regulates a Multigenic Resistance Program to Immune Checkpoint Blockade. *Cell*, 167(6):1540–1554.e12, December 2016.

[172] Gwo-Hsiao Chen, Roderick A McDonald, Jason C Wells, Gary B Huffnagle, Nicholas W Lukacs, and Galen B Toews. The gamma interferon receptor is required for the protective pulmonary inflammatory response to Cryptococcus neoformans. *Infect. Immun.*, 73(3):1788–1796, March 2005.

[173] Ralph R Weichselbaum, Hemant Ishwaran, Taewon Yoon, Dimitry S A Nuyten, Samuel W Baker, Nikolai Khodarev, Andy W Su, Arif Y Shaikh, Paul Roach, Bas Kreike, Bernard Roizman, Jonas Bergh, Yudi Pawitan, Marc J van de Vijver, and Andy J Minn. An interferon-related gene signature for DNA damage resistance is a predictive marker for chemotherapy and radiation for breast cancer. *Proc. Natl. Acad. Sci. U.S.A.*, 105(47):18490–18495, November 2008.

[174] Michael S Rooney, Sachet A Shukla, Catherine J Wu, Gad Getz, and Nir Hacohen. Molecular and Genetic Properties of Tumors Associated with Local Immune Cytolytic Activity. *Cell*, 160(1-2):48–61, January 2015.

[175] Christopher J Nirschl, Mayte Suárez-Fariñas, Benjamin Izar, Sanjay Prakadan, Ruth Dannenfelser, Itay Tirosh, Yong Liu, Qian Zhu, K Sanjana P Devi, Shaina L Carroll, David Chau, Melika Rezaee, Tae-Gyun Kim, Ruiqi Huang, Judilyn Fuentes-Duculan, George X Song-Zhao, Nicholas Gulati, Michelle A Lowes, Sandra L King, Francisco J Quintana, Young-Suk Lee, James G Krueger, Kavita Y Sarin, Charles H Yoon, Levi Garraway, Aviv Regev, Alex K Shalek, Olga Troyanskaya, and Niroshana Anandasabapathy. IFNγ-Dependent Tissue-Immune Homeostasis Is Co-opted in the Tumor Microenvironment. *Cell*, 170(1):127–141.e15, June 2017.

[176] K Abiko, N Matsumura, J Hamanishi, N Horikawa, R Murakami, K Yamaguchi, Y Yoshioka, T Baba, I Konishi, and M Mandai. IFN-γ from lymphocytes induces PD-L1 expression and promotes progression of ovarian cancer. *Br. J. Cancer*, 112(9):1501–1509, March 2015.

[177] Jae-Ouk Kim, Ho Won Kim, Kyoung-Min Baek, and Chang-Yuil Kang. NF-κB and AP-1 regulate activation-dependent CD137 (4-1BB) expression in T cells. *FEBS Letters*, 541(1-3):163–170, April 2003.

[178] Gustavo J Martinez, Renata M Pereira, Tarmo Äijö, Edward Y Kim, Francesco Marangoni, Matthew E Pipkin, Susan Togher, Vigo Heissmeyer, Yi Chen Zhang, Shane Crotty, Edward D Lamperti, K Mark Ansel, Thorsten R Mempel, Harri Lähdesmäki, Patrick G Hogan, and Anjana Rao. The Transcription Factor NFAT Promotes Exhaustion of Activated CD8+ T Cells. *Immunity*, 42(2):265–278, February 2015.

[179] Romina S Goldszmid, Amiran Dzutsev, and Giorgio Trinchieri. Host Immune Response to Infection and Cancer: Unexpected Commonalities. *Cell Host and Microbe*, 15(3):295–305, March 2014.

[180] Cameron R Cunningham, Ameya Champhekar, Michael V Tullius, Barbara Jane Dillon, Anjie Zhen, Justin Rafael de la Fuente, Jonathan Herskovitz, Heidi Elsaesser, Laura M Snell, Elizabeth B Wilson, Juan Carlos de la Torre, Scott G Kitchen, Marcus A Horwitz, Steven J Bensinger, Stephen T Smale, and David G Brooks. Type I and Type II Interferon Coordinately Regulate Suppressive Dendritic Cell Fate and Function during Viral Persistence. *PLoS Pathog*, 12(1):e1005356, January 2016.

[181] Laura M Snell and David G Brooks. New insights into type I interferon and the immunopathogenesis of persistent viral infections. *Curr. Opin. Immunol.*, 34:91–98, June 2015.

[182] R H Schwartz, D L Mueller, M K Jenkins, and H Quill. T-cell clonal anergy. *Cold Spring Harb. Symp. Quant. Biol.*, 54 Pt 2:605–610, 1989.

[183] K Araki, A J Zajac, S Gangappa, J N Blattman, K Murali-Krishna, D L Dillehay, B T Rouse, D J Sourdive, C P Larsen, M Suresh, J D Altman, and R Ahmed. Viral

immune evasion due to persistence of activated T cells without effector function. *J. Exp. Med.*, 188(12):2205–2213, December 1998.

[184] Andrea Schietinger and Philip D Greenberg. Tolerance and exhaustion: defining mechanisms of T cell dysfunction. *Trends in Immunology*, 35(2):51–60, February 2014.

[185] Vijay K Kuchroo, Ana C Anderson, and Constantinos Petrovas. Coinhibitory receptors and CD8 T cell exhaustion in chronic infections. *Current Opinion in HIV and AIDS*, 9(5):439–445, September 2014.

[186] E L Pearce, M C Poffenberger, C H Chang, and R G Jones. Fueling immunity: insights into metabolism and lymphocyte function. *Science*, 2013.

[187] Alison Crawford, Jill M Angelosanto, Charlly Kao, Travis A Doering, Pamela M Odorizzi, Burton E Barnett, and E John Wherry. Molecular and Transcriptional Basis of CD4(+) T Cell Dysfunction during Chronic Infection. *Immunity*, 40(2):289–302, February 2014.

[188] Derek L Clouthier, Angela C Zhou, and Tania H Watts. Anti-GITR agonist therapy intrinsically enhances CD8 T cell responses to chronic lymphocytic choriomeningitis virus (LCMV), thereby circumventing LCMV-induced downregulation of costimulatory GITR ligand on APC. *The Journal of Immunology*, 193(10):5033–5043, November 2014.

[189] Surojit Sarkar, Vandana Kalia, W Nicholas Haining, Bogumila T Konieczny, Shruti Subramaniam, and Rafi Ahmed. Functional and genomic profiling of effector CD8 T cell subsets with distinct memory fates. *J. Exp. Med.*, 205(3):625–640, March 2008.

[190] Susan M Kaech, Joyce T Tan, E John Wherry, Bogumila T Konieczny, Charles D Surh, and Rafi Ahmed. Selective expression of the interleukin 7 receptor identifies effector CD8 T cells that give rise to long-lived memory cells. *Nat Immunol*, 4(12):1191–1198, November 2003.

[191] Janet Lau, Jeanne Cheung, Armando Navarro, Steve Lianoglou, Benjamin Haley, Klara Totpal, Laura Sanders, Hartmut Koeppen, Patrick Caplazi, Jacqueline McBride, Henry Chiu, Rebecca Hong, Jane Grogan, Vincent Javinal, Robert Yauch, Bryan Irving, Marcia Belvin, Ira Mellman, Jeong M Kim, and Maike Schmidt. Tumour and host cell PD-L1 is required to mediate suppression of anti-tumour immunity in mice. *Nature Communications*, 8:14572, February 2017.

[192] Haidong Tang, Yong Liang, Robert A Anders, Janis M Taube, Xiangyan Qiu, Aditi Mulgaonkar, Xin Liu, Susan M Harrington, Jingya Guo, Yangchun Xin, Yahong Xiong, Kien Nham, William Silvers, Guiyang Hao, Xiankai Sun, Mingyi Chen, Raquibul Hannan, Jian Qiao, Haidong Dong, Hua Peng, and Yang-Xin Fu. PD-L1 on host cells is essential for PD-L1 blockade-mediated tumor regression. *J. Clin. Invest.*, 128(2):580–588, February 2018.

[193] Heng Lin, Shuang Wei, Elaine M Hurt, Michael D Green, Lili Zhao, Linda Vatan, Wojciech Szeliga, Ronald Herbst, Paul W Harms, Leslie A Fecher, Pankaj Vats, Arul M Chinnaiyan, Christopher D Lao, Theodore S Lawrence, Max Wicha, Junzo Hamanishi, Masaki Mandai, Ilona Kryczek, and Weiping Zou. Host expression of PD-L1 determines efficacy of PD-L1 pathway blockade-mediated tumor regression. *J. Clin. Invest.*, 128(2):805–815, February 2018.

[194] Vikram R Juneja, Kathleen A McGuire, Robert T Manguso, Martin W LaFleur, Natalie Collins, W Nicholas Haining, Gordon J Freeman, and Arlene H Sharpe. PD-L1 on tumor cells is sufficient for immune evasion in immunogenic tumors and inhibits CD8 T cell cytotoxicity. *J. Exp. Med.*, 214(4):895–904, April 2017.

[195] Shashank J Patel, Neville E Sanjana, Rigel J Kishton, Arash Eidizadeh, Suman K Vodnala, Maggie Cam, Jared J Gartner, Li Jia, Seth M Steinberg, Tori N Yamamoto, Anand S Merchant, Gautam U Mehta, Anna Chichura, Ophir Shalem, Eric Tran, Robert Eil, Madhusudhanan Sukumar, Eva Perez Guijarro, Chi-Ping Day, Paul Robbins, Steve Feldman, Glenn Merlino, Feng Zhang, and Nicholas P Restifo. Identification of essential genes for cancer immunotherapy. *Nature*, 548(7669):537–542, August 2017.

[196] Robert T Manguso, Hans W Pope, Margaret D Zimmer, Flavian D Brown, Kathleen B Yates, Brian C Miller, Natalie B Collins, Kevin Bi, Martin W LaFleur, Vikram R Juneja, Sarah A Weiss, Jennifer Lo, David E Fisher, Diana Miao, Eliezer Van Allen, David E Root, Arlene H Sharpe, John G Doench, and W Nicholas Haining. In vivo CRISPR screening identifies Ptpn2 as a cancer immunotherapy target. *Nature*, 375:1823, July 2017.

[197] Jingjing Zhu, Céline G Powis de Tenbossche, Stefania Cané, Didier Colau, Nicolas van Baren, Christophe Lurquin, Anne-Marie Schmitt-Verhulst, Peter Liljeström, Catherine Uyttenhove, and Benoît J Van den Eynde. Resistance to cancer immunotherapy mediated by apoptosis of tumor-infiltrating lymphocytes. *Nature Communications*, 8(1):1404, November 2017.

[198] B Huard, P Gaulard, F Faure, T Hercend, and F Triebel. Cellular expression and tissue distribution of the human LAG-3-encoded protein, an MHC class II ligand. *Immunogenetics*, 39(3):213–217, 1994.

[199] P Hemon, F Jean-Louis, K Ramgolam, C Brignone, M Viguier, H Bachelez, F Triebel, D Charron, F Aoudjit, R Al-Daccak, and L Michel. MHC Class II Engagement by Its Ligand LAG-3 (CD223) Contributes to Melanoma Resistance to Apoptosis. *The Journal of Immunology*, 186(9):5173–5183, April 2011.